

# **Leg 210 Preliminary Report**

Drilling the Newfoundland Half of the Newfoundland–  
Iberia Transect: The First Conjugate Margin Drilling  
in a Nonvolcanic Rift

6 July–6 September 2003

Shipboard Scientific Party

Ocean Drilling Program  
Texas A&M University  
1000 Discovery Drive  
College Station TX 77845-9547  
USA

November 2003

## **PUBLISHER'S NOTES**

This report was prepared from shipboard files by scientists who participated in the cruise. The report was assembled under time constraints and does not contain all works and findings that will appear in the *Initial Reports* of the ODP *Proceedings*. Reference to the whole or to part of this report should be made as follows:

Shipboard Scientific Party, 2003. Leg 210 Preliminary Report. *ODP Prelim. Rpt.*, 110 [Online]. Available from World Wide Web: <[http://www-odp.tamu.edu/publications/prelim/210\\_prel/210PREL.PDF](http://www-odp.tamu.edu/publications/prelim/210_prel/210PREL.PDF)>. [Cited YYYY-MM-DD]

Distribution: Electronic copies of this series may be obtained from the Ocean Drilling Program's World Wide Web site at <http://www-odp.tamu.edu/publications>.

This publication was prepared by the Ocean Drilling Program, Texas A&M University, as an account of work performed under the international Ocean Drilling Program, which is managed by Joint Oceanographic Institutions, Inc., under contract with the National Science Foundation. Funding for the program is provided by the following agencies:

Australia/Canada/Chinese Taipei/Korea Consortium for Ocean Drilling  
Deutsche Forschungsgemeinschaft (Federal Republic of Germany)  
European Science Foundation Consortium for Ocean Drilling (Belgium, Denmark, Finland, Iceland, Ireland, Italy, The Netherlands, Norway, Portugal, Spain, Sweden, and Switzerland)  
Institut National des Sciences de l'Univers–Centre National de la Recherche Scientifique (INSU-CNRS; France)  
Ocean Research Institute of the University of Tokyo (Japan)  
Marine High-Technology Bureau of the State Science and Technology Commission of the People's Republic of China  
National Science Foundation (United States)  
Natural Environment Research Council (United Kingdom)

## **DISCLAIMER**

Any opinions, findings, and conclusions or recommendations expressed in this publication are those of the author(s) and do not necessarily reflect the views of the National Science Foundation, the participating agencies, Joint Oceanographic Institutions, Inc., Texas A&M University, or Texas A&M Research Foundation.

The following scientists and personnel were aboard the *JOIDES Resolution* for Leg 210 of the Ocean Drilling Program:

**SHIPBOARD SCIENTIFIC PARTY**

**Co-Chief Scientist**

**Brian E. Tucholke**

Department of Geology and Geophysics  
Woods Hole Oceanographic Institution  
MS 22

Woods Hole MA 02543-1541

USA

Work: (508) 289-2494

Fax: (508) 457-2187

**btucholke@whoi.edu**

**Co-Chief Scientist**

**Jean-Claude Sibuet**

Ifremer Centre de Brest

BP 70

29280 Plouzané Cedex

France

Work: (33) 2-98-22-42-33

Fax: (33) 2-98-22-45-49

**jsibuet@ifremer.fr**

**Staff Scientist**

**Adam Klaus**

Ocean Drilling Program

Texas A&M University

1000 Discovery Drive

College Station TX 77845-9547

USA

Work: (979) 845-3055

Fax: (979) 845-0876

**aklaus@odpemail.tamu.edu**

**Michela Arnaboldi**

**Organic Geochemist**

Department of Geological Sciences

University of Michigan

2534 C.C. Little Building

425 East University Avenue

Ann Arbor MI 48109-1063

USA

Work: (734) 647-7925

Fax: (734) 763-4690

**marna@umich.edu**

**Heike Delius**

**Logging Staff Scientist**

Department of Geology

University of Leicester

University Road

Leicester LE1 7RH

United Kingdom

Work: (44) 116-252-3634

Fax: (44) 116-252-3918

**hd21@leicester.ac.uk**

**Anna V. Engström**

**Petrologist**

Department of Geology and Geochemistry

Stockholm University

106 91 Stockholm

Sweden

Work: (46) 8 164751

Fax: (46) 8 6747897

**anna@geo.su.se**

**Bruno Galbrun**

**Paleomagnetist**

Département de Géologie Sédimentaire

Université Pierre et Marie Curie

Case 117

4 Place Jussieu

75252 Paris Cedex 05

France

Work: (33) 1-44-27-5041

Fax: (33) 1-44-27-3831

**bgalbrun@ccr.jussieu.fr**

**Silvia Gardin**

**Paleontologist (nannofossils)**

Laboratoire de Micropaléontologie

Université Pierre et Marie Curie

4 Place Jussieu

75252 Paris Cedex 05

France

Work: (33) 1 44274986

Fax: (33) 1 44273831

**gardin@ccr.jussieu.fr**

**Richard N. Hiscott**

**Sedimentologist**

Earth Sciences Department

Memorial University of Newfoundland

St. John's NF A1B 3X5

Canada

Work: (709) 737-8394

Fax: (709) 737-2589

**rickh@sparky2.esd.mun.ca**

**Garry D. Karner**

**Physical Properties Specialist**

Marine Geology and Geophysics

Lamont-Doherty Earth Observatory

of Columbia University

PO Box 1000, 61 Route 9W

Palisades NY 10964

USA

Work: (845) 365-8355

Fax: (845) 365-8156

**garry@ldeo.columbia.edu**

**Bryan C. Ladner**  
**Paleontologist (nannofossils)**  
Department of Geological Sciences  
Florida State University  
108 Carraway Building  
Tallahassee FL 32306-4100  
USA  
Work: (850) 644-5860  
Fax: (850) 644-4214  
**ladner@gly.fsu.edu**

**R. Mark Leckie**  
**Paleontologist (foraminifers)**  
Department of Geosciences  
University of Massachusetts  
611 North Pleasant Street  
Amherst MA 01003  
USA  
Work: (413) 545-1948  
Fax: (413) 545-1200  
**mleckie@geo.umass.edu**

**Chao-Shing Lee**  
**Physical Properties Specialist**  
Institute of Applied Geophysics  
National Taiwan Ocean University  
2 Pei-Ning Road  
Keelung 202  
Taiwan  
Work: (886) 2-2463-1811  
Fax: (886) 2-2462-5038  
**leecs@mail.ntou.edu.tw**

**Gianreto Manatschal**  
**Structural Geologist**  
Centre de Géochimie de la Surface  
Ecole et Observatoire des Sciences de la Terre  
1 Rue Blessig  
67084 Strasbourg  
France  
Work: (33) 3 90 24 04 54  
Fax: (33) 3 88 36 72 35  
**manatschal@illite.u-strasbg.fr**

**Kathleen M. Marsaglia**  
**Sedimentologist**  
Department of Geological Sciences  
California State University, Northridge  
18111 Nordhoff Street  
Northridge CA 91330-8266  
USA  
Work: (818) 677-6309, ext 3541  
Fax: (818) 677-2820  
**kathie.marsaglia@csun.edu**

**Thomas K. Pletsch**  
**Sedimentologist**  
Technical Mineralogy and Sedimentology Section  
Bundesanstalt für Geowissenschaften und Rohstoffe  
Stilleweg 2  
30655 Hannover  
Germany  
Work: (49) 511-643-2828  
Fax: (49) 511-643-3664  
**t.pletsch@bgr.de**

**Jörg Pross**  
**Paleontologist (palynomorphs)**  
Institut für Geowissenschaften  
Universität Tübingen  
Sigwartstrasse 10  
72076 Tübingen  
Germany  
Work: (49) 7071-297 3068  
Fax: (49) 7071-295 727  
**joerg.pross@uni-tuebingen.de**

**Alastair H.F. Robertson**  
**Sedimentologist**  
Department of Geology and Geophysics  
University of Edinburgh  
West Mains Road  
Edinburgh, Lothian EH9 3JW  
United Kingdom  
Work: (44) 131-650-8546  
Fax: (44) 131-668-3184  
**alastair.robertson@glg.ed.ac.uk**

**Dale S. Sawyer**  
**Physical Properties Specialist**  
Department of Earth Science  
Rice University MS-126  
PO Box 1892  
Houston TX 77001-1892  
USA  
Work: (713) 348-5106  
Fax: (713) 348-5214  
**dale@rice.edu**

**Derek E. Sawyer**  
**Physical Properties Specialist**  
Department of Geosciences  
Pennsylvania State University  
320 Deike Building  
University Park PA 16802  
USA  
Work: (814) 863-9663  
Fax: (814) 863-7823  
**dsawyer@geosc.psu.edu**

**Donna Shillington**  
**Logging Scientist**

Department of Geology and Geophysics  
University of Wyoming  
PO Box 3006  
Laramie WY 82071-3006  
USA  
Work: (307) 766-3363  
Fax: (307) 766-6679  
**djs@uwyo.edu**

**Masaaki Shirai**  
**Sedimentologist**

Ocean Research Institute  
University of Tokyo  
1-15-1 Minamidai  
Nakano, Tokyo 164-8639  
Japan  
Work: (81) 3-5351-6559  
Fax: (81) 3-5351-6438  
**shirai@ori.u-tokyo.ac.jp**

**Thérèse Shryane**  
**Structural Geologist**

Galway Geofluids Research Centre  
Department of Earth and Oceanographic Science  
National University of Ireland, Galway  
Galway  
Ireland  
Work: (353) 1 524411  
Fax: (353) 1 752555  
**shryane@ireland.com**

**Sharon Audra Stant**  
**Student Trainee**

Department of Geological Sciences  
Florida State University  
108 Carraway Building  
Tallahassee FL 32306-4100  
USA  
Work: (850) 974-6490, (850) 644-5860  
Fax: (850) 644-4214  
**stant@gly.fsu.edu**

**Hiroyuki Takata**  
**Paleontologist (foraminifers)**

Research Center of Coastal Lagoon Environments  
Shimane University  
Nishi-kawatsu 1060  
Matsue, Shimane 690-8504  
Japan  
Work: (81) 852-32-6450  
Fax: (81) 852-32-6099  
**yu@soc.shimane-u.ac.jp**

**Elsbeth Urquhart**  
**Paleontologist (foraminifers/radiolarians)**

Rosenstiel School of Marine and Atmospheric Science  
University of Miami  
4600 Rickenbacker Causeway  
Miami FL 33149  
USA  
Work: (305) 361-4668  
Fax: (305) 361-4632  
**eurquhart@rsmas.miami.edu**

**Chris Wilson**  
**Sedimentologist**

Department of Earth Sciences  
The Open University  
Walton Hall  
Milton Keynes MK7 6AA  
United Kingdom  
Work: (44) 1908-653-228  
Fax: (44) 1908-655-151  
**r.c.l.wilson@open.ac.uk**

**Xixi Zhao**  
**Paleomagnetist**

Department of Earth Sciences  
University of California, Santa Cruz  
1156 High Street  
Santa Cruz CA 95064  
USA  
Work: (831) 459-4847  
Fax: (831) 459-3074  
**xzhao@es.ucsc.edu**

**TRANSOCEAN OFFICIALS**

**Pete Mowat**  
**Master of the Drilling Vessel**

Overseas Drilling Ltd.  
707 Texas Avenue South, Suite 213D  
College Station TX 77840-1917  
USA

**Tim McCown**  
**Drilling Superintendent**

Overseas Drilling Ltd.  
707 Texas Avenue South, Suite 213D  
College Station TX 77840-1917  
USA

**ODP SHIPBOARD PERSONNEL**

**Christopher Bennight**  
Marine Laboratory Specialist (Chemistry)

**Gerald W. Bode**  
Marine Laboratory Specialist (Curator)

**Timothy Bronk**  
Assistant Laboratory Officer

**Jason Deardorff**  
Marine Laboratory Specialist (Core)

**David Fackler**  
Programmer

**Kevin Grigar**  
Drilling Engineer

**Michael Hodge**  
Marine Computer Specialist

**Shannon Housley**  
Marine Laboratory Specialist (Photographer)

**Brian Jonasson**  
Operations Manager

**Peter Kannberg**  
Marine Laboratory Specialist (Core)

**Steve Kittredge**  
Schlumberger Engineer

**Jurie Kotzé**  
Marine Electronics Specialist

**William Mills**  
Laboratory Officer

**David Morley**  
Marine Computer Specialist

**Deborah L. Partain**  
Marine Laboratory Specialist (Yeoperson)

**Pieter Pretorius**  
Marine Electronics Specialist

**Patrick Riley**  
Marine Laboratory Specialist (Physical Properties)

**Johanna Suhonen**  
Marine Laboratory Specialist (Underway Geophysics)

**Paul Ténrière**  
Marine Laboratory Specialist (Paleomagnetism)

**Robert Wheatley**  
Marine Laboratory Specialist (Chemistry)

## ABSTRACT

Ocean Drilling Program Leg 210 was devoted to studying the history of rifting and postrift sedimentation in the Newfoundland–Iberia rift. Drilling was conducted in the Newfoundland Basin along a transect conjugate to previous drilling on the Iberia margin (Legs 149 and 173). This was the first time that deep-sea drilling has been conducted on both sides of a nonvolcanic rift in order to understand the structural and sedimentary evolution of the complete rift system. The prime site during Leg 210 (Site 1276) was drilled in “transitional” crust between known continental crust and known oceanic crust identified by magnetic anomalies M3 to M0 (Barremian–Aptian). On the conjugate Iberia margin extensive geophysical work and deep-sea drilling have shown that the transition zone crust is exhumed mantle that is extensively serpentinized in its upper part. Transition zone crust on the Newfoundland side, however, is typically a kilometer or more shallower and has much smoother topography, and seismic refraction data suggest that the crust may be thin (~4 km) oceanic crust. These features indicate that the rift may have developed asymmetrically. A major goal at Site 1276 was to investigate these differences by sampling basement and the facies responsible for a strong overlying, basin-wide reflection (U) that is poorly developed on the conjugate Iberia margin, together with the intervening section.

Site 1276 was cored from 800 to 1739 m below seafloor with excellent recovery (average = 85%). Before drilling was terminated because of unstable conditions in the uncased hole, drilling reached sills >10 m thick that are estimated to be 100–200 m above basement. The sills are alkaline diabbases, they have sedimentary contacts that show extensive hydrothermal metamorphism, and associated sediment structural features indicate that they were intruded at shallow levels below the seafloor. The top of the upper sill is approximately coincident with U, which correlates with lower Albian fine- to coarse-grained sedimentary gravity flows. The nature of basement at this site remains uncertain, but the presence of the deep sills indicates that there was a significant postrift magmatic event that may have affected much of the basin. This feature of the basin could help to explain the asymmetry in basement depth and basement roughness on the conjugate Newfoundland and Iberia margins.

The overlying Albian–lower Oligocene sediments record paleoceanographic conditions similar to those in the main North Atlantic Basin and on the Iberia margin, including deposition of Cretaceous “black shales,” but they show an extensive component of gravity flow deposits throughout. Major paleoceanographic events including a number of Ocean Anoxic Events, the Cretaceous/Tertiary boundary, and the recovery from the Paleocene/Eocene Thermal Maximum are well represented in the cored section. A prominent seismic marker that is correlated with the initiation of deep circulation in the North Atlantic was cored, and preliminary biostratigraphic data indicate that it is a hiatus dating to the middle Eocene, perhaps several million years older than proposed in previous interpretations.

Site 1277 was drilled 80 m into a shallow basement high ~40 km southeast of Site 1276. This crust, presumed to be oceanic, is on the young side of a magnetic anomaly interpreted as M1. Cores from the upper part of basement at this site recovered a remarkable assemblage of basalt flows interleaved with gravity flows containing slivers of gabbro, serpentinized peridotite, and sediments (e.g., fine- to coarse-grained sandstones). Below these largely allochthonous rocks, basement is serpentinized peridotite with veins of gabbro and this rock is interpreted as being in situ. These rocks were emplaced in a magma-limited, highly extensional environment which we interpret as very slow spreading ocean crust.

## INTRODUCTION

Rifting of a continent and birth of a new oceanic spreading center are fundamental yet poorly understood parts of the plate tectonic cycle. Rifted margins are commonly classified into two types, volcanic and nonvolcanic (Mutter et al., 1988; White and McKenzie, 1989; White et al., 1987), although a relatively continuous range of margin types that vary in character according to tectonic stress, lithospheric strength, and mantle conditions is likely (Mutter, 1993). Two principal models of lithospheric extension have been proposed for nonvolcanic margins. In the pure shear model (McKenzie, 1978), crustal thinning is relatively uniform across a rift; brittle deformation causes thinning and faulting of the upper crust and ductile deformation thins the lower crust. This model predicts that conjugate margins will have generally similar crustal thickness, structure, composition, and subsidence history. Progress in modeling of continental rift structure and extensional tectonics, however, together with observations of significant asymmetries in conjugate margins, suggests that many rifts may develop by a simple shear mechanism (e.g., Lister et al., 1986, 1991; Rosendahl, 1987; Wernicke, 1985). Simple shear predicts an upper plate margin consisting of weakly structured upper continental crust with a rift stage history of uplift and a lower plate margin dominated by highly structured lower continental crust and a history of subsidence. Melt generation and attendant volcanism, compared to a pure shear environment, is probably minimal (Buck, 1991; Latin and White, 1990).

As continental plates separate, crustal thinning, volcanism, faulting, uplift, subsidence, and sedimentation profoundly modify the structure of the rifted margins. To understand these processes we need detailed information on the resulting geological record, particularly the basement architecture and the overlying sedimentary framework. Furthermore, in order to evaluate the role of pure shear, simple shear, or other mechanisms of rift extension, it is essential to examine the geological record of *conjugate* rifted margins. This is best done by acquiring and analyzing wide-angle reflection/refraction and vertical-incidence reflection data along carefully chosen conjugate margin transects and then by sampling critical sections by drilling.

In the early 1990s, the Joint Oceanographic Institutions for Deep Earth Sampling (JOIDES) North Atlantic Rifted Margins Detailed Planning Group recommended the Newfoundland and Iberia conjugate margins as high-priority drilling targets to understand the evolution of nonvolcanic rifts (Fig. F1). These margins presented several advantages for such a study:

1. They are considered to be representative of nonvolcanic rifting.
2. Rifting is complete, so the entire rift history can be studied.
3. The along-rift spatial relations of crustal conjugates are well constrained in plate reconstructions.
4. Sediments are comparatively thin, so important basement targets can be imaged by seismic reflection/refraction and they are accessible to the drill.
5. The locations are logistically convenient, thus facilitating access.

By design of the JOIDES advisory and planning structure, extensive drilling (Ocean Drilling Program [ODP] Legs 149 and 173) was conducted on the Iberia half of the rift (Fig. F1). This complemented earlier drilling (ODP Leg 103) on the western margin of Galicia Bank, and it was supported by extensive geophysical work (e.g., Whitmarsh et al., 1990, 1996; Pinheiro et al., 1992; Reston et al., 1995; Whitmarsh and Miles, 1995; Reston, 1996; Pickup et al., 1996; Discovery 215 Working Group, 1998). An early drill site from Deep Sea Drilling Project (DSDP) Leg 47B (Site 398) also provided valuable information near the Leg 149/173 transect. These studies, summarized below, provided surprising results about the composition and

origin of crust in the transitional zone between known continental and known oceanic crust on the Iberia margin. They also raised major questions about how the Newfoundland–Iberia rift developed and whether rifting was symmetrical or asymmetrical. To answer these questions, it is necessary to investigate the structure and evolution of the conjugate Newfoundland margin, which was the major objective of Leg 210. The following section outlines the geological setting of the Newfoundland–Iberia rift and summarizes the results of a site survey that was conducted in preparation for drilling on the Newfoundland margin.

## **Geological Setting**

### **Rift Development and Basement Structure**

The Newfoundland and Iberia margins first experienced significant extension in Late Triassic time when rift basins initially formed within the Grand Banks and on the Iberia margin (Lusitania Basin) (Figs. F2, F3). The Grand Banks basins accumulated siliciclastic “redbed” sediments, and these were succeeded by deposition of evaporite deposits, which extended into the earliest Jurassic in both the Grand Banks and Lusitania basins (Jansa and Wade, 1975; Wilson, 1988; Rasmussen et al., 1998). A second prolonged rift phase in the Late Jurassic through Early Cretaceous extended the crust in several subbasins, but it ultimately focused extension between the Grand Banks and Iberia (Tankard and Welsink, 1987; Enachescu, 1987; Wilson, 1989). This culminated in continental breakup and formation of the first oceanic crust no later than Barremian to Aptian time. Excepting the Southeast Newfoundland Ridge at the southernmost edge of the rift, no significant thickness of volcanic rocks or magmatic underplating is known to be present in the rift. Thus the system is considered to be nonvolcanic.

Plate reconstruction of the Newfoundland–Iberia conjugate margins at the time of Anomaly M0 (Barremian/Aptian boundary; ~121 Ma) (Fig. F3) provides a regional overview of the rift and the conjugate margins. At this time, thick continental crust of Flemish Cap was close to extended continental crust of Galicia Bank at the northern end of the rift. To the south, geophysical studies and magnetic anomaly identifications suggest that ocean crust was present, extending landward from a seafloor-spreading axis to at least Anomaly M3 (see shaded area in Fig. F3). Along-axis, the Newfoundland–Iberia rift can be roughly divided into three segments: (1) a northern segment containing Flemish Cap and Galicia Bank, (2) a central segment bounded on the south by the Newfoundland Seamounts and Tore Seamount, and (3) a southern segment extending south to the Southeast Newfoundland Ridge and the present-day Gorringe Bank off southwestern Iberia. Each of these is reviewed below.

In the northern segment, Flemish Cap has full continental crust thickness of ~30 km (Funck et al., in press) and it is separated from the shallow Grand Banks by thinned continental crust under the Flemish Pass Basin and Flemish Cap Graben (Enachescu, 1987). Galicia Bank is extended continental crust that has a maximum thickness of ~20 km in its central part and thins to zero thickness at its western margin; it is separated from Iberia by the Galicia Interior Basin, which contains rifted continental crust that is thinned to ~10 km (González et al., 1999; Perez-Gussinye et al., 2003). Anomaly M0 appears to occur just seaward of the edges of continental crust in these conjugate segments (Srivastava et al., 2000), but there are no older M-series magnetic anomalies present. At the seaward margin of Galicia Bank (ODP Site 637), the westward transition from continental to ocean crust is marked by a prominent ridge composed of serpentinized peridotite (Boillot et al., 1987, 1995).

On the Iberia margin the southern limit of this rift segment lies roughly at the southern edge of Galicia Bank. In this location, the shallow crust of the bank is expressed in a series of rift-parallel ridges that plunge to the south and lose a large portion of their amplitude beneath the southern Iberia Abyssal Plain. It is along this transition that the Leg 149/173 transect was drilled. The seaward edge of known

continental crust passes southeastward through this transect near ODP Site 1069, then probably to the south toward Estremadura Spur (Fig. F3). On the Newfoundland margin, continental crust reaches seaward at least to the Flemish Hinge near Flemish Cap and to a hinge line at the eastern edge of Salar-Bonniton Basin to the south. Seaward of the hinge, no along-strike change has been identified in basement structure that would correlate with the structural change at the southern margin of the conjugate Galicia Bank.

The central segment on both margins has an abrupt transition from shallow continental shelf to deep basin, although there are rift basins beneath the continental shelves that are completely filled with sediments (Fig. F3). On the Newfoundland margin these are the Jeanne d'Arc, Carson, and Salar-Bonniton basins, and the Lusitania Basin is present on the Iberia margin. These basins are in extended continental crust that reaches seaward an uncertain distance beneath the continental slope and rise, and they contain evaporites of Triassic age (Jansa et al., 1980; Austin et al., 1989). Farther seaward, the basement is deep and is considered to be "transitional" crust out to a point where magnetic anomalies M3 to M0 are identified (Fig. F4).

The origin of the transitional crust has been a matter of intense debate. Structural trends in the basement are oriented north-northeast to northeast, subparallel to the M0 rift axis. Srivastava et al. (2000) suggested that magnetic anomalies as old as M17 (early Berriasian; ~140 Ma) are present in this segment, but it is unclear whether the low-amplitude anomalies represent polarity reversals or are related to the basement relief. In the transition zone at the northern margin of the segment, Leg 149 and 173 drilling recovered serpentinized peridotites from basement (Fig. F4). In seismic data to the south (line IAM9; Fig. F4), a thin (1.0–2.5 km) unreflective basement layer is observed overlying a more reflective layer (Pickup et al., 1996). This upper layer also has been interpreted to be serpentinized upper mantle peridotite, grading downward into less altered and unaltered peridotite. Seismic refraction experiments there seem to agree, defining a low-velocity "crust" that is only 2–4 km thick and that overlies a layer with velocities of ~7.1–7.7 km/s that is thought to be partially serpentinized peridotite (Whitmarsh et al., 1990; Discovery 215 Working Group, 1998; Dean et al., 2000). In the conjugate central Newfoundland Basin, similar "crustal" thicknesses and velocity structure have been detected in the transition zone (Srivastava et al., 2000). The transition zone width in the central segment is ~150 km on both margins.

The southern segment is like the central segment in that it has deep and thin crust in the transition zone and the zone is ~130–150 km wide. On the Newfoundland side, refraction data of Reid (1994) indicate the presence of very thin crust (~2 km) over apparently serpentinized mantle (7.2–7.5 km/s) that extends at least ~50 km east of the seaward hinge of the Salar-Bonniton Basin. Very similar results have been reported for the conjugate Iberia transitional crust beneath Tagus Abyssal Plain (Pinheiro et al., 1992). Srivastava et al. (2000) suggested that the transitional crust in the southern segment is oceanic and that it is Tithonian (Anomaly M20; ~145 Ma) in its oldest part. The landward portions of the southern segment differ from the central and northern segments in that there are no major proximal rift basins in the continental crust, excepting the southern Salar-Bonniton Basin on the Newfoundland side. On the Newfoundland margin, the southeasternmost Grand Banks is intact continental crust that has been in a subaerial or shallow-shelf environment throughout the Mesozoic and Cenozoic (Jansa and Wade, 1975).

Just as the three rift segments differ from one another, the conjugate sides of each segment also show dissimilarities. In the northern segment, the major distinction is in the amount of crustal extension (i.e., the thick, intact crust of Flemish Cap vs. the extended and structured crust of Galicia Bank). In the central and southern segments, the major differences are in crustal depth and crustal roughness. The Newfoundland transitional basement averages a kilometer or more shallower than the Iberia basement

(Fig. F4), even when corrected for sediment loading. In addition, Newfoundland basement is relatively smooth compared to that off Iberia, where >1 km of basement relief is common.

Structural trends in the transitional basement (Fig. F3) tend to show some convergence toward the north. This, together with the northward-narrowing zone of ocean crust in the M0 reconstruction, suggests that the rift may have opened from south to north, which is consistent with a stage pole of opening a short distance north of the rift (Whitmarsh et al., 1990; Srivastava et al., 2000). Considering the segment-to-segment differences in extent of rifting in the shallower continental crust, the southern part of the rift may have switched from continental rifting to seafloor spreading relatively early and abruptly, while the northern part experienced prolonged continental extension and a delayed change to normal seafloor spreading.

### **Insights from Newfoundland Basin Geophysical Survey**

Additional constraints on basement structure and sedimentary stratigraphy of the Newfoundland transition zone were obtained in 2000 during the Study of Continental Rifting and Extension on the Eastern Canadian Shelf (SCREECH) program (*Ewing* Cruise 00-07). In this program, multichannel seismic (MCS) and Ocean Bottom Hydrophone/Seismometer surveys were made in three major transects across the Newfoundland margin (Figs. F3B, F5, F6). Each transect extended from full-thickness continental crust on the landward end seaward to known oceanic crust beyond magnetic Anomaly M0. Transect 2 was located so that it is conjugate to the Leg 149/173 drilling on the Iberia margin (Fig. F3B), and it is along this transect that Leg 210 drilling was conducted (Fig. F7). To provide regional perspective, the principal results for all three transects are summarized below.

#### **Transect 1**

Transect 1 across Flemish Cap is in a position conjugate to Leg 103 drilling conducted on the seaward margin of Galicia Bank (Fig. F3B). It shows that continental crust thins rapidly from ~30 km beneath Flemish Cap to ~2 km beneath the lower continental slope at Flemish Hinge (Funck et al., in press; Hopper et al., in press). Farther seaward, probable ocean crust appears first with oceanic Layer 2/3 velocity structure, and it is 3–4 km thick. It then changes eastward to Layer 2 velocity structure and is only 1 km thick. This crust reaches to slightly beyond Anomaly M0, where more normal thickness ocean crust is present. Both the thin continental and thin ocean crust overlie a layer of probably serpentinized mantle ( $V_p = 7.6\text{--}7.9$  km/s) that is 3–5 km thick.

#### **Transect 2**

Transect 2, as noted above, is conjugate to Leg 149 and 173 drilling on the Iberia margin and is the focus of drilling during Leg 210 (Fig. F3B). On this transect continental crust thins quickly seaward beneath the continental slope from 30 km to ~7–8 km over a distance of 60 km, and then over the next 50 km it thins more slowly to ~5 km at the Flemish Hinge (Fig. F3). Beyond this, transition zone crust out to Anomaly ~M3 is only 3–5 km thick. Like part of transect 1, this crust has velocities characteristic of oceanic Layers 2/3, but there appears to be no significant underlying zone of possibly serpentinized mantle (Nunes, 2002). This contrasts with transect 1 and with the velocity structure on the conjugate Iberia margin, where a thick zone of serpentinized mantle appears to be present at and south of the Leg 149/173 drilling transect. Also unlike the Iberia conjugate, transect 2 seismic reflection data show no unreflective upper basement layer that might be highly serpentinized peridotite.

### ***Transect 3***

Transect 3 exhibits still another set of basement structures. Although continental crust thins rapidly from 35 to <10 km under the continental slope near the seaward edge of Salar-Bonnet Basin (Fig. F3B), thin (<5 km) continental crust above serpentinized mantle appears to reach seaward 50 km into the transition zone. The remainder of the transition zone to the east has extremely thin (~2 km thick) “crust” that may be either a serpentinized layer of exhumed mantle or thin ocean crust (Lau et al., 2003).

A common feature of all three transects is that there is thin crust and apparently very limited magmatism in the transition zone. The transects differ, however, in how magmatism was expressed, in distribution and character of tectonic extension, and in development of serpentinized “lower crust.” Thus, it appears that the balance between tectonic extension and limited magmatism was heterogeneous both along and across the rift.

## **Sedimentary Seismic Sequences**

### ***Basal Sequence (Seismic Sequence A)***

In the transition zone off Newfoundland there is a very flat, high-amplitude reflection (U) that closely overlies or intersects basement (Figs. F4, F8, F9). This reflection reaches some 600 km south to north in the basin and up to ~150 km across the transition zone. Where traced landward it merges with the Lower to mid-Cretaceous Avalon unconformity on the Grand Banks (Tucholke et al., 1989). At its seaward edge it normally pinches out on crust of about Anomaly M3 age (Hauterivian–Barremian) (Fig. F9). These features suggest that the horizon has an Early Cretaceous age.

The sedimentary sequence between basement and U is defined here as seismic Sequence A. It is seismically laminated, exhibits strong and laterally coherent reflections, and is up to ~0.5 s (two-way traveltime) thick along the proximal part of the margin (Figs. F8, F9, F10). At many locations, basement below U is not identified as a distinct reflection but as a downward disappearance of reflections (Fig. F8A, F8B). This indicates that the impedance of Sequence A is high and is probably close to that of the underlying basement. The sequence is often faulted near its seaward margin, but it is seldom faulted at other locations in the transition zone (Tucholke et al., 1989). The apparent age of U and underlying sediments is similar to that of the Blake-Bahama Formation (Hauterivian–Barremian limestones, capped by Horizon  $\beta$ ) in the western North Atlantic Basin (Tucholke and Mountain, 1979; Jansa et al., 1979). The reflection character is also similar, although the U horizon is a much stronger reflection than Horizon  $\beta$ . These features suggest that Sequence A may be equivalent to the Blake-Bahama Formation in the western North Atlantic Basin.

Locally, U appears to truncate the underlying basement (Tucholke et al., 1989). The possible truncations, areal extent, and flatness of the horizon led Tucholke et al. (1989) to suggest that it could be an unconformity eroded at or above sea level on extended continental crust. This interpretation has been evaluated with thermal-mechanical modeling (B. Tucholke and N. Driscoll, unpub. data). The results indicate that if erosion occurred at sea level, it would have to be on continental crust at least ~18 km thick, given reasonable upper mantle temperatures of 1300°–1400°C. Thus, if the reflection originated in this way, it must be a synrift unconformity and not a “breakup unconformity.”

U and Sequence A can also be compared to a similar deep reflection sequence across probable continental crust of southern Galicia Bank on the Iberia margin (see Figs. F28, F29). The sequence there is capped by the “orange” reflection and it has been drilled at Site 398 (Shipboard Scientific Party, 1979). It is represented by lithologic Unit 4C, of Aptian age, which is composed of bioturbated mudstones, turbiditic mudstones, thin laminated and cross-bedded fine-grained sandstones and siltstones, and debris flows or

mud flows. The unit was interpreted as a fining-upward submarine fan sequence that began to be deposited in Barremian time, with fan deposition gradually waning during the late Aptian. Seismic profiles and the mapped distribution of this sequence (seismic Unit 4 of Réhault and Mauffret [1979]) show that it fills in basement depressions (Fig. F30). A deeper lithologic, just unit above basement (lithologic Unit 5), consists of nannofossil limestones interbedded with laminated mudstones. Velocity in lithologic Units 4 and 5 at Site 398 probably increases with depth, but a mean assumed velocity of 3.59 km/s results in good fit between seismic reflections and a synthetic seismogram based on borehole physical property data (Bouquigny and Willm, 1979). Thus, velocities and impedance in the deep part of the section are high and may be close to those of the underlying basement, much as interpreted on the Newfoundland margin. However, the regional reflectivity of the orange reflection and the upper part of the sequence appear to be lower than the reflectivity of Sequence A on the Newfoundland margin.

### ***Shallower Sedimentary Sequences***

Reflection profiles in the Newfoundland Basin show five principal seismic sequences in the section above U. These are differentiated from one another by broad changes in reflection character, which in turn suggest general changes in depositional conditions and/or deformation. The sequences are summarized below, from base to top.

1. ***Seismic Sequence B.*** This sequence is conformable to the underlying U reflection and extends upward to the base of a strongly laminated zone near middepth in the sedimentary column (Fig. F8). In the landward part of the transition zone it has a thickness of ~0.5 s two-way traveltime. Reflections in Sequence B have low amplitude compared to reflections in the underlying and overlying sequences, but they are still relatively well defined and are mostly laterally continuous over distances of tens to hundreds of kilometers. Reflections tend to be more coherent and readily traced in the lower part of the sequence than in the upper part, where they are sometimes disrupted or even chaotic. At some locations in the upper part of Sequence B, reflections show seaward downlap and landward onlap of reflections that suggest local control of depositional patterns (e.g., in a fan-channel system). The top of the sequence is marked by an apparent unconformity that truncates progressively deeper beds in a landward direction. The predicted age of this sequence is mid-Cretaceous, which would include black shales equivalent to the Hatteras Formation farther south in the main North Atlantic Basin.
2. ***Seismic Sequence C.*** Sequence C exhibits a series of very strong, flat, coherent reflections that are easily traced laterally for distances of 100 km or more. The interval represents ~0.3 s of reflection time and occurs midway in the sedimentary section. Reflection character of this sequence indicates that it consists of interbedded high- and low-velocity layers (e.g., turbidites). In its landward portions, the upper part of Sequence C remains strongly layered in its lower section but its upper section expands and contains chaotic reflections; these reflections appear to be caused by debris flows and other downslope mass movements.

The reflection that marks the top of Sequence C, as discussed below, appears to be equivalent to Horizon A<sup>u</sup> in the western North Atlantic, suggesting that Sequence C is Eocene at its top; it probably extends into the Paleocene or possibly the Upper Cretaceous at its base. The following formations would be included in this sequence, from base to top: black shales of the Hatteras Formation, reddish and multicolored pelagic shales of the Plantagenet Formation ( $\pm$  Maastrichtian limestones of the Crescent Peaks Member), and siliceous shales and cherts of the Bermuda Rise Formation (Jansa et al., 1979).

3. **Seismic Sequence D.** This sequence is characterized by reflections with distinctive pinch-and-swell morphology that indicates current-controlled deposition and formation of sediment waves, much like Oligocene–Miocene seismic sequences along the eastern margin of North America to the south (Mountain and Tucholke, 1985). The sequence is thickest close to the margin (~0.4 s reflection time) and sediment waves are best developed there. Seaward, it thins to ~0.1 s. A number of strong reflections are well developed and continuous through the sequence, but weaker intervening reflections are often broken up, particularly in the lower part of the sequence and in its thinner section away from the margin. The semichaotic character of these reflections suggests that debris flows and mass wasting deposits may form part of the sequence.

The base of this sequence is interpreted to be equivalent to Horizon A<sup>u</sup> in the western North Atlantic south of Newfoundland Basin. There, the horizon is a widespread unconformity that was eroded when strong abyssal circulation (Deep Western Boundary Current [DWBC]) developed in the basin (Tucholke and Mountain, 1979). On the Newfoundland margin the reflection shows truncation of the underlying irregular beds of upper Sequence C beneath the inner continental rise, but farther seaward it is mostly conformable to deeper bedding. The source of bottom water for the DWBC is thought to be in the sub-Arctic/Arctic seas, so the Newfoundland Basin is the “gateway” region through which this current flowed southward and it may contain an important record of how abyssal circulation developed in the North Atlantic Ocean. The DWBC is interpreted to have developed in the latest Eocene to early Oligocene (Miller and Tucholke, 1983; Davies et al., 2001). The predicted age of Sequence D is lower Oligocene at the base, extending up into the Miocene at the top.

4. **Seismic Sequence E.** This sequence is well developed all along the Newfoundland margin. It is consistently thicker close to the margin (~0.8 s two-way traveltime) and thins seaward to as little as ~0.2 s beneath the outermost continental rise and abyssal plain. Sequence E has a very distinctive seismic signature. It is marked by undulating and contorted reflections that usually can be traced for only limited distances. Some reflections have the form of poorly developed sediment waves. In its upper part the sequence contains channels that are filled with chaotic debris, and other portions also show chaotic signature that probably represents rapid deposition of mass-wasting deposits. The sequence is also permeated by small-throw normal faults, almost none of which extend into the underlying or overlying sequences. These features are commonly developed in abyssal fans; they suggest that the sediments were deposited rapidly while trapping pore fluids and that they later failed as the sediments dewatered. Similar seismic sequences appear along the U.S. East Coast margin (Mountain and Tucholke, 1985) and on other margins across the globe in the middle Miocene to Pliocene–Pleistocene. They appear to document a global period of margin progradation (Bartek et al., 1991).
5. **Seismic Sequence F.** This is the topmost seismic sequence in the Newfoundland Basin and it consists of reflective, flat-lying turbidites that form an abyssal plain seaward of the lower continental rise. The turbidites interfinger with and lap landward onto underlying fan Sequence E. Thus the base of the sequence is time-transgressive, becoming younger landward. Within the turbidites, it is common to observe chaotic beds up to ~0.1 s thick and extending for many tens of kilometers. These appear to be debris flows that originated on the continental rise fan. The predicted age of the turbidities is late Pliocene to Quaternary.

## Leg 210 Objectives

Drilling objectives for Leg 210 were twofold. The primary objective was to sample the deep sedimentary structure and basement in order to investigate early rift development. A related objective was to study the shallower stratigraphy and to elucidate the postrift sedimentation processes and paleoceanographic history of this gateway between the North Atlantic and the sub-Arctic sea. The background for each of these objectives is summarized below.

### Origin of Transitional Crust

Drilling results from the Iberia margin and geophysical data from both sides of the Newfoundland–Iberia rift show clearly that the rift was characterized by very limited volcanism, that there are marked asymmetries between margin conjugates, and that there is significant structural variability along strike between rift segments. These features are particularly manifested in the transition zones between known continental and known oceanic crust on the opposing margins. We have posed three hypotheses to explain the crustal structure and basal stratigraphy in the Newfoundland and Iberia transition zones and the cross-rift asymmetries between these zones (e.g., Tucholke et al., 1999) (Fig. F11). Leg 210 provided the first direct test of these hypotheses by drilling in the transition zone along transect 2 on the Newfoundland margin (Figs. F3, F4, F7, F8B).

#### ***Hypothesis 1: Newfoundland Transition Zone Is Highly Thinned Continental Crust***

Newfoundland transitional crust is shallower and has less roughness than Iberia crust, and it could be the upper plate in an asymmetric detachment system (Fig. F11B). According to this hypothesis, the lower Iberia plate east of Anomaly ~M3 would be exhumed lower continental crust and mantle (e.g., Whitmarsh et al., 2001). Strong thinning of the Newfoundland crust without significant brittle extension might be possible if the lower crust thinned by ductile flow (e.g., Driscoll and Karner, 1998) (Fig. F11). This should be reflected in rapid synrift subsidence of the Newfoundland basement. If U corresponded to a subaerially eroded unconformity, the rapid subsidence would be recorded in the sedimentary section above the reflection.

There are two other possible explanations of U. One is that it corresponds to the top of basalt flows emplaced either subaerially (i.e., it is synrift on continental crust) or on the seafloor (Enachescu, 1988). If melt was extracted from the rising lower plate and emplaced in the Newfoundland upper plate (see, e.g., Fig. F11C), the exhumed Iberia mantle could be virtually melt-free, as has been suggested by existing Iberia drilling (Whitmarsh and Sawyer, 1996). Although it seems unlikely that smooth basalt flows could be as widespread as is indicated by the distribution of U, there are documented instances where such flows are known to be extensive (e.g., Larson and Schlanger, 1981; Driscoll and Diebold, 1999).

Another explanation is that U corresponds to the top of high-velocity sedimentary deposits that were shed from the Grand Banks, probably in Early Cretaceous time. As already noted, this sequence could be similar to the Aptian fan deposits recorded on the conjugate Iberia margin, although the stronger seismic signature on the Newfoundland margin suggests much higher-velocity beds that possibly are very coarse grained or carbonate rich.

#### ***Hypothesis 2: Transition Zones Reflect Extreme Extension in an Amagmatic Rift***

According to this hypothesis, continental extension proceeded under nearly amagmatic conditions to a state where only mantle was exposed, and at some point an asymmetric shear developed within the exposed mantle (Fig. F11C). This hypothesis differs from the one above in that Newfoundland transitional

crust would be exhumed, probably serpentinized mantle. U could not correspond to a subaerial unconformity because it would be impossible to uplift extending mantle to sea level. The U–basement interval could correlate with basalt flows, with melt generated from the rising lower plate in an asymmetric extensional system, or it could be high-velocity sedimentary beds, as noted above.

***Hypothesis 3: Newfoundland Transitional Crust Was Formed by Ultra-Slow Seafloor Spreading***

Slow seafloor spreading (Fig. F11D) is known to expose lower crust and mantle (e.g., in the Labrador Sea [Chian and Loudon, 1995; Osler and Loudon, 1995]), and it could explain the transitional crust in the Newfoundland Basin. However, symmetrical ultra-slow seafloor spreading in the rift seems unlikely because it does not explain the extensive mantle exposures off Iberia, nor does it explain the asymmetries in crustal structure and depth between the conjugate transition zones. It is possible that extension first exposed mantle in the rift, that ultra-slow seafloor spreading then occurred on the Newfoundland side of the rift, and that this ocean crust was then isolated on the Newfoundland margin by an eastward jump of the spreading axis (Fig. F11D). This hypothesis precludes U from corresponding to a subaerial unconformity because it would overlie thin ocean crust. As in the above hypotheses, U might correlate with either basalt flows or the top of high-velocity sedimentary beds.

**Sedimentary History and Paleooceanography**

Rifting between Labrador and Greenland, and between Greenland and Eurasia (Rockall Trough), began in the Early Cretaceous, leading to Late Cretaceous seafloor spreading in the Labrador Sea and Paleocene spreading east of Greenland (e.g., Srivastava and Roest, 1999; Eldholm et al., 1990). The Newfoundland–Iberia rift was a gateway between the main North Atlantic and these developing ocean basins, so it is in a key position to investigate sedimentary history and paleooceanographic links through the northward-expanding ocean basins.

Two features of the predicted sedimentary record above U were of particular interest during Leg 210. The main basin of the adjacent North Atlantic was accumulating black shales of the Hatteras Formation in Barremian–Cenomanian time, followed by deposition of the Plantagenet Formation under oxygenated seafloor conditions in the Late Cretaceous (Jansa et al., 1979). The Newfoundland Basin Cretaceous sedimentary record provided an opportunity to examine whether this record of reduced and then increased ventilation of the deep basin extended northward into the developing ocean basins, as well as information on the timing of that record. It also provided important information on paleobiogeography in a zone where Tethyan and boreal flora and fauna were expected to have mixed.

The second feature of interest was the upper Eocene–lower Oligocene sedimentary record, which could contain important information on the first development of strong abyssal circulation in the North Atlantic. As already noted, the source of the bottom water for this developing circulation has been interpreted to be the sub-Arctic seas and the timing has been estimated as latest Eocene to early Oligocene (Miller and Tucholke, 1983; Davies et al., 2001). However, these predictions are based largely on the occurrences of hiatuses in boreholes farther south in the North Atlantic, and the lack of sedimentary records in the critical intervals there makes it difficult to verify the predictions. New data from the gateway region could help to constrain the source and timing of the circulation event.

**Drilling Strategy**

The most direct and productive method to test our hypotheses about basement structure and the deep reflection sequence in the Newfoundland transition zone was to drill a deep hole (up to ~2200 m) into

that zone. Such a hole would also recover an expanded Cretaceous and Tertiary sedimentary record with which to investigate the paleoceanographic history in this gateway between the sub-Arctic seas and the main North Atlantic Basin. The prime site that was selected to accomplish these objectives is proposed Site NNB01A (Site 1276), located in the westernmost edge of the abyssal plain at the foot of the Newfoundland continental rise. In the event that our basement and deep sedimentary objectives could not be achieved at this site and sufficient drilling time remained during Leg 210, we also developed a series of alternate sites that extend seaward to known oceanic crust that could be drilled in order to partially satisfy our objectives.

Depths of major seismic horizons, including basement, were predicted from semblance velocity analysis of multichannel seismic reflection data obtained along the drilling transect during the SCREECH site survey program in 2000. This analysis indicated that the major drilling objectives at proposed Site NNB01A (i.e., U and basement) were at depths of ~1860 and 2080 meters below seafloor (mbsf), respectively (Table T1). Sampling to these great depths in one drilling leg was considered to be an ambitious goal, but the objectives were deemed to be achievable by following a plan of drilling, casing, and logging the hole as shown in Figure F12. To improve our chances of meeting the objectives within the time available for drilling, it was agreed that the upper 800 m of the hole would be drilled without coring. Thus, we expected that the first sediments recovered from the hole would be of Oligocene age, above Horizon A<sup>u</sup>.

Actual hole conditions and time constraints necessitated modification of this plan in real time during Leg 210. Nonetheless, we were able to follow part of the drilling and casing plan at proposed Site NNB01A (Site 1276) (Fig. F32), and we achieved a significant part of our objectives. In addition, we drilled a short hole ~95 m into basement at proposed alternate Site NNB04A (Site 1277). Results of both sites are summarized below.

## **SITE 1276 SYNTHESIS**

### **Lithostratigraphy**

Coring at Site 1276 started at ~800 mbsf. Recovery was excellent throughout the entire cored interval, averaging 85% and approaching or exceeding 100% for many cores. Five lithologic units are recognized (Fig. F13), ranging in age from Albian–uppermost Aptian(?) to Eocene. The units are defined primarily by the proportions of sediment types, sedimentary facies, and mineralogy of detrital and biogenic components. The sedimentary succession consists mainly of background hemipelagic mudrocks (bioturbated claystone and mudstone) with interbedded gravity flow deposits that vary from minor in some intervals to dominant in others. For example, Unit 2 and Subunits 5A and 5C are largely gravity flow deposits, whereas Subunit 5B is primarily hemipelagic mudstones and claystones. An exception to this general organization is Unit 4, in which the reddish brown, intensely burrowed muddy sandstones that occur (Fig. F14) are inferred to have been reworked by bottom currents on a well-oxygenated seafloor.

Gravity flow deposits show remarkable variability. They include the deposits of debris flows (Figs. F15, F16), low-density turbidity currents (Fig. F17), and mud-laden, viscous gravity flows that formed spectacular contorted structures in many beds (Figs. F18, F19). Texturally, the gravity-flow deposits range from siliciclastic mudrocks, siltstones, and sandstones to carbonate grainstones and marlstones. The sand fraction in these sediments is mainly (a) quartz, feldspar, mica, and rock fragments derived from metamorphic and plutonic source rocks; (b) recycled carbonate components derived from unlithified to loosely consolidated outer-shelf to slope sediments; (c) contemporaneous biogenic components; and (d)

minor ash (e.g., in the mid-Paleocene). Bioclasts include benthic and planktonic foraminifers, red algae, bryozoans, mollusk fragments, and echinoderms. Other locally common particles include carbonate intraclasts and glauconite pellets. With rare exceptions, only the gravity flow deposits contain significant biogenic carbonate. This consists of bioclasts in grainstones and nannofossils in mudstones and marlstones. Most of the interbedded hemipelagic sediments are noncalcareous, reflecting deposition mainly below the calcite compensation depth (CCD).

Diagenesis is moderate throughout the succession, with minor mobilization and precipitation of silica in Units 1 through 3 and common carbonate cementation of grainstones, sandstones, and siltstones in Units 2 through 5. Authigenic siderite and dolomite form many concretionary bands and nodules in the hemipelagic mudrocks of Subunit 5B. Downhole changes in clay mineral assemblages, from mostly illite-smectite in Unit 1 through Subunit 5A to kaolinite-chlorite below Subunit 5A, are attributed to paleoenvironmental changes rather than to burial diagenesis.

Subunit 5C is intruded by two major diabase sills that locally altered and contact-metamorphosed their host sediments (Fig. F20). The remainder of the Albian–Turonian Unit 5 is very thick (>700 m). In addition to gravity flow deposits, it is characterized by ~5% finely laminated, organic-rich calcareous claystones to marlstones (“black shales”) (Fig. F21) with total organic carbon (TOC) reaching ~10 wt% in some beds. The carbonate is mainly in the form of nannofossils. These laminites record times of enhanced input of mostly terrestrial organic matter under low oxygen conditions, with the notable exception of Ocean Anoxic Event (OAE) 2 (Cenomanian/Turonian), which contains significant amounts of marine organic matter.

Cored sediments at Site 1276 record postrift burial of irregular basement topography. Accumulation rate was rapid during the Albian to Turonian (maximum = ~100 m/m.y.) but then dropped steeply to <15 m/m.y. thereafter (Fig. F24). The Albian sediment influx is attributed to enhanced continental weathering in a warm humid climate, possibly accentuated by clastic input from active rifts farther north. After initial accumulation in a restricted ocean basin (i.e., black shale deposition), Site 1276 experienced a pulse of bottom-current reworking during the Turonian–Santonian that is inferred to originate from the establishment of a deep-ocean connection between the North and South Atlantic; the effect may have extended into the nascent Labrador Sea.

A hiatus in the middle Eocene at the boundary of Units 1 and 2 correlates with a discontinuity in the seismic reflection record that separates parallel reflections below from large sedimentary waveforms above. This may mark the initiation of strong abyssal circulation along the foot of the Newfoundland margin, correlative with Horizon A<sup>u</sup> in the western North Atlantic.

The Albian–Eocene succession at Site 1276 has stratigraphic and facies similarities with DSDP and ODP sites in the western North Atlantic (Fig. F22) and on the conjugate Iberia margin. For example, dark-colored, locally carbon-rich mudrocks in the Albian–Turonian interval at Site 1276 are like those of the Barremian–Cenomanian Hatteras Formation. Also, the younger parts of the Site 1276 succession are comparable to the Plantagenet, Bermuda Rise, and Blake Ridge formations. Site 398 on the conjugate continental margin off Iberia is similar but contains significant nannofossil-rich sediment, indicating that it was above the CCD from the Campanian to early Oligocene.

### **Igneous and Metamorphic Petrology**

One of the major discoveries at Site 1276 was two diabase sills emplaced within lower Albian sediments, 100–200 m above basement as estimated from seismic reflection data. The upper sill is ~100 m thick, and the lower sill, which was not fully penetrated, is thicker than 10 m. Indirect constraints suggest

emplacement soon after sediment deposition and at a very shallow level beneath the seafloor. These constraints are (1) the occurrence of vesicles in the sill, (2) the growth of porphyroblastic calcite occurring in contact metamorphosed sediments and predating compaction of these sediments, and (3) compaction folding of a calcite vein that was emplaced vertically in the sediments probably at the time of intrusion. The sills preserve chilled margins, and toward their centers they show an increase in average crystal size and a change of magmatic textures from predominantly interstitial to subophitic or ophitic (Fig. 23). Sill/sediment contacts preserve a thermal overprint marked by color changes, recrystallization processes, and very high reflectance of organic matter.

The sills are predominantly aphyric diabase, composed of primary plagioclase (40%–60%), pyroxene (10%–30%), magnetite (<5%), olivine (<5%), and glass (<20%). More differentiated rocks occur in segregation bands (e.g., sample 4i in Fig. F23) that form <5% of the rocks in the sills. Hydrothermal alteration in the sills ranges from high to complete at the margins to moderate toward the centers (see the alteration column in Fig. F23). The diabases are silica-poor basanites, with SiO<sub>2</sub> values that range from 40 to 46 wt% and follow an alkaline differentiation trend. Samples taken from less altered parts of the sill show surprisingly coherent patterns for elements like K<sub>2</sub>O, NaO<sub>2</sub>, and CaO, assuming that the sills preserve their initial magmatic signature. Future petrological, geochemical, and age-dating studies of these rocks are expected to provide further information on the nature and evolution of the mantle source underlying the Newfoundland margin, as well as on the age of emplacement.

### **Biostratigraphy**

Paleogene and Cretaceous sediments cored at Site 1276 were deposited in abyssal depths (>2000 m) below the CCD. Hence, calcareous microfossil assemblages, particularly the planktonic foraminifers, were severely affected by dissolution in most intervals of Site 1276. High-resolution biostratigraphic analysis will ultimately depend on full integration of organic walled microfossils (palynomorphs: dinocysts, spores, and pollen), calcareous plankton (calcareous nannofossils and planktonic foraminifers), and siliceous microfossils (radiolarians). In situ agglutinated and redeposited calcareous benthic foraminifers also provide both a biostratigraphic and paleoenvironmental assessment of the deep western North Atlantic and the adjacent Newfoundland continental margin. Shipboard analysis of these varied microfossil groups provided a robust model of age vs. depth in the hole, as well as important insights into the changing paleoceanographic and depositional conditions during latest Aptian(?)–early Albian to early Oligocene time.

Calcareous nannofossils provided excellent biostratigraphic control for most of the section, and planktonic foraminifers preserved in turbiditic sandstones proved helpful in refining that biostratigraphy. Palynomorphs provided a critical component for biostratigraphic age control in carbonate-free intervals. Calcareous benthic foraminifers indicated changes in the source areas for the turbidites cored at Site 1276. Reworking is a constant component in assemblages of all fossil groups, rendering the use of last occurrence datums problematic, particularly in the Paleogene section where reworking of older material is pervasive. On the other hand, a uniform age progression of the samples and minimal reworking of older material in the Cretaceous section indicates that redepositional processes appear to have been largely penecontemporaneous.

### **Age-Depth Model for Site 1276 and Comparison to the Iberian Margin (DSDP Site 398)**

The age-depth model reveals marked changes in sedimentation rate, including at least one unconformity and two condensed intervals (see Fig. F24 for calculated sedimentation rates). The changes

in slope correspond closely to lithologic unit boundaries. An unconformity marks the boundary between lithologic Units 1 and 2 based on palynomorph and nannoplankton data. The hiatus at this level indicates similarities in rift-wide sedimentation patterns when one considers results from studies on Sites 398, 900, 1067, 1068, and 1069 on the conjugate Iberian margin (McGonigal and Wise, 2001). Over the full stratigraphic section, comparison of the sedimentation rate at Site 1276 with that at Site 398 shows striking similarity not only in the positions of hiatuses or condensed intervals, but also in overall sedimentation rate (Fig. F24).

### **Abyssal Paleoceanography and History of the CCD**

The paleoceanographic history of the opening of the North Atlantic is documented in the faunal composition of benthic foraminifers recovered at Site 1276. Exceptionally well preserved autochthonous deepwater agglutinated foraminifers (e.g., Kuhnt and Urquhart, 2001) throughout most of the sedimentary sequence imply that Site 1276 has remained at abyssal depths (>2000 m) since at least latest Aptian(?)–early Albian time. Times of possible depression of the CCD are recognized in the late Albian, late Campanian, latest Maastrichtian, and late Paleocene.

### **Paleoceanography and Paleoenvironment**

All microfossil groups examined indicate that Site 1276 was influenced by transitional surface water masses during much of the Cretaceous and early Paleogene. This is suggested by the presence of select Boreal taxa and the absence or paucity of key Tethyan taxa. Hence, these taxa will be invaluable in determining oceanographic communication routes between the northwestern Atlantic, Tethys, and eastern Atlantic.

Although many of the sediments recovered are barren of calcareous fossils, debris flows and turbidites brought in more well preserved assemblages. Specifically, in the Paleocene and Eocene sections many debris flows contain robust assemblages of shallow-water origin, including calcareous benthic foraminifers indicating a neritic facies and abundant holococcoliths not generally preserved in deepwater sections. These taxa can provide insights into the paleoceanographic history of the nearby shallow-water areas. These allochthonous faunas indicate original depositional environments, together with the provenance of turbiditic packages and the timing of climatic change and/or tectonic disturbance.

For the extended Albian–Turonian section of Site 1276, palynological data indicate a strong terrestrial influence, which is documented by very high amounts of terrigenous organic matter. There is an overall trend toward a downhole increase of terrestrial influence. Samples from Albian black mudstones seem to be characterized by especially high amounts of terrestrial palynoclasts and sporomorphs. This is tentatively interpreted to indicate an accelerated hydrological cycle during the time of black mudstone deposition.

### **Critical Events**

A series of “critical events” in Earth’s history were cored at Site 1276. The recovered records are affected by abyssal burial depths below the CCD and by frequent turbidites, which make lithologic and microfossil information discontinuous. Nevertheless, the integrated results from the different microfossil groups, together with chemical and sedimentologic data, provide a preliminary documentation of the stratigraphy and environmental conditions during these intervals.

### ***Paleocene/Eocene Boundary***

Worldwide, uppermost Paleocene marine sections are characterized by a sudden shift from carbonate-marl deposition to clayey, calcite-free deposition. The Paleocene/Eocene boundary interval is also characterized by an abrupt worldwide warming event referred to as the Paleocene/Eocene Thermal Maximum (PETM). In addition to the dissolution interval, the Paleocene–Eocene transition in the oceanic sedimentary record is also distinguished by a sharp negative  $\delta^{13}\text{C}$  excursion and by a benthic foraminiferal extinction event (Zachos et al., 1993; Thomas and Shackleton, 1996). The widespread pattern of decreased carbonate content is consistent with the hypothesis of a massive methane flux in the ocean-atmosphere inorganic carbon reservoir, which caused a short-term “super greenhouse” event (Dickens et al., 1997).

A nearly complete uppermost Paleocene to lower Eocene section is present at Site 1276. Even though the specific clay boundary layer is missing, probably due to incomplete core recovery, a complete succession of the calcareous nannofossil events occurring immediately above the boundary clay layer is recognized in Cores 210-1276A-13R and 14R. At the Paleocene–Eocene transition, the calcareous nanoplankton community shows a great turnover characterized by peculiar biotic changes (Bralower et al., 1995; Angori and Monechi, 1996), which are recognized at Site 1276. This material is sufficiently well preserved to document a detailed biostratigraphic and evolutionary history of this fossil group, which can then be compared with other sections of the Atlantic domain in the framework of biochronological and paleoenvironmental changes associated with the PETM.

### ***Cretaceous/Tertiary Boundary***

The Cretaceous/Tertiary (K/T) boundary records one of the most catastrophic perturbations to the Earth’s biosphere and coupled ocean-climate system. A wealth of ODP research has provided data on the link between the K/T boundary mass extinction and a large-body impact on the Yucatan Peninsula. The Caribbean and North Atlantic sections are crucial to understand not only the marine biotic response to this event, but also to document disruption of the stratigraphic record as a consequence of the impact.

One of the few nearly complete upper Maastrichtian to lower Danian abyssal sections was recovered at Site 1276. Extensive reworking and frequent carbonate-free sediments prevent this section from being suitable for analyzing extinction processes, but the succession of biotic changes is obvious. The sequence includes a sharp increase of calcareous dinoflagellates (“*Thoracosphaera* bloom?”) and an increase in Cretaceous survivor species, followed by blooms of dwarf earliest Danian species (“dwarf *Biscutum* bloom;” Gardin and Monechi, 1998). Penecontemporaneous reworking of planktonic foraminifers preserved in turbiditic sandstones provide an additional record of biotic extinction and recovery including an interval characterized by Cretaceous survivors (*Guembelitra*), together with earliest Danian species (*Parvulorugoglobigerina eugubina*, *Woodringina* sp.) and *Thoracosphaera*. The high sedimentation rates in the early Paleocene allow good resolution to study biotic recovery following the impact.

### ***Oceanic Anoxic Events***

Oceanic Anoxic Events were short-lived episodes of widespread organic carbon burial, typically coupled with rapid changes in the ocean-climate system and marine biosphere. These perturbations in the global carbon cycle occurred during times of elevated tectonic activity, high global sea level, and generally warm climates of the mid- to Late Cretaceous (Leckie et al., 2002). A thick interval of gray to olive-black mudrocks was cored at Site 1276 (lithologic Unit 5). Much of the organic matter preserved in these hemipelagic and turbiditic sediments is likely of terrigenous origin, based on preliminary geochemical analyses and the preponderance of terrestrial organic matter observed in foraminiferal and palynomorph preparations. However, within Subunits 5A and 5C, there are several thin intervals characterized by

laminated black shale, high TOC contents (3–7 wt%), and hydrogen index (HI) values (231–452 mg HC/g TOC) characteristic of marine algal organic matter. The black shales in Core 210-1276A-31R correlate with the latest Cenomanian–earliest Turonian OAE 2 (“Bonarelli” event). OAE 2 is one of the most widespread black shale events recognized in the marine record. It represents a time of enhanced productivity, perhaps triggered by tectonic activity or changes in ocean circulation. Black shale in Core 210-1276A-94R is potentially correlated with OAE 1b (“Paquier” event). A black shale in Core 210-1276A-98R, bounded by bioturbated sediments and located 8 cm above the lower sill cored at Site 1276, has yielded only strongly thermally altered palynoclasts.

## **Paleomagnetism**

Paleomagnetic studies consisted of routine measurements of natural remanent magnetization (NRM) and magnetic susceptibility of archive-half split cores of recovered sediments and rocks. Paleomagnetic data obtained from Site 1276 samples exhibit considerable variations in demagnetization behavior among various lithologies, and only one magnetic reversal was detected in the entire hole.

In the lower Oligocene–middle Eocene cores in lithologic Unit 1, varicolored mudstone and claystone have low NRM intensity and low magnetic susceptibility. A few discrete peaks of higher NRM and susceptibility values could in some cases be tied directly to visible presence of pyrite. Although the NRM intensity of the middle Eocene–upper Paleocene sediments in lithologic Unit 2 was also low, we were able to define the characteristic remanent magnetization (ChRM) direction from a few intact cores. Both magnetic susceptibility and NRM intensity records show an anomalous peak at approximately the lower/upper Paleocene boundary. Lower Paleocene–upper Campanian lithologic Unit 3 has relatively high NRM intensity and magnetic susceptibility; it is caused by the presence of numerous dark burrowed beds that have relatively high concentrations of magnetic minerals. NRM intensity and magnetic susceptibility for lithologic Unit 4 are relatively high, perhaps because of the presence of fine-grained iron oxides. A strong drilling-induced overprint is present throughout this unit, which severely limits paleomagnetic work. Sedimentary cores from lithologic Unit 5 consist of lower Turonian to Albian–uppermost Aptian(?) claystones and mudstones that have low NRM intensity and low magnetic susceptibility. There are more significant variations in susceptibility within lithologic Unit 5 than in lithologic Unit 4. Characteristic susceptibility peaks reflect carbonate and sandstone layers, and troughs correspond to green and gray claystones and mudstones. The susceptibility peaks correlating with the carbonates may reflect an iron component in these rocks, most likely in siderite.

Drilling in Subunit 5C recovered two diabase sills. The inclinations of the ChRM direction for these sills are all positive. The simplest explanation of the positive inclinations is that they represent normal polarity magnetization, probably acquired within the Cretaceous Normal Superchron. Significant changes in inclination and intensity values within the upper sill suggest that it may contain two intrusive units.

In order to test the archive-half data and to identify magnetic carriers in sediments of this hole, selected discrete samples from the five different lithologic units were demagnetized with stepwise alternating fields or were thermally demagnetized. Most samples show unblocking temperatures between 350°–550°C, indicating that titanomagnetites are the likely magnetic carriers in these samples. Results from discrete sample measurements confirm the pass-through observation that no reversed magnetization polarity is present in these cores.

Time-series analysis was conducted on magnetic susceptibility and natural gamma ray data for several pelagic marlstone cores in lithologic Unit 5, with the goal of identifying paleoclimatic cycles driven by changes in the Earth’s orbit (Milankovitch cycles). Preliminary results are encouraging, and they

demonstrate that certain Leg 210 cores seem to be suitable for magnetic detection and extraction of climatic cycles and sedimentary changes in the Cretaceous.

### **Geochemistry**

At Site 1276 an extensive Albian–Cenomanian black shale/mudstone sequence was cored. This lithologic unit (Unit 5) extends for >700 m (1064.24–1719.40 mbsf). It is characterized by moderately enriched TOC contents (mostly <2 wt%) (Fig. F25). This turbidite-dominated sequence shows low hydrogen index values (HI < 100 mg HC/g TOC) and C/N ratios averaging ~20 (Fig. F25), suggesting a strong influence of terrestrially derived organic matter. A positive correlation between C/N ratios and TOC contents supports the importance of a terrigenous contribution to the sedimentary organic matter.  $T_{\max}$  values ranging between 435° and 470°C could indicate that kerogen present in the sediments may be derived mainly from reworked, preheated terrestrial components (Wagner and Pletsch, 2001). Higher values of Ni/Al ratios in Unit 5 confirm the importance of anoxia, and therefore preservation, in the accumulation of organic matter throughout the sequence.

Headspace methane ( $C_1$ ) concentrations start to increase above background levels downhole only at a depth of 1140 mbsf in lithologic Subunit 5B (Fig. F25). In Unit 5, a possible weak correlation exists between higher organic carbon percentages and higher methane concentrations, suggesting that the concentration of organic matter may play a role in the generation of methane.  $C_1$  concentrations increase dramatically immediately below the upper diabase sill (Subunit 5C1; 1624.01 mbsf) and particularly in Cores 210-1276A-96R and 97R (1692.33–1703.5 mbsf) above the lower sill. These latter increases correspond to layers of anomalously underconsolidated high-porosity clays. Here, the methane concentrations are directly linked to the lithology of the formation; the sills probably formed seals and prevented gas and interstitial water from escaping. Low  $C_1/C_2$  ratios and the presence, but small concentrations, of longer-chain volatile hydrocarbons in the deeper part of the hole, indicate that some thermogenically derived gas is present; it could have either migrated to this location or been generated in situ.

### **Oceanic Anoxic Events**

Within lithologic Unit 5, six sedimentary intervals have high TOC contents, in several instances coupled with high HI (characteristic of marine derived organic matter) and high  $S_2$ , and they may record oceanic anoxic events.

The top of lithologic Subunit 5A (Cores 210-1276A-30R and 31R) is upper Cenomanian–lowermost Turonian and it likely corresponds to the “Bonarelli” event, OAE 2. Core 210-1276A-33R (middle of Subunit 5A) probably represents the “mid-Cenomanian event” (Leckie et al., 2002). In lithologic Subunit 5B, Core 210-1276A-55R (characterized by terrestrially derived kerogen) may correspond to OAE 1c. The bottom of Subunit 5B (Core 210-1276A-73R) does not correspond to any of the known OAEs; however, it has the potential to represent an OAE-type layer. The top of Subunit 5B (Cores 210-1276A-42R to 44R) is late Albian and may correspond to OAE 1d, dominated by terrigenous organic matter (Leckie et al., 2002). Core 210-1276A-94R, in the middle of lithologic Subunit 5C is lower Albian and it might represent the “Paquier” event, OAE 1b.

## Physical Properties

Leg 210 physical property data for rocks and sediments include measurements of seismic velocity, density, porosity, natural gamma radiation (NGR), magnetic susceptibility, and thermal conductivity. Such data are a critical component for seismic stratigraphic studies and for understanding the complex physical and chemical processes responsible for the development of rift systems and passive margin sedimentation. At Site 1276, an excellent physical property data set was facilitated by very high core recovery through ~930 m of section. NGR, vertical velocity, bulk density, and porosity profiles are presented for Site 1276 in Figure F26. The data are color-coded to indicate lithology as defined from the barrel sheets, allowing assessment of sedimentary facies control on physical properties behavior of sediments and rocks. We are hoping that this type of display becomes standard procedure on future Integrated Ocean Drilling Program (IODP) legs.

Bulk density and porosity mirror one another downhole, with bulk density increasing from ~1.9 to 2.3 g/cm<sup>3</sup> and porosity decreasing from ~50% to 20%. These trends result from the progressive mechanical reduction of void space with increasing burial depth. Abrupt variations in the general density and porosity trend correlate well with lithologic unit boundaries. High-density and low-porosity outliers tend to be associated with siderite-enriched carbonate concretions and grainstone and sandstone cementation. In marked contrast, a relatively thick zone of low density and high porosity at ~1690 mbsf defines a zone of undercompacted and low-density plastic mudstones.

Vertical (*z*-) velocity generally increases downhole from 1900 to 2600 m/s, and it is apparently insensitive to gross lithologic variations (Fig. F26). Rather, the velocity trend appears to be primarily a function of bulk density and porosity. Numerous high-velocity outliers exist, however, and they invariably relate to zones of increased cementation (both siliceous and carbonate cements) and zones of siderite precipitation. Low-velocity outliers (1650–1800 m/s) correlate with a zone of undercompacted, low-density mudstones between 1690 and 1710 mbsf.

The NGR profile shows a general increase downhole, with several large spikes that tie closely to lithologic unit boundaries. In general, NGR reflects changes in the relative amounts of sand (low NGR) and terrigenous clays (high NGR). The observed general decrease of NGR uphole may reflect the progressive increase of paleowater depth following rifting and breakup of the region, and thus the slow transition from terrigenous to pelagic sedimentation. This regional trend should be punctuated by eustatically enhanced sediment delivery to the deep basins.

### Undercompacted Systems: High-Porosity and Low-Velocity Mudstones

From 1690 to 1710 mbsf, a zone of mudstones and calcareous mudstones have unusually high porosities (27%–39%) and low velocities (1690–1960 m/s) for their depth of burial (Fig. F27). Furthermore, these sediments are very soft, with consistencies comparable to modeling clay. The porosity, velocity, density, and apparent plasticity of these mudstones are comparable to those of normally compacted sediments recovered higher in the section from 840 to 1020 mbsf (Fig. F27), and they clearly demonstrate that the sediments are significantly undercompacted with respect to their depth.

We surmise that the mechanical compaction of these mudstones was halted at a relatively shallow burial depth, perhaps related to the emplacement of two diabase sills, one above and one below the mudstones (Fig. F27). It is possible, but not necessary, that this interval was overpressured prior to Leg 210 drilling. Evidence of past fluid flow exists in the hydrothermally altered sediment immediately above the lower sill and underlying the undercompacted mudstones (Fig. F27). Furthermore, the highest measured concentration of hydrocarbons exists in this 20-m interval. Geochemical analysis measured C<sub>1</sub> (methane)

levels of nearly 19,000 ppm (Fig. F27), implying that fluids in this interval were trapped. This interval of section clearly was made incapable of normally compacting and expelling pore fluids, and perhaps it was sealed off due to the emplacement and effects of the bounding igneous intrusions.

## **SITE 1277 SYNTHESIS**

### **Lithostratigraphy**

Site 1277 was located on a basement ridge beneath thin sediment cover (Figs. F8B, F9). The main objective was to recover samples of basement, so the site was drilled without coring from 0 to 103.90 mbsf. It was predicted that the bit would be some tens of meters above the sediment-basement contact at that depth. During drilling, a “wash” core barrel was in place. When retrieved, this core barrel contained 2.29 m of fractured igneous rock and associated volcanoclastic sediments (Core 210-1277A-1W) that are indistinguishable from rock in the top of the next core, Core 2R. During drilling, hard zones were encountered at 85–89 and 97.5–100 mbsf. Thus, it is believed that recovery in Core 210-1277A-1W comes from depths between 85 and 103.90 mbsf, and the top of basement (Unit 1) is set at 85 mbsf.

Two lithologic units are recognized. Unit 1 is a succession of alternating basalt flows (~50%), coarse breccia units containing a wide variety of clasts of gabbro and serpentinite (~20%), and minor volcanoclastic and ferruginous sediments (~10%). There are also variably deformed gabbroic rocks (~20%). Interpreted depth of this unit is 85–142.10 mbsf. The principal characteristic of Unit 1 is that it is a sedimentary and volcanic succession. The sedimentary units are derived entirely from rock types characteristic of the underlying basement at this site.

Lithologic Unit 2 (142.18 mbsf to the bottom of the hole at 180.30 mbsf) consists almost entirely of tectonized, altered ultramafic rocks including harzburgite, dunite, and serpentinite mylonite. There is a gabbro cataclasite at the top of the unit. The entirety of Unit 2 is cut pervasively by secondary veins that record several stages of veining and mineral precipitation. Many of the smaller veins cutting the serpentinitized peridotite are composed of talc, magnetite, and calcite. There are no sediments or lavas in Unit 2 that would indicate proximity to the seafloor. The rocks are interpreted as mantle that was exposed by tectonic extension and that was associated with pervasive deformation and hydrothermal alteration. After their exhumation, these serpentinites were buried by the lavas, allochthonous debris, and coarse sediments of Unit 1. The allochthonous debris was shed from local seafloor topography along the crest of the basement ridge.

### **Biostratigraphy**

No shipboard biostratigraphic analysis was conducted on the few sedimentary rocks recovered at Site 1277 because no suitable materials were recovered.

### **Paleomagnetism**

We made pass-through magnetometer measurements and magnetic susceptibility measurements on all split-core archive sections at 2-cm intervals. To isolate the ChRM, cores were subjected to alternating-field demagnetization up to 60 mT. We analyzed the results in Zijderveld diagrams (Zijderveld, 1967) and calculated ChRM direction using principal component analysis (Kirschvink, 1980). We also determined magnetic susceptibility on all whole cores at 2.5-cm intervals as part of the multisensor track analysis, and

we measured split-core sections at 2-cm intervals with the point-susceptibility meter. No shipboard discrete samples were taken because of time constraints at the end of the leg.

Paleomagnetic data exhibit significant variations in demagnetization behavior among recovered lithologies. As at Site 1276, there was drilling-induced remagnetization, but it was reduced compared to Site 1276 sediments. Greenish volcanoclastic breccia in Core 210-1277A-2R has the lowest NRM intensity (~0.02–0.3 A/m), contrasting with relatively fresh aphyric basalt in Cores 1R and 3R (~1–4 A/m), gabbro in Cores 4R and 5R (0.5 A/m), and serpentinite in Core 9R (1–9 A/m). The basalts appear to record a stable component of magnetization with normal inclinations (~45°). The green breccia, on the other hand, displayed variable inclinations (from positive shallow to negative shallow). Gabbros and adjacent sediments have the same stable inclination values (~40°), similar to those of the basalt.

The serpentinitized peridotites in different parts of long, coherent core pieces in Core 210-1277A-9R showed ChRM inclinations that cluster around a mean of 40°, generally in agreement with inclinations in the basalt and gabbros. Because NRM intensities of the serpentinitized peridotites are on the order of 1–9 A/m, they could contribute significantly to the regional magnetic anomaly. There is a distinct difference between gabbro, with relatively low magnetic susceptibility and high median destructive field (MDF), and serpentinite, with high susceptibility and low MDF. This difference may be explained by either the finer grain size of the gabbros or their higher degree of low-temperature alteration, or both.

### **Geochemistry**

Because of time constraints at the end of the leg, no shipboard geochemical analyses were conducted on rocks from Site 1277.

### **Physical Properties**

Evaluation of physical properties at Site 1277 included nondestructive measurements of density, porosity, velocity, and thermal conductivity. Porosity varied between 2% and 25%, bulk densities varied between 2.0 and 3.8 g/cm<sup>3</sup>, and grain densities varied between 2.18 and 4.36 g/cm<sup>3</sup>. Compressional wave velocity varied between 3300 and 6300 m/s. Velocity was lowest in highly altered and veined breccias (Section 210-1277A-4R-2), and it was highest in a coarse-grained gabbro (Section 5R-3). Thermal conductivity ranged from 1.6 to 2.3 W/(m·K), with no obvious trend in the values.

## **COMPARISON OF SITE 1276 WITH IBERIA MARGIN STRATIGRAPHY**

It is instructive to compare seismic reflection profiles, lithologic units, and sediment accumulation patterns on the conjugate margins of the Newfoundland–Iberia rift. This is true particularly for the deepest parts of the sedimentary section, which were deposited at a time when the two margins were close to one another. For this comparison we consider Site 1276 and Site 398 (DSDP Leg 47B), drilled on continental crust of southern Galicia Bank on the Iberia margin (Fig. F28). This site has the most complete and expanded stratigraphic range of sediments among the Iberia margin sites. Other sites drilled during Legs 149 and 173 were on basement highs and did not penetrate significant sections of pre-Tertiary sediments. At the time of Anomaly M0 (Aptian; ~121 Ma), Sites 1276 and 398 were separated by only ~250 km (Fig. F3). The paleoceanographic environment in this young ocean basin should have been similar on both margins. Indeed, we observe comparable occurrences of mid-Cretaceous black shales and Upper Cretaceous red-brown and multicolored shales, although there are some significant differences in details

of sedimentary processes. Below, we summarize and compare principal features of the sedimentary sequences on the two margins.

### **Seismic and Sedimentary Succession at Site 1276**

Seismic sequences in the Newfoundland Basin around Site 1276, outlined more fully in “Geological Setting,” in “Introduction,” are summarized in Figure F29. The deepest sequence, A, is seismically laminated, flat-lying, and contains intervals with sufficiently high impedance contrasts that signal penetration to the underlying basement and appears to be limited. Its top is the flat, strong, basin-wide U reflection. The sequence covers and smooths the underlying basement topography, with its greatest thicknesses between underlying basement blocks (Fig. F10). Correlation of the exact top of the seismic sequence to Site 1276 borehole results is not certain. In one interpretation the upper of two diabase sills (at 1612 mbsf) correlates with U, and in an alternate interpretation the lower sill at 1705 mbsf is correlative. Both sills intruded into dark mudstones, siltstones, and sandstones of early Albian age (nannofossil biozone NC8a–NC8b).

Seismic Sequence B is not strongly laminated compared to the underlying interval. It correlates with dominantly green-gray to black claystones and mudstones, with variable amounts of siltstones and sandstones. The sediments were deposited in the lowermost Albian to upper Turonian.

The overlying seismic Sequence C is flat-lying and strongly reflective. It correlates with brown sandy mudstones, overlain by multicolored (e.g., brown, red, and gray green to black) hemipelagic claystones interrupted by frequent turbidites. The sediments are latest Turonian to middle Eocene in age.

Seismic Sequence D was sampled at Site 1276 only in its lower part, where it consists of middle Eocene to lower Oligocene(?) gray-green hemipelagic claystones and mudstones. Although the sequence shows distinct sediment waves in the landward seismic section (Figs. F8, F28), there is little indication of current-controlled deposition at Site 1276 and the section is dominated by turbidites and debris flow deposits.

Seismic Sequences E and F were not sampled during Leg 210, although they can reasonably be interpreted from their seismic signature. Sequence E is an abyssal fan marked by irregular reflections, poorly developed sediment waves, and local debris-filled channels. Sequence F is an abyssal plain with widespread planar reflections that are very characteristic of turbidite deposits. Both sequences record extensive downslope sedimentation during Oligocene to recent time. The Sequence F turbidites most likely are latest Pliocene and Quaternary.

### **Seismic and Sedimentary Succession at Site 398**

Site 398 was drilled at a depth of 3900 mbsf, ~20 km south of Vigo Seamount on the southern margin of Galicia Bank (Fig. F3A). The site is on thinned continental crust on the seaward side of Galicia Interior Basin and ~40 km north of the Leg 149/173 drilling transect. A representative MCS reflection profile extending northwest–southeast through the site (GP-19; Figs. F28, F29) displays a complete sedimentary sequence that shows little apparent interruption by unconformities or condensed sections.

Basement on profile GP-19 exhibits some coherent internal reflections and apparent fault blocks that appear to record tectonic extension of the continental crust (Figs. F28, F29). The overlying moderately smooth and seismically laminated seismic sequence is named acoustic Unit 4 (Groupe Galice, 1979), and it is capped by a moderately strong reflection termed the orange reflection. In the lowest part of the sequence, reflections are moderately conformable to basement and locally may diverge, but reflections in the upper part are unconformable and lap against the flanks of the fault blocks. This sequence was interpreted as being deposited during tilting of the fault blocks (Groupe Galice, 1979; Shipboard Scientific

Party, 1979), but the onlap relations indicate that at least the upper part of the sequence is postrift. Site 398 drilling results show that the sequence consists of thin sand-silt-clay graded beds that are interbedded with thick slumps or debris flows (Shipboard Scientific Party, 1979). The sequence is interpreted as an upward-fining set of abyssal fan deposits. Its top (orange reflection) appears to match a small stratigraphic gap at the Aptian/Albian boundary (Sigal, 1979). At its base is an interval of white indurated limestone and marlstone/siltstone of Hauterivian–Barremian age (Shipboard Scientific Party, 1979). This has been interpreted as part of the basement complex at Site 398.

A large set of MCS profiles in this area allows us to correlate acoustic Unit 4 from the thinned continental crust of Galicia Bank southward onto the transitional crust beneath the Iberia Abyssal Plain (Fig. F30). Mapped thickness patterns show that on Galicia Bank the sequence is deposited between north-south-oriented basement blocks that plunge to the south under the abyssal plain. Just south of the Leg 149/173 drilling transect, the surface of the sequence reaches across the tops of all these blocks. The sequence also thins toward the west, indicating a source of the clastic sediments along the shallow Iberia margin. It pinches out on crust of late Barremian age ~30 km west of ODP Site 1070.

The overlying acoustic Unit 3 is a weakly reflective layer in which faint, semicontinuous reflections are observed. It correlates with a series of dark gray to black laminated to homogeneous claystone and interbedded mudstone that includes black shale and calcareous mudstone overlain by nannofossil chalk and claystone. The sediments are lower Albian–lower Cenomanian.

Acoustic Unit 2 is flat-lying and highly stratified, and it consists of siliceous mudstone, red marly chalk, and brown, dark reddish, and reddish gray mudstone and claystone, predominantly massive and unborrowed. Ages of the sequence at Site 398 are Coniacian to early Eocene.

The shallowest acoustic Unit 1 is stratified in its lower part but has only weak reflections in its upper part. The lower part is marly nannofossil chalk, nannofossil chalk, and siliceous marly chalk, and the upper part is rhythmically bedded marly nannofossil ooze. Although the sequence locally is eroded away, apparently by bottom currents (Fig. F28), its internal reflections are flat-lying and show few if any signs of current-controlled erosion or deposition. Ages of the sequence range from middle Eocene to Quaternary.

### **Comparison of Seismic Sequences at Site 1276 and Site 398**

It is clear that there are significant similarities in the deeper parts of the seismic sections and in the correlative lithofacies of the conjugate Newfoundland and Iberia margins (Figs. F28, F29). These similarities persist up through seismic Sequence C on the Newfoundland margin and the correlative acoustic Unit 2 on the Iberia margin. They indicate that the two margins shared common depositional environments when the ocean basin was young and relatively narrow. At shallower levels in the sedimentary record the seismic signatures become significantly different, reflecting divergence in sedimentation patterns as the margins became more widely separated. We summarize this development below.

Basal seismic Sequence A off Newfoundland and acoustic Unit 4 on Galicia Bank show comparable seismic signatures. The age at the base of the sequence at Site 1276 is unknown, but it may be very similar to the Hauterivian age of basement limestones cored at Site 398. Magnetic anomalies M3 and M0 lie to the east of Site 1276. If the crust at the drill site is oceanic and we extrapolate a crustal age from these anomalies to the drill site (assuming constant spreading rate), the basement dates to ~126 Ma at the Hauterivian/Barremian boundary. Although the top of seismic Sequence A appears to be slightly younger than that of acoustic Unit 4 (lower Albian vs. Aptian/Albian boundary), depositional conditions were comparable on both margins. Dark-colored, low-carbonate hemipelagic sediments indicate that the basin

was a low-oxygen environment below the CCD, but sedimentation was dominated by turbidity currents and debris flows. Widespread dispersal of these flows across the basin floor accounts for the seismically laminated signature of the interval.

Newfoundland seismic Sequence B matches the seismic signature of Iberia acoustic Unit 3. The correlative sedimentary section on both margins is Albian to lower Cenomanian–upper Turonian gray-green and black shales, similar to the Hatteras Formation in the main North Atlantic Basin (Jansa et al., 1979). At Site 1276 these shales are hemipelagic through most of the section, with gravity-flow deposits being important at the top and base of the section. At Site 398 gravity-flow deposits are important at the top, but sediments are hemipelagic in the middle and mostly calcareous at the base. During the Albian–Turonian, the basin width increased from 600 to 1000 km. Nonetheless, the two margins show remarkable correspondence in sediment facies, and they also have very similar sediment accumulation patterns. Notably, there are high rates (to 55 m/m.y.) in the lower part of the section and somewhat reduced rates (to 18 m/m.y.) at the top of the section on both margins (Fig. F31). These correlations indicate that both margins provided similar source areas for sediment input to the deep basin. The deep seafloor was at least intermittently anoxic and was below the CCD.

In the Late Cretaceous (approximately Cenomanian–Campanian), both margins developed either hiatuses or had severely reduced sedimentation rates (Fig. F31). This condensed or missing record corresponds to the top of seismic Sequence B off Newfoundland, where truncations of reflections indicate that an unconformity is present. Similar truncation in the Iberia GP-19 seismic profile is not apparent, although a slight unconformity was identified on other profiles (Groupe Galice, 1979). This correlation between margins indicates a rift-wide event, possibly the development or invigoration of deep circulation that marked the end of significant black shale deposition. This is consistent with the presence of red and brown sediments deposited on a more oxygenated seafloor in the overlying section on both margins.

Similar seismic signatures between margins persist upward into seismic Sequence C off Newfoundland and acoustic Unit 2 off Iberia. Basin width increased from 1000 to 2000 km during this period (Turonian–middle Eocene). The sequences are red-brown mudstones on the Newfoundland margin and marly chinks on the Iberia margin, deposited under mostly oxygenated seafloor conditions. Turbidity currents delivered carbonate sediments to the deep seafloor in large quantities on the western side, but they mostly bypassed Site 398, where pelagic carbonates are abundant (50–60 wt%). Even so, sedimentation rates were similar (5.7 m/m.y.) on both margins. The difference in sedimentation processes at the two drill sites is not apparent in the seismic signature.

Beginning with the middle–late Eocene record, there is significant divergence in the seismic signature of sediments on the two margins. Newfoundland seismic Sequence D shows clear evidence of sediment waves developed by strong abyssal circulation, but there is no similar seismic signature on the Iberia side (Figs. F8A, F8B, F29). The reflection at the base of Newfoundland seismic Sequence D appears to correlate with an unconformity between lithologic Units 1 and 2 at Site 1276, and biostratigraphic data indicate a middle Eocene hiatus at this level (Fig. F31; see “Biostratigraphy,” in “Site 1276 Synthesis”). All these features indicate that the reflection may be equivalent to Horizon A<sup>u</sup> in the western North Atlantic, which marks the influx of cool bottom waters from the Norwegian-Greenland Sea and corresponds to initiation of strong abyssal circulation in the basin (e.g., Miller and Tucholke, 1983). Because of the Coriolis effect, the deep currents were primarily concentrated along the western boundaries of the ocean basins. Although the currents seem not to have affected the seismic architecture of the Iberia margin at Site 398, there is an indication of a short middle Eocene hiatus there (Fig. F31), so there may be some subtle erosion or attenuation of the sedimentary record.

The uppermost sedimentary sections on the opposing margins are markedly different in seismic character (Figs. F28, F29), and they clearly show a divergence in sedimentary processes during the late Cenozoic. As already noted, seismic Sequences E and F on the Newfoundland margin are dominated by downslope sedimentation. In contrast, acoustic Unit 1 around Site 398 is a less reflective sequence of largely pelagic sediments. It is clear that this southern part of Galicia Bank became progressively isolated from downslope sedimentation throughout the Cenozoic.

## **SUMMARY AND CONCLUSIONS**

### **Overview**

The prime drilling objectives of Leg 210 were to sample basement and facies corresponding to the overlying U reflection in the Newfoundland Basin, both of which were deep targets. Additional objectives included investigation of the Cretaceous paleoceanography of the Newfoundland–Iberia rift and the record of how abyssal circulation developed in Paleogene time through this gateway to the sub-Arctic and Arctic seas.

At our prime site, 1276, basement was estimated to be at 2080 mbsf and depth of U was estimated at 1866 mbsf. Drilling and coring to these depths presented considerable engineering and operational challenges, both expected and unexpected. We were able to follow our operational plan to case the hole at Site 1276 with both 20- and 16-in casing as planned (Fig. F12), but very tight hole conditions prevented us from installing liners to greater depths. Ultimately, these hole conditions also prevented us from logging the hole.

Despite these difficulties, drilling at Site 1276 was an outstanding success. We cored from 800 to 1736.9 mbsf with a remarkable average core recovery of 85%, and we obtained a detailed record of sedimentation from the time that the Newfoundland–Iberia rift was a very narrow ocean basin (latest Aptian[?] to earliest Albian) up to the early Oligocene. This record captures an extensive series of major oceanographic events that affected the expanding North Atlantic Ocean during this time period, and it allowed us to accomplish virtually all of our major paleoceanographic objectives.

Site 1276 bottomed in diabase sills that appear to have been intruded into lower Albian sediments at very shallow subbottom depths. These sills are estimated to lie only 100–200 m above basement, and it appears completely feasible that future drilling at this site can core to, and into, basement. The sills were intruded at the level of U, and this basin-wide horizon is interpreted to represent a combination of extensive gravity flow deposits and intrusive sills. The occurrence of the sills raises intriguing new questions about the magmatic history of the Newfoundland side of the rift and about its relation to the nonmagmatic exhumation of mantle on the conjugate Iberia margin.

With a few days remaining on Leg 210, we were able to drill at Site 1277, a shallow-penetration basement site ~40 km southeast of Site 1276 on presumed ocean crust. Here we recovered a unique assemblage of ~35 m of basalt flows interleaved with allochthonous slivers of gabbro, serpentinized peridotite, and fine- to coarse-grained sediments at the top of basement. These overlie at least ~45 m of serpentinized peridotite that appears to represent intact basement. The Site 1277 basement rocks record complex processes of magmatism, deep-crust and mantle exhumation, and mass wasting at the eastern margin of the Newfoundland transition zone, in ocean crust that probably accreted at very slow spreading rates.

## **Engineering and Drilling Challenges**

The hole at Site 1276 was cased to 750 mbsf, and the engineering plan was to extend casing liners to a depth as great as 2060 mbsf, just above projected basement depth (Fig. F12). Hole conditions below the casing, however, prevented liners from being installed. Tight spots at numerous intervals (see “Operations,”) indicated that the hole was persistently closing on the drill string, and it was clear that liner could not be forced into this section, even with predrilled, oversize hole. Engineering assessment is that, if drill-in casing had been available for this section, it most likely could have been successfully emplaced and latched into the reentry cone.

Tight spots in the (ultimately) 987 m of open hole below the casing slowed operations throughout the drilling, requiring frequent wiper trips to condition the hole as well as significant redrilling each time we tripped the pipe and reentered. This persistent hole closure also prevented lowering of logging tools, and we ultimately were unable to obtain any logs. Fortunately, the excellent core recovery allowed us to obtain an extensive set of laboratory physical property data that will be used for hole-seismic correlation and synthetic seismogram modeling.

Reentry was another significant operational challenge. Beginning with the first reentry, the reentry cone was found to be completely covered by sediment and its location could only be determined from an overlying craterlike depression in the seafloor. On a number of reentries, muddy water streaming from the crater largely obscured it, and reentry was accomplished only by careful tracking of the crater in both sonar images and in the very limited visual images. Currents presented an additional problem. Bottom currents at times appeared to approach 50 cm/s (estimated from the streaming sediment noted above), and this displaced the drill bit up to 75 m laterally from the location of the moonpool. The conventional assumption on reentry is that the drill bit is within a few meters to tens of meters directly below the ship, so this unexpected offset at one point caused a long search for the cone. We ultimately found the cone by working “upstream” along the trail of muddy water noted above. Subsequently, a transponder was placed on the vibration-isolated television (VIT) frame; this allowed us to track the location of the drill bit with respect to the cone, and it greatly facilitated further reentries.

## **Highlights of Scientific Results**

### **Site 1276**

#### ***Sills***

We drilled two sills, one at 1613–1623 mbsf and a second from 1719 mbsf to the bottom of the hole at 1737 mbsf (the sill base was not reached or recovered). These are alkaline diabases, tentatively identified as “basanites.” They were intruded at very shallow levels beneath the seafloor, in lowermost Albian to uppermost Aptian(?) sediments at or near the level of U. They exhibit chilled margins and they developed striking hydrothermal metamorphic effects in the enclosing sediments. It appears that the upper sill may have formed a seal over the underlying sediments, preventing them from becoming normally compacted and isolating fluids (including methane) in the section. Seismic signal reflection from the strong impedance contrasts created by these interbedded igneous and sedimentary rocks appears to explain the poor seismic signal penetration through U, and thus the typically poor reflection definition of underlying basement.

Careful examination of SCREECH site survey seismic reflection data indicates that U may be a double wavelet at Site 1276, and we infer that this character may be related to the presence of the sills. With further study, we identified similar double wavelets at or near U in seismic profiles from a number of

locations throughout the Newfoundland Basin. If, indeed, this is a signature characteristic of sills, then such sills may be a common feature in the basin. The double wavelets typically extend for a few kilometers or less, and many coincide with subtle disruptions of the underlying sub-U reflections or with basement highs. This subtle disruption appears to be present at Site 1276. Shore-based synthetic-seismogram studies will examine more closely how variations in sill thickness and spacing may affect the seismic signature in reflection profiles.

The source of magmatism that created the sills is presently unknown, and such magmatism certainly is unexpected considering the nonvolcanic nature of the conjugate transition zone crust off Iberia. A source (hotspot?) associated with development of the Newfoundland Seamounts ~180 km to the south seems to be unlikely, considering the basin-wide scattering of double wavelets (?sills) noted above. However, some kind of regional, postrift magmatic or thermal effect could help to explain the marked asymmetry of basement depth and roughness between the conjugate Newfoundland and Iberia margins (Fig. F4). Shore-based analysis of the Newfoundland Basin reflection data, together with synthetic seismogram modeling based on the Site 1276 physical property data, age dating, and geochemical analyses, are expected to provide significant insights into this issue.

### ***U Reflection***

Preliminary shipboard synthetic seismogram modeling and velocity-depth analysis indicate that U is at or near the top of the upper sill noted above. In the lithologic column this level is close to the top of extensive lower Albian sedimentary gravity flows. This is much like the Iberia margin where the orange reflection, coincident with uppermost Aptian fan deposits, lies at the top of a similar, although weaker, reflection sequence. Off Newfoundland, it is somewhat puzzling that there is not a stronger lithologic or physical property contrast at the top of the gravity flow deposits, in light of the fact that U is a very strong reflection throughout the basin. It seems very unlikely that the reflection is widely accentuated by intrusion of sills because the reflection covers a very large area (~600 km × ~150 km) and because its seismic signature is very regular, except for the scattered double wavelets noted above. New insights provided by future analysis of physical property results, however, may help to resolve this question.

### ***Black Shales and Oceanic Anoxic Events***

A greatly expanded sedimentary sequence of Cretaceous black shales, equivalent to the Hatteras Formation in the western North Atlantic, was cored at Site 1276. The sequence extends from the lowermost Albian, or possibly the uppermost Aptian, upward to the Cenomanian/Turonian boundary. It reflects deposition under relatively low oxygen conditions in the deep basin, probably punctuated by intervals of total anoxia. Various black, organic carbon-rich layers contain either terrestrial or marine carbon, or both, indicating that both sources intermittently created reducing conditions at and below the seafloor. There is an overall trend from strong input of terrestrial carbon in the lower part of the section to reduced input in the upper part. This correlates generally with relative abundance of gravity flow deposits derived from the shallow margin, which also decreases upsection. The trend probably reflects, at least in part, increasing sequestration of terrestrial debris on the continental shelf as sea level rose in the mid-Cretaceous.

Site 1276 recovered sediments that may include five major OAEs. These are the latest Cenomanian–earliest Turonian OAE 2 (“Bonarelli” event), the mid-Cenomanian event, and OAE 1b (“Paquier” event), OAE 1c, and OAE 1d in the Albian. In addition, one other, possibly new, Albian event is recognized from its characteristic black color coupled with high total organic carbon and related geochemical indicators (see “Geochemistry” and “Biostratigraphy,” both in “Site 1276 Synthesis”). Analysis of these sediments

will provide a rich data set to examine the paleoceanography of the Cretaceous North Atlantic Ocean as it expanded northward through the Newfoundland–Iberia rift.

Interestingly, similar dark sediments with locally black layers were recovered in parts of the uppermost Cretaceous and Paleocene section. This kind of occurrence has also been observed on the southern Bermuda Rise at Site 387 (Tucholke and Vogt, 1979), suggesting that low-oxygen conditions intermittently affected the North Atlantic at times well after the main episodes of anoxia that are documented in the OAEs.

### ***Upper Cretaceous Multicolored Mudstones***

Most Turonian and younger sediments are facies characterized by reddish, brown, green gray, and other light colors that indicate a well-oxygenated basin, in marked contrast to the underlying black shales. This change is well documented in the main North Atlantic Basin, where the multicolored sediments form the Plantagenet Formation (Jansa et al., 1979). The paleoceanographic change is thought to be associated with development of longitudinal deep circulation between the North and South Atlantic Oceans when these two oceans first became fully connected at abyssal depths near the end of Cenomanian time (Tucholke and Vogt, 1979). Documentation of this oceanographic change off Newfoundland indicates that the widening rift probably was connected to the main North Atlantic over full ocean depth.

### ***Cretaceous/Tertiary Boundary***

We recovered one of the few nearly complete upper Maastrichtian to lower Danian abyssal sedimentary sections across the K/T boundary at Site 1276. Extensive reworking and frequent carbonate-free sediments prevent this section from being suitable for analyzing processes of biotic extinction, but the succession of biotic changes is obvious. High sedimentation rates in the lower Paleocene section will facilitate high-resolution study of biotic recovery following the impact event at the K/T boundary.

### ***Paleocene/Eocene Thermal Maximum***

The Paleocene/Eocene boundary interval is characterized worldwide by an abrupt warming event referred to as the PETM, which is recorded by clay-rich precursor beds, followed by a sharp negative  $\delta^{13}\text{C}$  excursion and a benthic foraminiferal extinction event. We cored this sequence at Site 1276. Although the specific boundary clay layer appears to be missing in our cores, a complete succession of the calcareous nannofossil events occurring immediately above the boundary clay layer was recognized, and it will provide important information on biotic recovery after this event.

### ***Initiation of Abyssal Circulation***

Sedimentation patterns in the North and South Atlantic Oceans have been profoundly affected by bottom currents ever since the initiation of strong abyssal circulation in Paleogene time. Determining when this initiation occurred, however, has been problematic because the currents created major unconformities (e.g., Horizon A<sup>u</sup> in the main North Atlantic Basin) and thus left little lithologic or biostratigraphic record to establish the timing of the event. Current interpretations are that the abyssal circulation developed near the Eocene/Oligocene boundary (Miller and Tucholke, 1983; Davies et al., 2001).

At Site 1276 we cored through a seismic marker that appears to coincide with this circulation event. It matches an unconformity between lithologic Units 1 and 2 and a middle Eocene hiatus identified from preliminary biostratigraphy. The hiatus seems to represent a limited length of geologic time compared to other places where the unconformity has been cored, probably because gravity flows were flooding the Newfoundland deepwater margin with abundant sediment at the time. If our preliminary shipboard

conclusions about the age of the hiatus are correct, then the age of this major paleoceanographic event may be 4–7 m.y. older than previously supposed. Shore-based analyses are planned to investigate this phenomenon in detail.

### **Site 1277**

With only 3 days of Leg 210 remaining, we moved 40 km southeast of Site 1276 and drilled into the crest of a prominent basement ridge at Site 1277 (Figs. F8B, F9). The crust here is just on the young side of a magnetic anomaly identified as M1, and it therefore is presumed to be oceanic. We cored the basement from 103.9 mbsf (wash core) to 180.3 mbsf and recovered a spectacular section of mixed basalts, fine to very coarse grained gabbros, serpentinized peridotites, fine- to coarse-grained sediments, and calcite-cemented conglomerates. Most of these rocks appear to have been displaced to their present location in local slumps, slides, and debris flows. The distance of transport cannot have been large because they were cored from the crest of the ridge, and they must have been displaced only from local basement irregularities. The deepest four cores, below ~135 mbsf, consist dominantly of serpentinized peridotite with minor gabbros and a cataclastic damage zone. The serpentinites are interpreted to may represent in situ basement.

The occurrence of coarse-grained gabbros and serpentinites at the crest of this ridge suggests that the ridge must have been formed by large-scale fault displacement that unroofed lower crust and upper mantle or that magmatic crust at this site is extremely thin, or both. Both of these features are expected in very slow spreading ocean crust that is characterized by limited magma supply and extreme tectonic extension. We conclude that at least this section of ocean crust in the Newfoundland Basin was formed at very slow spreading rates.

## **Concluding Remarks**

We undertook Leg 210 with a full understanding that drilling, casing, coring, and logging a 2+ km hole during only one drilling leg would be a major challenge. Although we were unable fully to meet this objective at Site 1276, in the final analysis we judge that the leg was a clear success. We cored to 1739 mbsf and recovered an exceptionally complete sedimentary record. Engineering analysis indicates that Site 1276 can reasonably be deepened to reach and core basement if casing is drilled into the lower part of the hole. In addition, Site 1277 returned a remarkable record of lower oceanic crust and upper mantle from a very short-penetration hole. As is true of the best scientific problems, results from these two sites raise exciting new questions. Among the most important of these is: How do we reconcile a record of extreme tectonic extension in an apparently slow spreading and magma starved environment (Site 1277) with a record of significant postrift magmatism in nearby crust at Site 1276? We look forward to future drilling in the Newfoundland Basin to answer this kind of question and to determine the nature of the crust in the Newfoundland transition zone.

## **OPERATIONS**

### **Bermuda Port Call**

Leg 210 began at 1712 hr on Sunday, 6 July 2003, when the ship arrived in St. Georges, Bermuda. As the ship arrived 1 day early, the planned berth at the Royal Naval Dockyard on the west end of the island was not yet available. Immigration and custom clearance was completed that day. Because of the change in

berth location, only one ODP container and the airfreight could be loaded on Monday, 7 July. The drill crew continued to work on replacing the drill line; unfortunately the new drill line reel was larger, necessitating significant reworking of the mounting structure.

On Tuesday, 8 July the ship moved to the Royal Naval Dockyard (RND) on the west end of Bermuda. After the pilot boarded (0745 hr), all lines were released (0824 hr), and the tug pulled the ship clear of the harbor (0831 hr), the ship began the transit to the RND. The first line was ashore at the RND at 1035 hr. The early arrival in Bermuda and berth change resulted in port call activities not effectively starting until 8 July.

The ODP crew change was completed at 1430 hr on 8 July. This crew change was extended so that the technical staff could be informed about the status of IODP and changes in medical and retirement benefits. The Lawrence Berkley National Labs X-ray computed tomography imaging (CAT) scanner was installed, and testing, calibration, and training began. Three containers of fresh groceries were loaded on Tuesday. Although the reefers had been left without power by dockworkers for ~24 hr, no spoilage occurred. ODP offloaded three 20-ft containers of supplies. We began loading 1400 metric tons of fuel on 8 July. Due to the small transfer hose size, this took 2 days; it shut down all drill floor activities for the drill line replacement because of welding restrictions. Potable water was delivered to the ship by small truck on an hourly basis.

Other activities on 8 July included the following:

1. A laboratory tour for staff from the Bermuda Underwater Exploration Institute was conducted.
2. Vendor engineers installed the antivibration bracket for the active heave compensator (AHC) motion reference unit (MRU).
3. The ODP operations engineer uncrated the APS Drilling Sensor Sub (DSS), spare parts, tools, and batteries and began testing the system with the Remote Memory Module (RMM).
4. Installation and testing of the electronics and firmware for the weight-on-bit (WOB) filter continued.

Activities related to troubleshooting AHC problems continued on Wednesday, 9 July with a technical review meeting with the Leg 209 ODP electronics technician, the Transocean operations manager, and the vendor service engineers. The rental MRU was mounted and the existing MRU was diagnosed with severe calibration problems.

On 9 July the ship had to shift down the dock to make way for another arriving ship. The pilot was on board at 0915 hr, and the lines were cleared at 0950 hr; a tug was tied to the stern, and we started shifting along the pier. At 1020 hr, the vessel was secured to the wharf two ship lengths down the pier. Testing continued on the DSS and the RMM as well as the WOB filter. The departing ODP dry ice and foreign airfreight shipments were sent out and all departing ODP surface freight was staged on the dock. One of the drill collar (DC) racks was cleared out and then loaded with eight DCs and three tapered drill collars (TDCs). Delivery to the ship of the 30-ft DCs was difficult because of the very narrow roads in Bermuda. Two flats of DCs were placed on the dock in preparation for loading. American Bureau of Shipping surveyors were on board carrying out various required ship inspections. More tours were conducted for staff of the Bermuda Biological Station and Texas A&M University Research Foundation representatives.

The Transocean crew crossover occurred on Thursday, 10 July. The new drill crew reorganized the DC rack and loaded the remaining 16 DCs. The reentry cone was spotted in the moonpool for assembly. The drill line installation was completed at 2100 hr. The AHC vendor engineers began testing and calibrating the AHC and then provided training for the drillers regarding set up and operating procedures for the

AHC. The remaining ODP airfreight arrived on the dock on late Thursday evening, and the departing ODP containers were sealed for shipment.

On Friday, 11 July, the Leg 210 airfreight was loaded. The pilot and tug were ordered for a 1500 hr departure. A comprehensive safety equipment and lifeboat orientation was held for new oncoming personnel and the science party.

### **Transit to Site 1276 (Proposed Site NNB-01A)**

The pilot boarded at 1631 hr on Friday 11 July, the tug boats secured to the ship at 1638 hr, and the last line was released at 1648 hr. Once the tugs were clear of the ship (1655 hr) we transited to the pilot station with beautiful blue skies and calm seas. The pilot departed the ship and we began the transit to Site 1276 (proposed Site NNB-01A) at 1813 hr. The Schlumberger logging engineer boarded the ship via the pilot vessel on 11 July.

During the transit from Bermuda, we assembled the reentry cone, picked up and determined the space-out of the bottom-hole assembly (BHA) for drilling in the 20-in casing, and performed general rig maintenance. On 14 July, we crossed the Gulf Stream and entered dense fog and cooler weather. That evening, we slowed to 9.5 nmi/hr as we entered marked fishing grounds in fog. During the final approach to Site 1276, we had to change heading slightly to avoid some research vessels that were towing gear. After a transit of 1227 nmi at an average speed of 11 nmi/hr, we arrived at Site 1276 at 0800 hr on Wednesday, 16 July.

### **Site 1276**

Once we arrived at Global Positioning System (GPS) coordinates of Site 1276 (45°24.23'N, 44°47.15'W), the thrusters were lowered and switched to dynamic positioning (DP) mode at 0815 hr on 16 July. A seafloor positioning beacon was deployed at 0844 hr. The precision depth recorder indicated a water depth of 4564.5 meters below sea level (mbsl) (4575.4 meters below rig floor [mbrf]).

### **Hole 1276A**

Figure F32 shows a diagram of drilling, casing, and coring in Hole 1276A, and Figure F33 gives a breakdown of operations activities while on site.

#### ***Installation of Reentry Cone and 20-in Casing***

During the transit we had prepared the 20-in casing running tools (CRTs), BHA components, pilot bit, underreamer, centralizer, casing shoe, and reentry cone. The underreamer arms were set for 22 in. After the ship was on location in DP mode, we assembled DCs into five stands and stored them in the derrick. The upper guide horn was removed and stored in the DC rack so the reentry cone could be centered over the moonpool.

A DC was attached to the top of the CRT, and the CRT was attached to the 20-in casing hanger and secured in the derrick. At 1430 hr on 16 July, we started rigging up for assembling eight joints of 20-in casing (total length = 101.9 m below the reentry cone mud skirt). The casing shoe joint was positioned in the rotary table and the casing assembled; the lower three casing connections were spot welded. Once the casing hanger was attached to the top, we lowered the 20-in casing through the reentry cone and latched the hanger into it. We lifted the entire casing and reentry cone assembly to ensure it was securely attached and to determine its weight (casing = 24,000 lb; casing + reentry cone = 38,000 lb). We then disconnected

the CRT from the casing hanger and welded the casing to the reentry cone. The CRT, with two joints of DCs attached to the top, was stored in the derrick.

Our next step was to assemble the drill-in BHA. At 1930 hr, the drill crew started assembling a BHA consisting of an 18-in bit, bit sub with float, underreamer, crossover sub, mud motor, 14-in stabilizer, and 10 DCs to allow the bit to extend 4.83 m below the bottom of the casing. Once the mud motor was attached above the bit and underreamer, we flow tested this setup to ensure the mud motor and underreamer were functioning properly.

The drill-in BHA (total length = 106.73 m below reentry cone mud skirt) was lowered through the reentry cone and 20-in casing, and the CRT was attached to the top and latched into reentry cone at 0105 hr on 17 July. After visually inspecting the latching of the casing to the reentry cone and the CRT to the casing hanger, the entire assembly was raised to confirm that it was securely attached and to obtain a total weight (casing = 25,000 lb; casing + reentry cone = 40,000 lb; drill-in BHA below the CRT = 40,000 lb; BHA above CRT = 10,000 lb). We lowered the reentry assembly through the moonpool (0205 hr) and prepared the rig floor for running the assembly to the seafloor. As the assembly was lowered to 2701 mbrf, we filled the drill pipe with seawater every 10 stands.

Because of the deep water at Site 1276 and planned penetration depth, we had to use some drill pipe that had not been used for a year. This resulted in some extra time expended to remove pipe thread protectors that were difficult to remove and to clean the threads. Because of rust inside the drill string, each time we picked up a stand we had to run a rabbit through the pipe; we used a rabbit with a smaller outside diameter than normal to ensure the inside of this drill string was open.

To minimize the risk that a large quantity of rust particles could be flushed down the drill string, potentially damaging the mud motor, we circulated a complete drill string volume of seawater through the drill pipe when the bit was at 2701 and 3621 mbrf. We deployed the VIT camera system and continued to lower the drill string. We then picked up the top drive, spaced out the drill string, and established circulation; mud motor circulation rates were recorded just off bottom.

Based on a reduction in drill string weight, the driller tagged seafloor at 2045 hr on 17 July, initiating Hole 1276A. The seafloor depth as felt by the drill bit was 4563 mbrf (4552.1 mbsl), but this was later corrected to 4560 mbrf (4549.1 mbsl), as the reentry cone landed and could not be lowered past this depth. It took a total of 28 hr to drill the 20-in casing to 4662.0 mbrf (102.0 mbsf).

We experienced highly variable penetration rates due to the presence of several hard layers and, at times, what appeared to be a plugged jet in the bit. Drilling times were mostly between 2 and 40 min/m, except for some very hard layers at 16, 56, and 62 mbsf that took 150, 80, and 210 min/m, respectively. We infer that these were intervals containing glacial dropstones. In general, the driller was using 100–140 spm (500–700 gpm) while drilling, with a resulting torque of 5000 ft·lb at the bit with a bit rotation of ~70 rpm. Penetration slowed again while drilling the last few meters, and the reentry cone appeared to land on the seafloor 3 m shallower than expected.

After drilling in the casing (completed at 0045 hr on 19 July), our next step was to activate the CRT to release the drill string from the 20-in casing and reentry cone. The driller reduced the string weight by 40,000 lb (the neutral point for the casing at the CRT) and then attempted to release the CRT at 0230 hr. Although it should have released relatively quickly, the CRT finally released at 0500 hr, when the driller rapidly increased the WOB. Even then, it still required repeated raising and lowering of the drill string to fully release the BHA from the casing. This sticking may have been due to the underreamer arms not being completely retracted or because the CRT was sticking in the casing hanger. Using the subsea camera system, we observed that sediment was completely covering the reentry cone. To better visualize the cone and seafloor, we retrieved the camera to change the guide funnel so it could pass over the CRT and reach

down to the bit. During camera retrieval, we circulated seawater to attempt to wash away some of the sediment in the core. When the camera was redeployed and had passed over the CRT, we reconfirmed that the reentry cone was covered by sediment, although a “crater” in the sediment could be clearly imaged on the sonar. It appeared that we may have set the reentry cone base slightly below the seafloor. We raised the bit until it was just inside the reentry cone and jetted with seawater to try to clear the sediments. The bit cleared the seafloor at 1000 hr.

Next, we retrieved the camera system and then pulled the drill string out of the hole. The drilling assembly was then disassembled (DC stands stored in the derrick, CRT detorqued, and mud motor and underreamer flow tested and then flushed with fresh water). The bit cleared the rotary table at 2300 hr.

Once the underreamer and bit were back on the rig floor, we observed that the underreamer’s nozzles were damaged. The damage was likely due to plugging of the nozzles as well as to clay and glacial dropstones packed inside the bit and underreamer. The sediment (late Pliocene age, uppermost part of fan deposits) and rocks were passed to the scientific party. The underreamer was subsequently repaired for drilling in the 16-in casing.

### ***Installation of 16-in Casing to 800 mbsf***

Our next operation was to install 16-in casing to 750 mbsf. The first step was to drill a 21-in hole to 800 mbsf. We started assembling the BHA at 0115 hr on 20 July. The BHA consisted of a 9<sup>7</sup>/<sub>8</sub>-in wobble (pilot) bit, bit stabilizer, a 21-in bicenter reamer, a float sub, eight DCs, the DSS (which measures downhole WOB, torque, and pressure), 10 DCs, and a TDC. The 174-m-long BHA weighed 50,000 lb, allowing a maximum WOB of 35,000 lb. The bicenter reamer could pass through a diameter of 18 in and was capable of drilling a 21-in hole beneath the 20-in casing.

While lowering the BHA to the seafloor, the subsea camera system was deployed. At 1245 hr (with the bit at 4539 mbsl), the drill string length was adjusted in preparation to reenter Hole 1276A. The bit reentered the hole at 1300 hr. The reentry cone was buried in the sediment and only visible as a dark conical depression in the seafloor; the sonar could clearly image the sedimentary crater above the cone.

The top drive was picked up and we tagged the bottom of the at hole 4666.9 mbrf (106.9 mbsf). We alternated between passive and active heave compensation while drilling to check recent AHC calibrations and drilling procedures (detailed engineering report is available from ODP).

The rate of penetration (ROP) varied from 21 to 3 m/hr, generally decreasing downhole. Substantial reductions in ROP occurred at 503 mbsf (from 13 to 7 m/hr) and at 685 mbsf (from 7 to 3–4 m/hr). A failed connection in the top drive circulation system interrupted drilling for 3 hr when the bit was at 666 mbsf (0915 hr on 23 July). The bit was raised off the bottom (to 5165 mbrf [605 mbsf]) to repair the top drive. After the repair, we drilled back to bottom (609–666 mbsf), encountering 10–15 m of soft fill.

The wobble bit with bicenter reamer drilled smoothly with no indication of drag along the borehole walls. We circulated sepiolite mud (20 bbl) every 50 m while drilling. The bit reached 800 mbsf at 2330 hr on 24 July.

We circulated 50 bbl of sepiolite mud to clean the hole and then raised the bit back up to the bottom of the 20-in casing shoe (102 mbsf). No tight sections of hole were encountered on the way up. While lowering the bit back down, the bit encountered some resistance from 615 to 634 mbsf. We washed from there down to 800 mbsf and had to wash 15 m of soft fill from the bottom of the hole. We circulated another 40 bbl of mud to clean out the hole and then put 375 bbl of mud in the bottom of the hole so that mud would cover the tight interval at 615–634 mbsf. As the drill string was raised, additional tight spots were found at 576–432, 423–412, and 288–103 mbsf and they required use of the top drive. Once the bit was at the reentry cone and before pulling completely out, we circulated seawater to clean

sediments from the reentry cone in order to make it easier for us to find the cone on the next reentry. The bit cleared the seafloor at 2100 hr on 25 July.

The BHA was taken apart and the bit was on the rig floor at 0640 hr on 26 July. The DSS was moved near the downhole laboratory so the data could be downloaded. The wobble bit and bicenter reamer had experienced 84 hr of rotation with 25,000–35,000 lb WOB (70–75 rpm) and could not be reused because of loose bearings.

Another problem with the top drive's seawater circulation system was observed when tripping out of the hole; water was leaking between the swivel and top drive shaft while circulating. At 0645 hr on 26 July, we started troubleshooting the top drive and swivel. The top drive was repaired, pressure tested to 1000 psi, and back in service by 1330 hr. Finally, preventative maintenance had to be done on the drill line (slip and cut).

We started preparing the rig floor for assembling the 16-in casing at 1515 hr. Once we were finished assembling the casing (749.11 m; 0200 hr on 27 July) the CRT was attached to the casing hanger and the casing was lowered below the rig floor and hung off on the moonpool doors. The CRT was disconnected, and we started assembling the 16-in drilling BHA through the 16-in casing. The BHA consisted of a 14-in tricone bit, underreamer (arms set to 20 in), a mud motor, a 14-in centralizer/stabilizer, 12 DCs, and 21 stands plus a double of drill pipe. The BHA length was 753.90 m, so the pilot bit extended 4.83 m below the 16-in casing shoe.

We attached the CRT to the top of the BHA (1115 hr), lowered it to the moonpool, and attached the CRT to the 16-in casing hanger. We picked up the entire drilling/casing assembly (1245 hr) and deployed the camera system to inspect the casing as well as to confirm the spacing of the bit and underreamer below the casing.

At 1415 hr we began lowering the assembly to the seafloor. The bit was at the seafloor and ready for reentry at 0000 hr on 28 July. After only 10 min (0010 hr), we reentered Hole 1276A. When the bit was at 4649 mbrf (89 mbsf; 0100 hr), we attached the top drive. The bit passed through the base of the 20-in casing (102.07 mbsf) at 0200 hr.

From the 20-in casing shoe to 4930.79 mbrf (370.79 mbsf), the drilling time for each 9.6-m interval was 3–12 min. The drilling parameters for this section were WOB = 4–14 klb, circulation rate = 80–110 spm, and pump pressure = 650–1200 psi. We started circulating 30 bbl of mud every stand starting at 284 mbsf. We continued drilling the casing in from 5017 to 5050 mbrf (457–490 mbsf; WOB = 20–30 klb, circulation = 150 spm, pressure = 2100 psi) until 0715 hr on July 29; at this time, it became apparent that the mud motor was not working properly. As we pumped 30 bbl of mud the pump pressure increased by 700 psi. Although this was not typical for a mud motor stall, we could not restart the mud motor despite repeated attempts at lifting off bottom or varying the circulating rate and WOB. At 1000 hr, we decided to retrieve the drill string to replace the mud motor.

The bit cleared the seafloor at 1415 hr, and the entire drilling/casing assembly was raised back to the ship. We hung the 16-in casing on the moonpool doors (2300 hr) and then began to take apart the BHA (2330 hr). Before taking apart the mud motor, underreamer, and bit, we tested the equipment by pumping seawater through it. The mud motor had seized up and would not rotate. Furthermore, the underreamer arms would not open and it was packed off with sand (including sand under the piston that actuates the arms). Later, we found pieces of rubber jammed in the nozzles of the underreamer; these were from inside the mud motor, further documenting the failure of its internal mechanism.

The underreamer had to be completely taken apart and nearly all moving parts were replaced. At 0430 hr on 30 July, we assembled the pilot bit, the rebuilt underreamer, and a new mud motor. Once this was

tested, we started to reassemble the drilling BHA (0900 hr). The BHA was latched into the 16-in casing hanger at 1130 hr, and we started lowering the drilling BHA and casing back down to the seafloor.

Once the bit was near the seafloor (2000 hr), it took 45 min to reenter Hole 1276A. The bit was lowered into the hole to 92 mbsf when we picked up the top drive to prepare for drilling. We began drilling the 16-in casing into the hole at 2200 hr. Drilling in the casing went quite quickly and smoothly down to 389.87 mbsf (drilling time = 2–14 min/9.6 m, WOB = 2–12 klb, circulation = 145–155 spm; pressure = 1900–2200 psi). We encountered what appeared to be a series of ledges at 392, 394, and 396 mbsf. It took 120 min to drill the interval from 389.87 to 399.47 mbsf. After each ledge was drilled we had to use 20 klb to work the casing past the ledge. While passing through this interval, the mud motor appeared to be experiencing torque, indicating that the underreamer arms were cutting hole. It is also possible that the underreamer arms were exposed to shock loads (perhaps as high as the full casing/BHA weight) when the casing would finally break through a ledge. From 389.87 to 754.05 mbsf, drilling time was 25–120 min/9.6 m; circulation was 155–160 spm; and pump pressure was 2150–2300 psi. Several hard intervals were encountered at 698, 703, and 743 mbsf. The casing hanger landed in the reentry cone at 1115 hr on 2 August with the bottom of the 16-in casing at 749.07 mbsf.

The 16-in casing landed 2.8 m higher than expected. We interpret that this was due to stretching of the drill pipe under the very heavy weight of the casing and drilling BHA; this is consistent with drill pipe stretch calculations. When we had deploying the 20-in casing and reentry cone, we calculated a drill pipe stretch of ~9.6 m. With the longer, much heavier 16-in casing string and drilling BHA, the calculated stretch was 12.4 m.

After landing the casing, it took only 30 min to release the CRT (1145 hr). We then reduced the circulation rate, pulled the bit and underreamer back into the casing, and started pulling out of the hole. The bit cleared the seafloor at 1440 hr. Before we could retrieve the drill string, we conducted routine preventative maintenance on the drill line (slip and cut). After the mud motor, underreamer, and pilot bit were flushed out with fresh water, the bit arrived back on the rig floor at 0340 hr on 3 August.

We observed that the underreamer was missing its three outer cones (cutting structure on the arms) as well as two sets of pins that control how far the arms extend. These were left in the hole. The body of the underreamer and bit exhibited some deep gouges, suggesting that the cones had been caught between these and the formation. We also observed water leaking from the hard covering over the top of the underreamer's bottom connection. Even after losing their cones, the underreamer arms appear to have continued cutting the formation because the outer parts of the arms had been worn back.

#### ***Attempted Cementing of the 16-in Casing***

After opening the hole to 800 mbsf and drilling the 16-in casing in to 749.07 mbsf, our next operation was to cement the casing in place. We had originally planned to use a cement retainer. Because this would have required an extra pipe trip, we decided to use a 16-in Cameron cup tester (CCT) for the cementing operation instead.

At 0345 hr on 3 August we tested the rig floor cementing equipment and then assembled the cementing BHA. The BHA consisted of a short piece of drill pipe, the CCT, an 8-in DC, a three-blade stabilizer, four DCs, a TDC, and five joints of 5½-in drill pipe (length = 110.09 m; weight = 27,000 lb).

We lowered the BHA and were ready for reentry at 1400 hr. The ship was positioned precisely at the same location where we had efficiently reentered before and where each time the bit was directly over the hole. However, this time there was no indication of the location of the hole on either the camera or sonar.

After spending 1 hr searching for the hole with no success and with the ship directly over the previous reentry coordinates, we decided to probe the seafloor with the drill string in an attempt to locate the hole.

The camera imaged a circular shadow, and we lowered into it at 1455 hr. It appeared that we had entered the hole because there was no reduction in drill string weight, and the drill string was lowered to 4643 mbrf (83 mbsf). At this point, we observed on the camera image that the drill string did not appear to be moving down into the seafloor. We immediately stopped lowering and raised it back up to 4569 mbrf (9.4 mbsf). We slowly lowered the drill string again and it started meeting resistance at 13.4 mbsf. At this point, we decided to circulate seawater to attempt to clear sediment from the area. We also decided to raise the camera and inspect the drill string for damage. Unfortunately, we observed that the TDC was severely bent, so we had to retrieve the drill string before continuing. First, we conducted a sonar search of the area. We saw a sonar return ~60 m from the bit location, but we did not move closer to investigate. At 1900 hr, we began retrieving the drill string. When the end of the drill string was at 107 mbrf (0230 hr on 4 August) we had to cut off the connection from the last joint of 5½-in drill pipe and we removed the bent (~20°) TDC.

We replaced the TDC and started lowering the BHA back to the seafloor at 0400 hr. This time we attached a transponder to the camera/sonar system frame so that its position (and the end of the drill string) could be accurately monitored.

When the drill pipe was ready for reentry (1230 hr; 4554 mbrf, or 6 m above seafloor), we observed that the end of the drill string was offset 55–70 m from the moonpool. This was caused by a significant increase in bottom-current strength since the previous reentries. Moving the drill pipe to the location where it had just previously been lowered into the seafloor, we observed in the camera image a ~1-m-diameter hole in the seafloor together with an adjacent smaller hole. After discussion, we decided that this marked the previous attempted reentry and it was not the location of the Hole 1276A cone. At this time, we began seeing plumes of sediment-laden water flowing from the southwest. We decided to trace these to their source, where we found a depression in the seafloor that turned out to be the sedimentary crater in Hole 1276A. The rim of the depression was visible on the sonar. Sediment-laden water was streaming from the seafloor around this depression, which was ~15 m in diameter. The next challenge was to lower the drill string into the 3.5-m-diameter cone that was obscured by sediment and flowing muddy water and had a 75-m offset between the moonpool and the bit position.

During our first reentry attempt (1920 hr), the CCT appeared to hang up on the throat of the reentry cone (4563 mbrf; 3 mbsf). We slowly lowered the drill string to 4589 mbrf (29 mbsf) where it encountered an obstruction. We started circulating seawater to wash down from 4589 mbrf (29 mbsf), but tagged something hard at 4594 mbrf (34 mbsf; 0200 hr on 5 August). It was clear that the CCT was hanging up in the reentry cone, so we pulled out of the seafloor at 0325 hr.

After ~1 hr of repositioning the drill pipe directly over the hole, we attempted another reentry (0522 hr). Once again, we could not lower past 4564.5 mbrf (4.5 mbsf) in the cone. After 2 hr of trying we decided to pull the pipe clear of the reentry cone (0730 hr) and cease attempts to use the CCT for cementing. The CCT reached the rig floor at 1630 hr. A total of 61 hr was expended while attempting reentry for the cementing job.

We decided to abandon attempts to cement the casing, as we felt that by now the formation had likely collapsed around the outside of the 16-in casing and additional time to cement would create even more risk to achieving any of the deep, primary leg objectives. We felt that it was important to verify that reentering Hole 1276A was possible and that the smaller 9<sup>7</sup>/<sub>8</sub>-in RCB bit was the best tool to use. Furthermore, we still did not know what impact the pieces of the underreamer previously lost in the hole would have on our ability to advance the hole.

***RCB Coring from 800 mbsf***

After preparing the rig floor (1830 hr on 5 August), we started assembling the BHA. The BHA consisted of a rotary core barrel (RCB) bit (C3), a mechanical bit release (MBR) (so we could log after coring), one DC, the DSS (to measure downhole WOB, torque, and pressure), 13 DCs, a TDC, and 6 joints of 5½-in drill pipe (length = 202.08 m; weight = 60,000 lb). When the bit was at 4550 mbrf (0500 hr on 6 August), we had to do drill line maintenance (slip and cut) before we started the coring operations. At 0630 hr, we started reentry attempts in Hole 1276A, where sediment-laden fluid was still billowing out of the seafloor around the hole. After almost 5 hr, we succeeded reentering the hole on our fourth attempt (1125 hr).

We lowered the drill pipe to 4.7 m below the 16-in casing (5313 mbrf; 754 mbsf), where the bit encountered some resistance. A core barrel (wash core) was deployed and we drilled down to 5360 mbrf (800 mbsf; WOB = 10 klb, bit rotation = 70 rpm; circulation = 85 spm at 1100 psi, torque = 150 A). After recovering the wash core (Core 1W; 2355 hr), we began RCB coring at 5360 mbrf (800 mbsf). By 0025 hr on 10 August, we had cored from 800 to 1059.7 mbsf and recovered 210 m of core (recovery = 81%). The time to cut each core varied primarily from 22 to 95 min (average = 50 min) except for Core 9R (876.8–886.4 mbsf) which took 120 min. Hole conditions remained good throughout the cored interval.

Coring parameters started at WOB = 12 klb, bit rotation = 70 rpm, and circulation = 85 spm at 1100 psi, but by Core 28R were WOB = 20–25 klb, bit rotation = 60–70 rpm, and circulation = 115 spm at 1800 psi. Thirty barrels of sepiolite mud was circulated every core. Particulate tracers for microbiological experiments were deployed while cutting Cores 8R, 18R, 19R, and 28R. The RMM was run on top of the core barrel while taking Cores 4R, 7R, 13R, and 24R to download data from the DSS. The AHC was used while cutting Cores 14R, 15R, 16R, 18R, 20R, and 22R. While cutting Core 22R, it developed a hydraulic leak, which was subsequently repaired.

RCB coring continued from 1059.7 to 1338.1 mbsf. Cores 29R to 57R penetrated 278.4 m of section and recovered 245.75 m (recovery = 88%). Coring parameters for Cores 29R through 32R were WOB = 20 klb, bit rotation = 70 rpm, circulation = 110 spm at 1600 psi, and torque = 175–200 A. During a wiper trip after Core 32R, we encountered no drag from the base of the hole (1098.2 mbsf) up to the 16-in casing at 749 mbsf. On the way back down to the bottom of the hole, tight spots had to be reamed out at 803, 864, and 874 mbsf. After 10 m of soft fill on bottom had been cleaned out, we pumped 50 bbl of sepiolite mud to clean cuttings out of the hole. After the 6.5-hr wiper trip, we resumed coring. From 1615 hr on 10 August to 0605 hr on 13 August, we cut Cores 33R to 57R (1098.2–1338.1 mbsf) and recovered 212.15 m (recovery = 88%). ROP varied from 19 to 6.4 m/hr and generally decreased downhole. Sepiolite mud (30 bbl) was circulated after each core. Coring parameters were WOB = 20 klb, bit rotation = 70 rpm, torque = 175 A, and circulation = 110 spm at 1600–1700 psi until the lower part of this section where WOB, torque, and pump rates started to increase (WOB = 25 klb, torque = 200–300 A, and circulation = 130 spm at 2300 psi, respectively). Particulate tracers for microbiological studies were deployed on Core 48R.

There was a significant decrease in recovery in Cores 55R to 57R. Recovery had been averaging 93% in Cores 33R to 54R, but it dropped to 30%–60% in Cores 55R to 57R. Torque and pump pressure also increased while cutting Core 57R (torque = 400 A and pressure = 2600 psi, respectively). When Core 57R was recovered, we immediately noticed that its diameter was significantly reduced. Although the bit had only 44.8 cutting hours, the sudden change in core quality indicated that one or more of the core guides may have been bent inward or perhaps a single cone was not rotating properly. We decided to stop coring because we wanted to minimize the chances that a bit failure might junk the hole, and we prepared to log the hole.

### **Attempted Logging of Hole 1276A**

Before we conducted a wiper trip to prepare for logging, we circulated 60 bbl of sepiolite mud to clean cuttings out of the hole and we then raised the bit up into the 16-in casing (0730–1030 hr on 13 August). We lowered the bit into the hole to 5626 mbrf (1066.8 mbsf; 1030–1215 hr), where we used the top drive to drill some tight spots down to 1095.6 mbsf. Once this section was clean, we removed the top drive and we were able to freely lower the bit to 1297 mbsf. At 1530 hr, we had to use the top drive again to drill from 1297 to 1338 mbsf. The bit was back at the bottom of the hole at 1630 hr. We circulated 50 bbl of mud and then displaced the hole with 185 bbl of mud before starting to pull out of the hole to drop the bit.

We raised the bit up with the top drive in place up to 1297 mbsf, where it was racked back. While we continued to pull out of the hole, the subsea camera/sonar system was deployed at 2015 hr so we could observe bit release and reentry for logging. The bit cleared the seafloor at 2210 hr, the ship was offset 50 m to the south, and at 2245 hr we lowered the rotary shifting tool (RST) on the wireline to release the bit. The bit did not release and we lowered the RST again to close the MBR ports. When the sleeve was shifted back in place over the ports, at 0020 hr on August 14, we observed the bit falling off onto the seafloor. At 0130 hr, the drill pipe was adjusted for reentry at 4553 mbrf (7 m above the seafloor).

At 0130 hr the DP operators began positioning the vessel for reentry. The offset between the beacon on the camera/sonar frame and the moonpool was 25–40 m. When the end of the pipe passed over the hole, we observed sediment-laden fluid still coming out of the hole and obscuring it. The sedimentary crater was ~15 m in diameter. After an initial failed stab at the hole, we successfully reentered Hole 1276A at 0400 hr.

The end of the pipe (EOP) was lowered to 186.6 mbsf, and we retrieved the camera/sonar system. At 0445 hr, we started preparing the rig floor to run the wireline logging tools. The camera system was back on deck at 0630 hr and we started assembling the triple combination (triple combo) tool string. Unfortunately, once the logging tools were deployed, they would not pass an obstruction ~5 m below the base of the 16-in casing (749 mbsf). We retrieved the logging tool and decided to try lowering the open EOP past the obstruction. We lowered the EOP to 821 mbsf (~21 m into the 9<sup>7</sup>/<sub>8</sub>-in RCB hole) and deployed the triple combo a second time. Once again, the tool did not pass more than 3 m out the end of the pipe. It was now clear that the logging tools could not get into the open hole, so we abandoned attempts to log and started to pull out of the hole to resume RCB coring. The triple combo tool was back on the rig floor at 2020 hr, and we began retrieving the drill string at 2230 hr. The EOP cleared the seafloor at 0020 hr on 15 August and was back on the rig floor at 0840 hr.

#### ***RCB Coring from 1338.1 mbsf***

After attaching a new RCB bit, a new MBR, and removing a damaged piece of 5½-in drill pipe, we lowered the coring BHA down to the seafloor. The subsea camera/sonar system was deployed at 1730 hr when the bit was at 4517 mbrf (42 m above seafloor). Before we could reenter, we conducted some preventative maintenance on the drill line (slip and cut); this took from 1800 to 1930 hr.

At 1930 hr, we began positioning for reentry with the bit at 4553 mbrf. We could clearly see the rim of the sediment crater above Hole 1276A on the camera image, but this time the hole was not shrouded by sediment-laden water. We reentered Hole 1276A on the second attempt at 2145 hr and lowered the bit to 736 mbsf. After retrieving the subsea camera/sonar system, we started lowering the bit into the open hole below the 16-in casing (0015 hr on 16 August). The bit encountered as much as 25 klb of drag, so we installed the top drive to drill and circulate back to the bottom of the hole at 1338.1 mbsf. Tight spots in

the hole had to be worked at 825, 834–839, 877–882, 904, 1005, 1053, 1085, 1148, 1170, 1236, and 1254 mbsf. These zones required WOB = up to 10 klb, bit rotation = 75 rpm, torque = 175–300 A, and circulation = 100 spm at 1100 psi. Thirty barrels of mud were circulated at 1120 mbsf. Fill had to be drilled and washed from the hole at 1264.6–1338.1 mbsf. Before coring, we circulated 50 bbl of mud at 1338 mbsf.

We started coring at 1330 hr on August 16. Cores 58R to 61R were taken from 1338.1 to 1372.9 mbsf, and we recovered 32.66 m (recovery = 93%). ROP was 10.2 m/hr, and coring parameters were WOB = 15–20 klb, bit rotation = 70 rpm, circulation = 120 spm at 2300 psi, and torque = 200–300 A. After cutting each core, 30 bbl of mud was circulated.

Cores 62R to 80R were cut from 1372.9 to 1555.4 mbsf (0225 hr on 17 August to 1450 hr on 19 August) and we recovered 170.27 m (recovery = 93%). Drilling parameters remained relatively constant in this interval: WOB = 20–25 klb, bit rotation = 70 rpm, torque = 200–250 A, and circulation = 120–130 spm at 2300–2500 psi. The ROP decreased downhole from 9.3 m/hr (Cores 62R to 70R) to 6.2 m/hr (Cores 71R to 77R) to 3.8 m/hr (Cores 78R to 80R). The AHC was used while cutting Core 64R and then used for all odd-numbered cores starting with Core 67R.

A full-length nonmagnetic RCB core barrel was deployed for all odd-numbered cores, and we continued to use a standard barrel for even-numbered cores. Particulate tracers for microbiological contamination testing were deployed every tenth core starting with Core 69R.

The bit encountered a hard interval at 1412.4 mbsf. A substantial reduction in penetration rate occurred between Cores 75R (85 min to cut 9.6 m; ROP = 6.7 m/hr) and Core 76R (170 min to cut 9.6 m; ROP = ~3.3 m/hr). This slow rate of penetration persisted while cutting Cores 77R to 80R. These cores also had slightly lower recovery. The recovered cores showed no obvious reason for the substantial change in penetration rate.

Because of the slow ROP and consistent torque, we decided to conduct a wiper trip up to the 16-in casing. At 1600 hr on 19 August, we circulated 50 bbl of sepiolite mud and then started raising the bit. The top drive was used to rotate and circulate as the bit was raised to 1284 mbsf. At 1830 hr, the top drive was removed and the bit was raised the rest of the way up to the 16-in casing. The wiper trip to this point lasted 5.75 hr.

We began lowering the bit back into the hole at 2045 hr. The bit immediately ran into a tight area at 851.5 mbsf, and we had to install the top drive to be able drill through it. Drilling did not start until 0000 hr on 20 August because we first had to replace a damaged 20-ft piece of drill pipe (“knobby”) at the rig floor.

It took 13.5 hr to drill back to the bottom of the hole at 1555.4 mbsf. On the way back to bottom, tight sections of hole had to be drilled through and reamed up and down (864–875, 885–887, 992, 1000, 1005–1024, 1093, 1285–1351, and 1365 mbsf). Torque of 400–500 A and pump pressures up to 1700 psi were recorded while drilling out the upper two intervals. Increased torque and pump pressures also occurred from 1285 to 1351 mbsf. The typical drilling parameters while reaming back to the bottom of the hole were WOB = 5–12 klb, bit rotation = 80 rpm, torque = 175–200 A, and circulation = 120 spm at 1200 psi. Sepiolite mud was circulated at 1300 mbsf (30 bbl) and 1514 mbsf (50 bbl).

Coring resumed at 1330 hr. Cores 81R to 84R were taken from 1555.4 to 1587.7 mbsf and we recovered 17.85 m (recovery = 55%). Coring parameters were WOB = 20–35 klb, bit rotation = 65–70 rpm, torque = 200–300 A, and circulation = 120 spm at 2000–2200 psi. We circulated 30 bbl of mud every core. The AHC was used while cutting Core 82R. Recovery for this core was very low (0.94 m), due to a mechanical problem with the check ball that allowed the full pump rate to pass through the core barrel.

Because of the slow and apparently decreasing rate of penetration (ROP = ~3 m/hr for Cores 81R through 83R and 1.8 m/hr for Core 84R), we decided to retrieve the drill string so we could change the bit to one better suited to hard formations.

### ***Top Drive Failure***

We deployed the wireline sinker bar to retrieve Core 84R at 0715 hr on 21 August. While lowering the sinker bar, the driller noticed that the top drive was leaking while he was circulating seawater (similar to the failure that occurred on 24 July). The situation changed drastically when the leak turned into a deluge. The driller immediately landed and secured the drill string on the rig floor elevators. Fortunately, the bit was off the bottom of the hole when this occurred, thus allowing the driller access to the tool joint on the 5.5-in drill pipe.

Once the drill pipe had been secured, our next concerns were to make sure the pipe didn't get stuck in the hole and to start retrieving the drill string as soon as possible. We needed to retrieve Core 84R, reestablish circulation, get the top drive out of the way, and then start pulling out of the hole.

Core 84R was pulled out of the pipe and recovered on the rig floor at 0830 hr on 21 August. The circulating head was then attached to the top of the drill pipe so that we could pump seawater to prevent the pipe from becoming stuck in the hole. The knobby drill pipe attached to the bottom of the top drive had to be removed before the top drive could be pulled out of the way. At 0830 hr, the 30-ft knobby was removed but the other 20-ft knobby had to be cut off because we could not reach the connection to loosen it. Once the knobbies were removed from the top drive, the top drive was rotated back away from the rig floor.

At 0930 hr, we started raising drill pipe out of the hole. The drill string encountered 50 klb of overpull and 25 klb of drag when raising and lowering the pipe through 1312 mbsf. Based on previous hole conditions when conducting wiper trips or pulling out of the hole, we were certain that circulation would be required to get out of the hole. Thus, we reinstalled the circulating head on the top of each stand of drill pipe. The pipe had to be worked up and down for ~2 hr before we could get through the interval from 1312 to 1323 mbsf. Tight hole conditions were encountered throughout the open hole and the pipe had to be worked up and down while circulating (pump rate = 30 spm at 300 psi). At 1930 hr, after 7.5 hr, the bit was raised back up inside the 16-in casing. We continued retrieving the drill string, which cleared the seafloor at 2055 hr and was back on the rig floor at 0455 hr on 22 August.

### ***Top Drive Repair***

At 0500 hr, we began to disassemble the top drive to evaluate what had broken. A severe crack was found in the swivel-shaft box connection. The swivel shaft bears the entire weight of the 6147-m-long drill string (~680,000 lb). The crack extended ~60% around the circumference of the shaft. It is a major miracle that we did not lose the drill string, lose the hole, and severely damage the derrick. We replaced the swivel shaft and then reassembled and tested the top drive. The top drive was fully repaired at 1530 hr.

### ***RCB Coring from 1587.7 mbsf***

We attached a new bit (CC-4) to the BHA and lowered it to the seafloor. The subsea camera system was launched at 0000 hr on 23 August. Before we could reenter Hole 1276A, we performed routine preventative maintenance on the drill line (slip and cut; 0045–0215 hr) and we picked up 10 new stands of 5-in drill pipe, measured length, and checked interior diameter.

We began searching for Hole 1276A at 0245 hr, and we reentered it on the second attempt at 0355 hr. The end of the drill string still had a 25 m offset from the moonpool due to currents, and there was 3 m of heave.

By 0545 hr, the bit was near the base of the 16-in casing. The bit was lowered to 1006 mbsf without using the top drive to rotate or circulate; this was the first time it entered so freely. The top drive was installed when the bit encountered drag (20–30 klb) at 1006 mbsf. The hole was redrilled from 1006 to 1587.7 mbsf (0930 hr on 22 August to 2045 hr on 23 August). Tight spots were encountered at 865, 990, 1006, 1070, and 1110 mbsf.

The RCB core barrel was dropped to start Core 85R at 2045 hr. While the core barrel was dropping to the bottom of the pipe, we continued to rotate and ream out the lowermost 8.5 m of hole.

Cores 85R and 86R were taken from 1587.7 to 1604.5 mbsf and recovered 14.59 m (recovery = 86%). We varied the coring parameters (WOB = 30 klb, bit rotation = 60 rpm, torque = 275 A, and circulation = 120 spm at 2300 psi) in an attempt to improve the rate of penetration (ROP = 2.3–2.7 m/hr), but there was no apparent improvement. Although the cores recovered alternating claystone and sandstone, there was no apparent change in drilling throughout the cored interval.

On 24 August, we cut Cores 85R to 90R from 6152.8 to 6200.8 mbrf (1592.8–1640.8 mbsf). Core recovery was 90%, and ROP was 3.0 m/hr. Coring parameters were WOB = 25–30 klb, bit rotation = 60 rpm, torque = 225–275 A, and circulation = 120 spm at 2300 psi. A sill was encountered at the bottom of Core 87R and in most of the upper part of Core 88R. Core 88R recovery was 97.1%, and ROP was 3.8 m/hr. The AHC was run on Cores 87R and 89R. Particulate tracers were deployed while cutting Core 89R. We continued to run full nonmagnetic core barrels on all odd-numbered cores.

On August 25, we cut Cores 90R to 95R from 6200.8 to 6242.9 mbsf (1640.8–1682.9 mbsf). Coring parameters were consistent: WOB = 25 klb, bit rotation = 60 rpm, torque = 225–275 A, and circulation = 120 spm at 2300 psi. Core recovery was 86.8%, and ROP was 3.2 m/hr. The AHC was run while cutting Core 91R, but it then had to be shut down because of a hydraulic leak.

By midnight on 25 August, sea conditions had deteriorated and we encountered maximum heave of nearly 3 m. Throughout 26 August, we continued to experience heave of 1.5–2.0 m.

On 26 August, we cut Cores 95R to 100R from 6242.9 to 6290.8 mbsf (1682.9–1730.8 mbsf). Particulate tracers were deployed while cutting Core 99R. Coring parameters were WOB = 20–30 klb, bit rotation = 60–70 rpm, circulation = 120 spm at 2200 psi, and torque = 225–350 A. Core recovery dropped from 80% in Core 96R to only 39% for Core 99R. For Cores 95R to 98R, ROP was 3–5 m/hr but then it dropped to 2.5 m/hr for Core 99R. We had to replace the lower 5-ft section of the nonmagnetic core barrel due to a cracked thread. This may have been damaged when we experienced the high heave late on 25 August or early 26 August. Although we held a constant WOB of 25 klb, WOB could have ranged from 12 to 37 klb because of the heave.

While we cut Core 100R, the circulating pressures dropped from 2200 to 1700–1800 psi and the torque increased to 400–500 A. After advancing only 2 m in 4 hr, we decided to retrieve the core to see if we could tell why the penetration rate had dropped so dramatically. When we recovered Core 100R it was empty. We deployed another core barrel and it did not appear to latch in properly, so it was immediately retrieved. When it was back on the rig floor, we noticed that the core catcher fingers inside the core barrel were damaged, as if something had poked through the middle of the core barrel when it landed. At this point we believed that the bit must have been jammed with rocks, so we ran a bit deplugger down on the end of a core barrel. This did not appear to land properly, so we ran in again with another type of deplugger.

At this point we felt that whatever was jamming the bit might be dislodged, so we deployed the barrel for Core 101R at 1200 hr on 27 August. While cutting this core, we observed relatively smooth torque of ~300 A during the first hour. After this, the torque became very erratic (200–500 A). After a 1-m advance (1731.1–1732.1 mbsf), we retrieved Core 101R at 1730 hr and it was empty.

It appeared that the bit was still jammed, so we decided to retrieve the drill string to replace the bit. We began raising the drill string at 1735 hr. The top drive was removed at 2245 hr when the bit was at 929 mbsf, but the circulating head had to be used from 865 to 813 mbsf to work through a section that had 30–40 klb of drag.

The bit cleared the seafloor at 0155 hr on August 28 and was back on the rig floor at 1005 hr. Pieces of diabase (~1.5 m total length) were jammed into the flapper valve. From all of the operations described above (especially the damaged core catcher fingers), we inferred that this 1.5 m of diabase most likely fell out of the core barrel while we were retrieving Core 99R. In addition, the bit was severely damaged, with one cone missing and one cone completely seized up; the remaining two cones could be moved up and down nearly 1 in on the bit. The three remaining cones also had missing buttons and severe gouging, and the core guides were damaged.

Once the damaged bit and pieces of core were removed, we started to assemble a new C-7 bit to a boot basket sub (designed to catch broken pieces of metal in cavities along the outside of the sub) and then we lowered the pipe back to the seafloor. We changed the bit in order to minimize damage to the cutting structure by any remnants of the lost bit cone. We did not want to use conventional fishing tools or a magnet due to the poor hole conditions (it was taking 10–20 hr to drill back to bottom of hole each time) and because we wanted to continue coring if possible. Before we reentered the hole, we performed preventative maintenance on the drill line (slip and cut).

We positioned the drill pipe at 4553 mbrf and started to maneuver the ship for reentering Hole 1276A at 2115 hr on 29 August. Once again we had significant difficulties reentering the hole due to currents (surface and deep), a completely sediment-covered reentry cone, and significant offset of the moonpool from the bit (~75 m). After 24 hr and 15 attempts, we reentered Hole 1276A at 2110 hr on 30 August. On this last and successful attempt, it at first appeared that we had missed the hole yet again because of difficulty in lowering the drill pipe. However, when we offset the ship back over the hole, the bit slipped in. It may be that we had actually stabbed the hole on previous attempts, but it seems that the offset had caused the bit to stick in the throat of the reentry cone.

When we lowered the bit into the hole, we encountered 30 klb of drag at 800 mbsf and had to raise the bit to 784 mbsf and install the top drive. It took ~28 hr to drill back down to the bottom of the hole at 1732.1 mbsf. We encountered tight spots at 800–900, 1030, 1075, 1285, 1320, 1354, and 1410 mbsf. It took ~5 hr to ream out and clean up a tight spot at 1688 mbsf using a WOB of 20 klb and torque of 300–400 A. Another difficult section of hole was encountered between 1720 and 1726.8 mbsf where we needed to use a WOB of 20 klb and torque of 300–450 A.

We dropped the barrel for Core 102R at 0045 hr on 31 August and starting coring at 1732.1 mbsf. Because the cone that had broken off the previous bit was in the bottom of the hole, we used a low WOB and a slow rotation rate while lowering the bit 0.8 m to 1732.9 mbsf. It took 2 hr to advance these 2 m. Core 102R was recovered with only a single 2-cm-long piece of diabase. After cutting Core 103R from 1732.9 to 1734.9 mbsf (3 hr), it was retrieved and it was empty.

At 1030 hr on 31 August, we deployed a center bit to try to dislodge anything that might be jammed in the bit and preventing core recovery and to help break up any debris from the missing cone. At 1115 hr, when we were ready to lower the sinker bars to retrieve the center bit, torque increased to 400 A and pump pressure increased to 2750 psi. We did not deploy the sinker bars and we reamed the tight hole from 1726.8 to 1693.8 mbsf. While reaming we encountered drag of 40,000 lb, torque of 600 A, and pump pressures of 2750 psi.

At 1315 hr on 31 August, we retrieved the center bit, then lowered the bit back to the bottom of the hole (1693.8–1734.9 mbsf) and started cutting Core 104R. We took 4 hr to advance 2 m using WOB = 20

klb, bit rotation = 55 rpm, and circulation = 100 spm at 1750 psi. When Core 104R was recovered it was empty.

At 2215 hr, we dropped another center bit in a further attempt to dislodge anything that might be jammed in the bit and to help break up any debris from the missing cone. The center bit was recovered at 0115 hr on 1 September, and it showed significant damage, indicating that it had been grinding on the lost cone in the bottom of the hole. We deployed another center bit at 0115 hr; it was retrieved at 0400 hr, and it showed significant damage to the cutting structure, also indicating that it had been grinding on metal in the bottom of the hole.

At 0400 hr, we deployed yet another center bit. When the bit had been lowered back down to 1734.9 mbsf (2 m above the bottom of the hole), we lost the ability to rotate the drill string (even with torque of >550 A) and pump pressures climbed to 2600 psi. We started to try to work the pipe up and down with overpull of 130 klb and pump pressures up to 3000 psi. Rotation could not be reestablished even with torque of 600 A. By 0930 hr, we were able to remove only two singles of drill pipe and to raise the bit up to 1707.5 mbsf.

At 0930 hr, we lowered the wireline to remove the center bit. At 1045 hr, we removed the 30-ft knobby drill pipe below the top drive so that we would have more space in the rig to work the pipe up and down. We attempted to work the drill string from 1045 to 1230 hr with maximum overpulls of 160 klb, torque of 650 A, and pump pressures to 3000 psi, but we were unable to raise, lower, or rotate the drill string. At this time we decided to prepare for severing the drill string while we continued trying to free it.

At 1600 hr, the drill string began to move ever so slowly with WOB = 150 klb overpull and pump = 100 spm and 3000 psi. The hole problems seemed to be associated with a relatively unconsolidated sediment section recovered in Core 97R. This was the section of hole where we had problems on the previous day. By 1715 hr, we were able to remove another 9.6-m section of drill pipe. At this point, we could slowly raise the drill string with progressively less overpull. We were able to raise the drill string from 1698.1 to 1678.9 mbsf and remove two more singles of drill pipe with 80 klb overpull and pressures of 3000 psi.

We then raised the bit from 1678.9 to 1131.2 mbsf with WOB overpulls = 20–25 klb, torque = 400–500 A, and pump pressures = 2000 psi. We continued to raise the bit up into the base of the 16-in casing using the top drive. This required overpull of 10–25 klb and torque of 400 A from 950 to 750 mbsf.

By this time, it was clear that Hole 1276A could not be deepened without casing the open hole above total depth, so we decided to terminate operations at the site. Before we pulled out of the hole, we wanted to identify the location of Hole 1276A with a marker buoy deployed from the subsea camera/sonar system. The bit cleared the seafloor at 0600 hr on 2 September. At 0615 hr we released the marker buoy 15 m from Hole 1276A at an azimuth of 225°. We then continued to retrieve the drill string and subsea camera/sonar. At 0910 hr we released the seafloor positioning beacon and it was back on deck at 1015 hr. Once the bit was back on the rig floor (1530 hr) we began the transit to proposed Site NNB-04A (Site 1277).

### **Transit to Site 1277 (Proposed Site NNB-04A)**

We began the transit from Site 1276 to Site 1277 at 1530 hr on 2 September. The beginning of the transit was delayed by 45 min because of a problem with the propulsion control system. Once the problem was resolved, the ship was under way at 1615 hr. After a transit of 21 nmi, we arrived at Site 1277 at 1800 hr. The ship was positioned over the site using GPS, and the thrusters were lowered by 1815 hr.

### **Site 1277**

Our aim at Site 1277 was to sample the lowermost 30 m of sediment and then core into basement of a shallowly buried ridge before we had to leave for St. John's. Basement was estimated to be at 136 mbsf, so we decided to drill without coring to 100 mbsf and then core until time ran out.

We assembled a RCB BHA and started lowering it the seafloor at 1830 hr on 2 September. We attached the top drive and deployed a wash core barrel (0230 hr on 3 September) in preparation for drilling. The bit tagged the seafloor at 0300 hr at 4639.4 mbrf. We drilled with the wash core barrel in place from 0 to 103.9 mbsf. Hard intervals were penetrated at 85–89 and 97.5–100 mbsf. The wash core barrel was retrieved, and it recovered 2.29 m of basement-related rocks, mostly basalts.

Cores 2R to 9R penetrated 103.9–180.3 mbsf and recovered 29.34 m (recovery = 38%). Coring parameters were WOB = 20 klb, bit rotation = 70 rpm, torque = 175 A, and circulation = 70 spm at 800 psi. ROP was 5.5 m/hr. Cores 6R to 8R were taken without plastic core liners to try to minimize core jamming and, hence, low recovery that we were experiencing. The AHC was run while cutting Cores 6R and 8R. We circulated 70 bbl of mud after Core 6R. The final core of Site 1277, Leg 210, and ODP (Core 9R) was on the rig floor at 1200 hr on 4 September. The last core of ODP was truly spectacular—a 10.5-m (recovery = 106%) core consisting of green and brown serpentinitized peridotite with calcite veins.

We removed the top drive at 1300 hr and we began to retrieve the drill string. The seafloor positioning beacon was recovered and back on board at 1500 hr on 4 September. The bit cleared the rig floor at 2345 hr. The DCs were taken apart, and the ship was secured for transit at 0100 hr on 5 September.

### **Transit to St. John's, Newfoundland**

We began the transit to St. John's at 0100 hr on 5 September. After traveling 374 nmi, the last scientific expedition of the Ocean Drilling Program concluded with the last line ashore at 1500 hr on 6 September 2003.

## REFERENCES

- Angori, E., and Monechi, S., 1996. High-resolution calcareous nannofossil biostratigraphy across the Paleocene/Eocene boundary at Caravaca (southern Spain). *Israel J. Earth Sci.*, 44:197–206.
- Austin, J.A., Jr., Tucholke, B.E., and Uchupi, E., 1989. Upper Triassic–Lower Jurassic salt basin southeast of the Grand Banks. *Earth Planet. Sci. Lett.*, 92:357–370.
- Balkwill, H.R., and Legall, F.D., 1989. Whale basin, offshore Newfoundland: extension and salt diapirism. In Tankard, A.J., and Balkwill, H.R. (Eds.), *Extensional Tectonics and Stratigraphy of the North Atlantic Margins*. AAPG Mem., 46:233–246.
- Bartek, L.R., Vail, P.R., Anderson, J.B., Emmet, P.A., and Wu, S., 1991. Effect of Cenozoic ice sheet fluctuations in Antarctica on the stratigraphic signature of the Neogene. *J. Geophys. Res.*, 96:6753–6778.
- Beard, J.S., Fullagar, P.D., and Sinha, A.K., 2002. Gabbroic pegmatite intrusions, Iberia Abyssal Plain, ODP Leg 173, Site 1070: magmatism during a transition from non-volcanic rifting to sea-floor spreading. *J. Petrology*, 43:885–905.
- Berggren, W.A., Kent, D.V., Swisher, C.C., III, and Aubry, M.-P., 1995. A revised Cenozoic geochronology and chronostratigraphy. In Berggren, W.A., Kent, D.V., Aubry, M.-P., and Hardenbol, J. (Eds.), *Geochronology, Time Scales and Global Stratigraphic Correlation*. Spec. Publ.—SEPM (Soc. Sediment. Geol.), 54:129–212.
- Beslier, M.-O., 1996. Seismic line LG12 in the Iberia Abyssal Plain. In Whitmarsh, R.B., Sawyer, D.S., Klaus, A., and Masson, D.G. (Eds.), *Proc. ODP, Sci. Results*. 149: College Station, TX (Ocean Drilling Program), 737–7390.
- Blechs Schmidt, G., 1979. Biostratigraphy of calcareous nannofossils: Leg 47B, Deep Sea Drilling Project. In Sibuet, J.C., Ryan, W.B.F., et al., *Init. Repts. DSDP*, 47 (Pt. 2): Washington (U.S. Govt. Printing Office), 327–360.
- Boillot, G., Beslier, M.-O., and Girardeau, J., 1995. Nature, structure and evolution of the ocean-continent boundary: the lesson of the west Galicia margin (Spain). In Banda, E. (Ed.), *Rifted Ocean-Continent Boundaries*: Netherlands (Kluwer Academic Publishers), 219–229.
- Boillot, G., Winterer, E.L., Meyer, A.W., et al., 1987. *Proc. ODP, Init. Repts.*, 103: College Station, TX (Ocean Drilling Program).
- Bouguigny, R., and Wilm, C., 1979. Tentative calibration of Site 398 and special processing of parts of Lines GP-19 and GP-23. In Sibuet, J.-C., Ryan, W.B.F., et al., *Init. Repts. DSDP*, 47 (Pt. 2): Washington (U.S. Govt. Printing Office), 623–629.
- Bralower, T.J., Zachos, J.C., Thomas, E., Parrow, M., Paull, C.K., Kelly, D.C., Premoli Silva, I., Sliter, W.V., and Lohmann, K.C., 1995. Late Paleocene to Eocene paleoceanography of the equatorial Pacific Ocean: stable isotopes recorded at Ocean Drilling Program Site 865, Allison Guyot. *Paleoceanography*, 10:841–865.
- Buck, W.R., 1991. Modes of continental lithospheric extension. *J. Geophys. Res.*, 96:20161–20178.
- Chian, D., and Loudon, K.E., 1995. Crustal structure of the Labrador Sea conjugate margin and implications for the formation of nonvolcanic continental margins. *J. Geophys. Res.*, 100:24239–24253.

- Davies, R., Cartwright, J., Pike, J., and Line, C., 2001. Early Oligocene initiation of North Atlantic Deep Water formation. *Nature*, 410:917–920.
- Dean, S.M., Minshull, T.A., Whitmarsh, R.B., and Loudon, K.E., 2000. Deep structure of the ocean–continent transition in the southern Iberia abyssal plain from seismic refraction profiles: the IAM-9 transect at 40°20'N. *J. Geophys. Res.*, 105:5859–5886.
- Dickens, G.R., Castillo, M.M., and Walker, J.G.C., 1997. A blast of gas in the latest Paleocene: simulating first-order effects of massive dissociation of oceanic methane hydrate. *Geology*, 25:259–262.
- Discovery 215 Working Group, 1998. Deep structure in the vicinity of the ocean–continent transition zone under the southern Iberia Abyssal Plain. *Geology*, 8:743–746.
- Driscoll, N.W., and Diebold, J.B., 1999. Tectonic and stratigraphic development of the eastern Caribbean: new constraints from multichannel seismic data. In Mann, P. (Ed.), *Caribbean Basins. Sedimentary Basins of the World, 4*: Amsterdam (Elsevier), 591–626.
- Driscoll, N.W., Hogg, J.R., Christie-Blick, N., and Karner, G.D., 1995. Extensional tectonics in the Jeanne d'Arc Basin, offshore Newfoundland: implications for the timing of break-up between Grand Banks and Iberia. In Scrutton, R.A., Stoker, M.S., Shimmiel, G.B., and Tudhope, A.W. (Eds.), *The Tectonics, Sedimentation and Palaeoceanography of the North Atlantic Region*. Geol. Soc. Spec. Publ., 90:1–28.
- Driscoll, N.W., and Karner, G.D., 1998. Lower crustal extension along the Northern Carnarvon Basin, Australia: evidence for an eastward dipping detachment. *J. Geophys. Res.*, 103: 4975–4992.
- Eldholm, O., Skogseid, J., Sundvor, E., and Myhre, A.M., 1990. The Norwegian-Greenland Sea. In Grantz, A., Johnson, L., and Sweeney, J.F. (Eds.), *The Geology of North America (Vol. L): The Arctic Ocean Region*. Geol. Soc. Am., 351–364.
- Enachescu, M.E., 1988. Extended basement beneath the intracratonic rifted basins of the Grand Banks of Newfoundland. *Can. J. Expl. Geophys.* 24:48–65.
- , 1987. Tectonic and structural framework of the northeast Newfoundland continental margin. In Beaumont, C., and Tankard, A.J. (Eds.), *Sedimentary Basins and Basin-Forming Mechanisms*. Spec. Publ.—Atl. Geosci. Soc., 5:117–146.
- Funck, T.J., Hopper, J.R., Larsen, H.C., Loudon, K., Holbrook, W.S., and Tucholke, B.E., in press. Crustal structure of the ocean–continent transition at Flemish Cap: seismic refraction results, *J. Geophys. Res.*
- Gardin, S., and Monechi, S., 1998. Paleocological change in middle to low-latitude calcareous nannoplankton at the Cretaceous/Tertiary boundary. *Bull. Soc. Geol. Fr.*, 169:709–723.
- González, A., Córdoba, D., and Vales, D., 1999. Seismic crustal structure of Galicia continental margin, NW Iberian Peninsula. *Geophys. Res. Lett.*, 26:1061–1064.
- Gradstein, F.M., Agterberg, F.P., Ogg, J.G., Hardenbol, J., van Veen, P., Thierry, J., and Huang, Z., 1995. A Triassic, Jurassic and Cretaceous time scale. In Berggren, W.A., Kent, D.V., Aubry, M.P., and Hardenbol, J. (Eds.), *Geochronology, Time Scales and Global Stratigraphic Correlation*. Spec. Publ.—SEPM (Soc. Sediment. Geol.), 54:95–126.
- Groupe Galice, 1979. The continental margin off Galicia and Portugal: acoustical stratigraphy, dredge stratigraphy, and structural evolution. In Sibuet, J.-C., Ryan,

- W.B.F., et al., *Init. Repts. DSDP*, 47 (Pt. 2): Washington (U.S. Govt. Printing Office), 633–662.
- Hopper, J.R., Funck, T., Tucholke, B.E., Larsen, H.C., Holbrook, W.S., Loudon, K., Shillington, D., and Lau, K.W.H., in press. Continental breakup and the onset of ultra-slow seafloor spreading off Flemish Cap on the Newfoundland rifted margin. *Geology*.
- Jansa, L.F., Bujak, J.P., and Williams, G.L., 1980. Upper Triassic salt deposits of the western North Atlantic. *Can. J. Earth Sci.*, 17:547–559.
- Jansa, L.F., Enos, P., Tucholke, B.E., Gradstein, F.M., and Sheridan, R.E., 1979. Mesozoic–Cenozoic sedimentary formations of the North American Basin, western North Atlantic. In Talwani, M., Hay, W., and Ryan, W.B.F. (Eds.), *Deep Drilling Results in the Atlantic Ocean: Continental Margins and Paleoenvironment*. Am. Geophys. Union, Maurice Ewing Ser., 3:1–57.
- Jansa, L.F., and Wade, J.A., 1975. Geology of the continental margin off Nova Scotia and Newfoundland. In Linden, W.J.M., and Wade, J.A. (Eds.), *Offshore Geology of Eastern Canada: Volume 2, Regional Geology*. Pap.—Geol. Surv. Can., 51–105.
- Kuhnt, W., and Urquhart, E., 2001. Tethyan flysch-type benthic foraminiferal assemblages in the North Atlantic: Cretaceous to Paleogene deep-water agglutinated foraminifers from the Iberia Abyssal Plain (ODP Leg 173). *Rev. Micropaleontol.*, 44:27–59.
- Larson, R.L., and Schlanger, S.O., 1981. Geological evolution of the Nauru Basin, and regional implications. In Larson, R.L., Schlanger, S.O., et al., *Init. Repts. DSDP*, 61: Washington (U.S. Govt. Printing Office), 841–862.
- Latin, D., and White, N., 1990. Generating melt during lithospheric extension: pure shear vs. simple shear. *Geology*, 18:327–331.
- Lau, K.W.H., Loudon, K.E., Funck, T., Hall, J., Deemer, S., Tucholke, B., Holbrook, W.S., Larsen, H.C., and Hopper, J.R., 2003. Seismic velocity model across the eastern Newfoundland (Grand Banks) continental margin [paper presented at Geol. Soc. Am. Northeastern Section 38th Annu. Meet., Halifax, Nova Scotia, March 2003, pap. no. 42-4].
- Leckie, R.M., Bralower, T.J., and Cashman, R., 2002. Oceanic anoxic events and plankton evolution: biotic response to tectonic forcing during the mid-Cretaceous. *Paleoceanography*, 17:10.1029/2001PA000623.
- Lister, G.S., Etheridge, M.A., and Symonds, P.A., 1986. Detachment faulting and evolution of passive continental margins. *Geology*, 14:246–250.
- , 1991. Detachment models for the formation of passive continental margins. *Tectonics*, 10:1038–1064.
- Loubrieu, B., Sibuet, J.-C., Monti, S., and Mazé, J.-P., 2002. Bay of Biscay and northeast Atlantic bathymetric map. *Eos*, 83:1358.
- Mauffret, A., Mougnot, D., Miles, P.R., and Malod, J.A., 1989. Results from multichannel reflection profiling of the Tagus Abyssal Plain (Portugal)—comparison with the Canadian margin. In Tankard, A.J., and Balkwill, H.R. (Eds.), *Extensional Tectonics and Stratigraphy of the North Atlantic Margins*. AAPG Mem., 46:379–393.

- McGonigal, K.L., and Wise, S.W., Jr., 2001. Eocene calcareous nannofossil biostratigraphy and sediment accumulation of turbidite sequences on the Iberia Abyssal Plain, ODP Sites 1067–1069. In Beslier, M.-O., Whitmarsh, R.B., Wallace, P.J., and Girardeau, J. (Eds.), *Proc. ODP, Sci. Results*, 173, 1–35 [Online]. Available from World Wide Web: <[http://www-odp.tamu.edu/publications/173\\_SR/VOLUME/CHAPTERS/SR173\\_04.PDF](http://www-odp.tamu.edu/publications/173_SR/VOLUME/CHAPTERS/SR173_04.PDF)>. [Cited 2003-09-05]
- McKenzie, D., 1978. Some remarks on the development of sedimentary basins. *Earth Planet. Sci. Lett.*, 40:25–32.
- Miller, K.G., and Tucholke, B.E., 1983. Development of Cenozoic abyssal circulation south of the Greenland–Scotland Ridge. In Bott, M., Saxov, S., Talwani, M., and Thiede, J. (Eds.), *Structure and Development of the Greenland–Scotland Ridge: New Methods and Concepts*: New York (Plenum), 549–590.
- Mountain, G.S., and Tucholke, B.E., 1985. Mesozoic and Cenozoic geology of the U.S. Atlantic continental slope and rise. In Poag, C.W. (Ed.), *Geologic Evolution of the United States Atlantic Margin*: New York (Van Nostrand Reinhold), 293–341.
- Mutter, J.C., 1993. Margins declassified. *Nature*, 364:393–394.
- Mutter, J.C., Buck, W.R., and Zehnder, C.M., 1988. Convective partial melting, 1. A model for the formation of thick basaltic sequences during the initiation of spreading. *J. Geophys. Res.*, 93:1031–1048.
- Nunes, G.T., 2002. Crustal velocity structure of the Newfoundland nonvolcanic rifted margin [M.S. thesis]. Univ. of Wyoming, Laramie.
- ODP Leg 173 Shipboard Scientific Party, 1998. Drilling reveals transition from continental breakup to early magmatic crust. *Eos*, 79:173, 180–181.
- Osler, J.C., and Louden, K.E., 1995. The extinct spreading centre in the Labrador Sea: crustal structure from a 2-D seismic refraction velocity model. *J. Geophys. Res.*, 100:2261–2278.
- Pérez-Gussinyé, M., Ranero, C.R., Reston, T.J., and Sawyer, D., 2003. Mechanisms of extension at nonvolcanic margins: evidence from the Galicia Interior Basin, west of Iberia. *J. Geophys. Res.*, 108:10.1029/2001JB000901.
- Pickup, S.L.B., Whitmarsh, R.B., Fowler, C.M.R., and Reston, T.J., 1996. Insight into the nature of the ocean–continent transition off West Iberia from a deep multichannel seismic reflection profile. *Geology*, 24:1079–1082.
- Pinheiro, L.M., Whitmarsh, R.B., and Miles, P.R., 1992. The ocean-continent boundary off the western continental margin of Iberia, II. Crustal structure in the Tagus Abyssal Plain. *Geophys. J.*, 109:106–124.
- Rasmussen, E.S., Lomholt, S., Andersen, C., and Vejbaek, O.V., 1998. Aspects of the structural evolution of the Lusitanian Basin in Portugal and the shelf and slope area offshore Portugal. *Tectonophysics*, 300:199–225.
- Réhault, J.-P., and Mauffret, A., 1979. Relationships between tectonics and sedimentation around the northwestern Iberian margin. In Sibuet, J.-C., Ryan, W.B.F., et al., *Init. Repts. DSDP*, 47 (Pt. 2): Washington (U.S. Govt. Printing Office), 663–681.
- Reid, I.D., 1994. Crustal structure of a nonvolcanic rifted margin east of Newfoundland. *J. Geophys. Res.*, 99:15161–15180.

- Reston, T.J., 1996. The S reflector west of Galicia: the seismic signature of a detachment fault. *Geophys. J. Int.*, 127:230–244.
- Reston, T.J., Krawczyk, C.M., and Hoffmann, H.J., 1995. Detachment tectonics during Atlantic rifting: analysis and interpretation of the S reflection, the west Galicia margin. In Scrutton, R.A., Stoker, M.S., Shimmiel, G.B., Tudhope, A.W. (Eds.), *Tectonics of the North Atlantic Region*. Spec. Publ.—Geol. Soc. London, 90:93–109.
- Rosendahl, B.R., 1987. Architecture of continental rifts with special reference to East Africa. *Annu. Rev. Earth Planet. Sci.*, 15:445–503.
- Russell, S.M., and Whitmarsh, R.B., 2003. Magmatism at the West Iberia non-volcanic rifted continental margin: evidence from analyses of magnetic anomalies. *Geophys. J. Int.*, 154:706–730.
- Schärer, U., Girardeau, J., Cornen, G., and Boillot, G., 2000. 138–121 Ma asthenospheric magmatism prior to continental break-up in the North Atlantic and geodynamic implications. *Earth Planet. Sci. Lett.*, 181:555–572.
- Schärer, U., Kornprobst, J., Beslier, M.-O., Boillot, G., and Girardeau, J., 1995. Gabbro and related rock emplacement beneath rifting continental crust: U–Pb geochronological and geochemical constraints for the Galicia passive margin (Spain). *Earth Planet. Sci. Lett.*, 130:187–200.
- Shipboard Scientific Party, 1979. Site 398. In Sibuet, J.-C., Ryan, W.B.F., et al., *Init. Repts. DSDP*, 47 (Pt. 2): Washington (U.S. Govt. Printing Office), 25–233.
- Shipboard Scientific Party, 1998. Leg 173 introduction. In Whitmarsh, R.B., Beslier, M.O., Wallace, P.J., et al., *Proc. ODP, Init. Repts.*, 173: College Station, TX (Ocean Drilling Program), 7–23.
- Sigal, J., 1979. Chronostratigraphy and ecostratigraphy of Cretaceous formations recovered on DSDP Leg 47B, Site 398. In Sibuet, J.-C., Ryan, W.B.F., et al., *Init. Repts. DSDP*, 47 (Pt. 2): Washington (U.S. Govt. Printing Office), 287–326.
- Srivastava, S.P., and Roest, W.R., 1999. Extent of oceanic crust in the Labrador Sea. *Mar. Pet. Geol.*, 16:65–84.
- Srivastava, S.P., Sibuet, J.-C., Cande, S., Roest, W.R., and Reid, I.R., 2000. Magnetic evidence for slow seafloor spreading during the formation of the Newfoundland and Iberian margins. *Earth Planet. Sci. Lett.*, 182:61–76.
- Tankard, A.J., and Welsink, H.J., 1987. Extensional tectonics and stratigraphy of Hibernia oil field, Grand Banks, Newfoundland. *AAPG Bull.*, 71:1210–1232.
- Thomas, E., and Shackleton, N., 1996. The Palaeocene–Eocene benthic foraminiferal extinction and stable isotope anomalies. In Knox, R.W.O’B., Corfield, R.M., and Dunay, R.E. (Eds.), *Correlation of the Early Paleogene in Northwest Europe*. Spec. Publ.—Geol. Soc. London, 101:401–441.
- Tucholke, B.E., Austin, J.A., and Uchupi, E., 1989. Crustal structure and rift-drift evolution of the Newfoundland Basin. In Tankard, A.J., and Balkwell, H.R. (Eds.), *Extensional Tectonics and Stratigraphy of the North Atlantic Margins*. AAPG Mem., 46:247–263.
- Tucholke, B.E., Driscoll, N.W., and Holbrook, W.S., 1999. The asymmetric Newfoundland–Iberia rift. In *Non-Volcanic Rifting of Continental Margins: A Comparison of Evidence from Land and Sea*: London (Geol. Soc.), 48. (Abstract)

- Tucholke, B.E., and Ludwig, W.J., 1982. Structure and origin of the J Anomaly Ridge, western North Atlantic Ocean. *J. Geophys. Res.*, 87:9389–9407.
- Tucholke, B.E., and Mountain, G.S., 1979. Seismic stratigraphy, lithostratigraphy, and paleosedimentation patterns in the North American Basin. In Talwani, M., Hay, W., and Ryan, W.B.F. (Eds.), *Deep Drilling Results in the Atlantic Ocean: Continental Margins and Paleoenvironment*. Am. Geophys. Union, Maurice Ewing Ser., 3:58–86.
- Tucholke, B.E., Vogt, P.R., et al., 1979. *Init. Repts. DSDP*, 43: Washington (U.S. Govt. Printing Office).
- Wagner, T., and Pletsch, T., 2001. No major thermal event on the mid-Cretaceous Côte d'Ivoire-Ghana Transform Margin. *Terra Nova*, 13:165–171.
- Wernicke, B., 1985. Uniform sense normal simple shear of the continental crust. *Can. J. Earth Sci.*, 22:108–125.
- White, R.S., and McKenzie, D., 1989. Magmatism at rift zones: the generation of volcanic continental margins and flood basalts. *J. Geophys. Res.*, 94:7685–7729.
- White, R.S., Spence, G.D., Fowler, S.R., McKenzie, D.P., Westbrook, G.K., and Bowen, A.N., 1987. Magmatism at rifted continental margins. *Nature*, 330:439–444.
- Whitmarsh, R.B., Manatschal, G., and Minshull, T.A., 2001. Evolution of magma-poor continental margins from rifting to seafloor spreading. *Nature*, 413:150–154.
- Whitmarsh, R.B., and Miles, P.R., 1995. Models of the development of the West Iberia rifted continental margin at 40°30'N deduced from surface and deep-tow magnetic anomalies. *J. Geophys. Res.*, 100:3789–3806.
- Whitmarsh, R.B., Miles, P.R., and Mauffret, A., 1990. The ocean-continent boundary off the western continental margin of Iberia, I. Crustal structure at 40°30'N. *Geophys. J. Int.*, 103:509–531.
- Whitmarsh, R.B., and Sawyer, D.S., 1996. The ocean/continent transition beneath the Iberia Abyssal Plain and continental-rifting to seafloor-spreading processes. In Whitmarsh, R.B., Sawyer, D.S., Klaus, A., and Masson, D.G. (Eds.), *Proc. ODP, Sci. Results*, 149: College Station, TX (Ocean Drilling Program), 713–733.
- Whitmarsh, R.B., White, R.S., Horsefield, S.J., Sibuet, J.-C., Recq, M., and Louvel, V., 1996. The ocean-continent boundary off the western continental margin of Iberia: crustal structure west of Galicia Bank. *J. Geophys. Res.*, 101:28291–28314.
- Wilson, R.C.L., Hiscott, R.N., Willis, M.G., and Gradstein, F.M., 1989. The Lusitanian Basin of west-central Portugal: Mesozoic and Tertiary tectonic, stratigraphic, and subsidence history. In Tankard, A.J., and Balkwill, H.R. (Eds.), *Extensional Tectonics and Stratigraphy of the North Atlantic Margins*. AAPG Mem., 46:265–282.
- Wilson, R.C.L., Manatschal, G., and Wise, S., 2001. Rifting along non-volcanic passive margins: stratigraphic and seismic evidence from the Mesozoic of the Alps and Western Iberia. In Wilson, R.C.L., Whitmarsh, R.B., Taylor, B., and Froitzheim, N. (Eds.), *Non-Volcanic Rifting of Continental Margins: A Comparison of Evidence From Land and Sea*. Geol. Soc. Spec. Publ., 187:429–452.
- Zachos, J.C., Lohmann, K.C., Walker, J.C.G., and Wise, S.W., Jr., 1993. Abrupt climate changes and transient climates during the Paleogene: a marine perspective. *J. Geol.*, 101:191–213.

## TABLE CAPTIONS

Table T1. Predicted depths of major reflection boundaries at Site 1276 from MCS velocity data.

Table T2. Leg 210 coring summary.

## FIGURE CAPTIONS

Figure F1. Bathymetric map of the North Atlantic Ocean showing locations of Site 1276 in the Newfoundland Basin and DSDP and ODP drill sites on the western and southern margins of Galicia Bank on the conjugate Iberia margin (Legs 47B, 103, 149, 173).

Figure F2. Summary diagram of rift events in the Newfoundland–Iberia rift. Leg 210 drilling was at the boundary between the central and northern rift segments (black triangle at top of the figure). The green intervals show principal periods of rifting, and the vertically hatched intervals indicate hiatuses, most of which probably developed because of tectonic uplift associated with rifting. “E” at the bottom indicates evaporites deposited in shallow rift basins during the Late Triassic to Early Jurassic. Minor magmatism in the rift is documented south of Tagus Abyssal Plain in Gorringer Bank (Schärer et al., 2000) and on Galicia Bank (Schärer et al., 1995; Beard et al., 2002). The Southeast Newfoundland Ridge at the southern margin of Newfoundland Basin was a major locus of volcanism in the Barremian–Aptian (Tucholke and Ludwig, 1982). Open arrows = earliest proposed seafloor spreading, solid arrows = estimates for latest initiation of spreading. (Southern segment earliest = 145–131 Ma [Anomaly M20–M11] [Srivastava et al., 2000; Mauffret et al., 1989]; central segment earliest = 140 Ma [M17] [Srivastava et al., 2000], latest = 127–125 Ma [M5–M3] [Whitmarsh and Miles, 1995; Russell and Whitmarsh, 2003]; northern segment = ~122 Ma [M0] [Srivastava et al. 2000; Boillot et al., 1987]). Other data are compiled from Enachescu (1987), Tankard and Welsink (1987), Wilson (1988), Balkwill and Legall (1989), Murillas et al. (1990), Driscoll et al., (1995), Rasmussen et al. (1998), and Wilson et al. (2001).

Figure F3. **A.** Reconstruction of the Newfoundland–Iberia rift to Anomaly M0 time (121 Ma), based on the reconstruction pole of Srivastava et al., 2000. Newfoundland plate is fixed in present geographic coordinates. Solid circles = locations of Sites 1276 and 1277 in the Newfoundland Basin plus DSDP and ODP drill sites on the conjugate Iberia margin. Tectonic and other data are compiled from numerous sources (structural data from the SCREECH survey [Fig. F5] are not included). Light red = evaporites in continental rift basins. Ocean crust (center, blue) is presumed to have formed beginning near Anomaly M3. A south–north zipperlike opening would account for the observed splayed tectonic trends between the two margins and the northward-narrowing zone of ocean crust. On the Newfoundland side, U extends throughout the Newfoundland Basin and pinches out seaward near Anomaly M3. **B.** M0 reconstruction as in A, with locations of reflection profiles. Solid lines show locations of profiles in Figure F4 and dotted lines show positions of other SCREECH transects not illustrated here (see Fig. F5). BMT. = basement, SMT(S) = seamount(s). NFLD. = Newfoundland, A.P. = abyssal plain, FL. = Flemish, N.B. = Newfoundland Basin. F.Z. = fracture zone, T.Z. = transition zone.

**Figure F4.** Conjugate seismic reflection sections from the Newfoundland and Iberia margins, juxtaposed at Anomaly ~M1. Profiles are displayed north to south (top to bottom), and locations are shown in Figure F3B. Vertical exaggeration = ~12.5. On the Newfoundland side, sediments are shaded brown above basement and/or the intersecting U reflection; on the Iberia side, sediments are similarly shaded above basement. Top left: Simplified interpretation of SCREECH line 2MCS with location of Site 1276. Top right: Composite seismic section (*Sonne 16, JOIDES Resolution, Lusigal 12, OC 103*) along the conjugate Iberia drilling transect, adapted from ODP Leg 173 Scientific Party (Shipboard Scientific Party, 1998). Drill sites are numbered and lithology at the bottom of holes is indicated. Center left: *Conrad* multichannel seismic (MCS) line NB1 about 150 km south of SCREECH Line 2MCS, showing another view of Newfoundland basement structure and the overlying U reflection. Center right: MCS line IAM9 about 50 km south of *Lusigal 12* off Iberia. Bottom left: *Conrad* MCS line NB19 in southern Newfoundland Basin. Bottom right: Conjugate MCS profile *Lusitanie 86* over Tagus Abyssal Plain. Note the marked asymmetries in basement depth and roughness between the Newfoundland and Iberia sides of the rift.

**Figure F5.** Track line map showing three transects of the SCREECH survey (*Ewing* cruise 00-07) across the Newfoundland continental margin. Leg 210 drilling was on transect 2 (see Fig. F6). Bathymetric contour interval = 200 m.

**Figure F6.** Track line map of the SCREECH survey (*Ewing* cruise 00-07) along transect 2, conjugate to the ODP Leg 149/173 drilling transect on the Iberia margin (see Fig. F3B). Locations of Leg 210 Sites 1276 and 1277 are indicated. The black section of track line locates the section of reflection profile 2MCS illustrated in Figure F8. Bathymetric contour interval = 200 m.

**Figure F7.** Bathymetry of the northern Newfoundland Basin showing the locations of Sites 1276 and 1277.

**Figure F8.** SCREECH line 2MCS from the central Newfoundland continental rise seaward to oceanic crust east of Anomaly M0, illustrated in three sections. Location is shown in Figure F6. **A.** Lower continental rise. The basement block at center is the landward side of the Flemish Hinge and is capped by probably lower Mesozoic, prerift sediments. Major deep-basin reflections and seismic sequences to the east are identified. **B.** Lowermost continental rise and western margin of the abyssal plain with Sites 1276 and 1277, major reflections, seismic sequences, and magnetic anomaly locations identified. **C.** Seaward portion over the abyssal plain, with Horizon A<sup>u</sup> and location of Anomaly M0 indicated. CMP = common midpoint, Unc. = unconformity.

**Figure F9.** Simplified interpretation of SCREECH line 2MCS across the Newfoundland continental margin, with magnetic anomaly locations of Srivastava et al. (2000) indicated. Line location is shown in Figure F5.

**Figure F10.** Isopach map of the U–basement interval showing two-way traveltime between the U reflection and basement, based on MCS profiles of the SCREECH survey (*Ewing* cruise 00-07) along transect 2. Locations of Sites 1276 and 1277 are indicated. Note that the deposits below the U reflection fill depressions between basement ridges. Interpretation of an U–basement interval southeast of Site 1277 is tentative; the U reflection cannot be traced continuously to this location from farther west in existing seismic data, and the possible U reflection there is inferred only on the basis of reflection character and depth (see, e.g., Fig. F9 for one example of possible occurrence of U in this zone).

**Figure F11.** Schematic models to explain observed deep structural asymmetries between the Newfoundland (left) and Iberia (right) transition zones. **A.** Synrift extension of continental crust. In the central part of the rift, lower crust is thinned ductilely (dashes) but brittle upper crust has limited tectonic extension (e.g., Driscoll and Karner, 1998). **B.** Anomaly ~M3; the rift evolves asymmetrically, with a thin remnant of continental crust forming an upper, Newfoundland plate, and serpentinized peridotite and remnants of ductilely thinned lower crust forming a lower, Iberia plate. Bending stresses may account for faulting in the cold, brittle mantle footwall as it is exhumed on the Iberia side. Differences of basement depth on the two margins reflect buoyancy of thin continental crust (shallow) vs. serpentinized mantle (deep). The U reflection could be compared to a synrift unconformity developed near sea level, basalt flows, or high-velocity sediments (see C and D). **C.** Alternate model at Anomaly ~M3; mantle is exposed on both sides of the rift at an early stage, followed by development of an asymmetric shear. Melt extracted from the lower plate may permeate the Newfoundland upper plate and flood its surface to form the U-to-basement sequence in a submarine setting. Basement depth differences between the two margins reflect buoyancy differences caused by melt intrusion/extrusion on the Newfoundland side. **D.** Second alternate model at Anomaly ~M3; ultra-slow seafloor spreading. Symmetrical spreading is unlikely because it would not account for extensive exposure of serpentinized mantle on the Iberia side or asymmetry in basement structure of the transition zones on the two margins. Rather, ocean crust may have formed in the western part of the rift by seafloor spreading after initial exposure of mantle, with the ocean crust subsequently being isolated on the Newfoundland side by a jump of the spreading axis (from a failed rift [FR] eastward to a more central location). The U-basement sequence might be explained by basalt flows capping the ocean crust or as a high-velocity sedimentary sequence. More buoyant Newfoundland ocean crust would be shallower than serpentinized mantle on the Iberia side, and differences in basement roughness would reflect dissimilar tectonic extension in the two kinds of lithosphere. MOHO = Mohorovicic discontinuity.

**Figure F12.** Proposed drilling and casing plan for the deep hole drilled at Site 1276. RCB = rotary core barrel, VSP = vertical seismic profile.

**Figure F13.** Synthesis of lithostratigraphic units recognized at Site 1276. Columns show recovery (solid black boxes), age, lithology on a core-by-core basis (see separate key), grain size and color variation (pseudoweathering profile and separate color key), and primary characteristics.

**Figure F14.** Close-up photograph of typical poorly sorted muddy sandstone of lithologic Unit 4 (interval 210-1276-29R-1, 90–120 cm). Note the intense burrowing and reddish color attributed to well-oxygenated bottom waters.

**Figure F15.** Close-up photograph of massive, poorly sorted grainstone with carbonate granules (mainly bioclasts) and abundant large mud clasts in lithologic Unit 1 (interval 210-1276A-7R-2, 16–41). The sediment has a swirled appearance because of soft-sediment deformation and differential compaction.

**Figure F16.** Close-up photograph of central part of a chaotic mud-clast conglomerate in lithologic Subunit 5C (interval 210-1276A-93R-3, 70–97 cm). Note the range in color of the mudstone clasts and the variety of clast shapes.

**Figure F17.** Close-up photograph of an excellent example of repeated graded beds in lithologic Unit 2 (interval 210-1276A-9R-2, 96–120 cm). Note the sharp bases of these turbidites and upward fining into burrowed and laminated intervals.

**Figure F18.** Close-up photograph of planar-laminated carbonate grainstone grading upward into marlstone in lithologic Unit 3 (interval 210-1276A-19R-5, 80–112 cm). Above 99 cm, there are contorted and flattened laminae and pockets of silt that formed when the sediment was in a plastic state.

**Figure F19.** Close-up photograph of middle part of a highly disorganized gravity flow deposit in lithologic Subunit 5C (interval 210-1276A-89R-6, 80–115 cm). Note the planar lamination (at 104–111 cm) passing upward into a convoluted and swirled interval (at 81–100 cm). Such flow features characterize this lithologic subunit.

**Figure F20.** Comparison of **(A)** core photograph and **(B)** computed tomography (CT) scan of a porphyroblastic mudrock created by thermal and hydrothermal effects of the intrusion of the upper diabase sill in lithologic Subunit 5C (interval 210-1276A-87R-6, 18–27 cm). The CT scan is a horizontal slice through a three-dimensional reconstructed image, viewed with IMAGEJ software. Note the apparent near-random orientation of the porphyroblasts.

**Figure F21.** Close-up photograph of very finely laminated black shale with planar siltstone laminae and a small siltstone lens (at 96 cm) in lithologic Subunit 5B (interval 210-1276A-43R-2, 88–117 cm).

**Figure F22.** Simplified time-stratigraphic chart comparing the lithostratigraphic successions encountered on the Newfoundland and Iberia conjugate margins. For comparison, a similar summary is provided (at right) for the geographically separate North American Basin in the western central North Atlantic. Lithologic units are shown on the left sides of the columns, and the thickness of the units are shown on the right sides. TD = total depth.

**Figure F23.** Summary of core recovery and observations of segregation bands, grain size, degree of alteration, thin section sample locations, textures, and minerals from X-ray diffraction data for the upper igneous sill at Site 1276. Photomicrographs 2i, 13i, and 6i show the texture denoted in the texture column. Photomicrograph 4i shows the composition of a segregation band. The alteration is shown with gray shades, where dark gray is complete alteration and lighter shades are moderate. The recovery of the core is shown in red. Plag = plagioclase, cpx = clinopyroxene, mag = magnetite.

**Figure F24.** Age-depth plot based on first and last occurrences datums (FOs and LOs) of microfossils at Site 1276 and DSDP Site 398. Dashed lines represent intervals in which no samples were analyzed, age-diagnostic datums are uncertain, or in which samples were found to be barren. Approximate sedimentation rates at Site 1276 which are based on calcareous nannofossils are shown in blue, while those based on palynomorphs are depicted in red.

**Figure F25.** Downhole plots of  $\text{CaCO}_3$ , TOC,  $C_1$ , and  $C_2$  concentrations and C/N ratios, Site 1276. Core lithology and recovery are shown on the left.

**Figure F26.** Composite physical property plots of smoothed NGR, z-velocity, bulk density, and porosity plotted against depth and for Site 1276, with lithology, lithologic boundaries, and grain size also indicated. Lithology and sedimentary facies keys are also shown.

**Figure F27.** Schematic lithologic column in a “weathering profile,”  $\alpha$ -velocity, porosity, and methane ( $\phi$ ) plots vs. depth for the lowermost 50 m of Site 1276 (1675–1725 mbsf). Right-hand border on the lithologic column indicates relative degree of compaction. Black circles indicate shipboard measurements. Dashed red lines are trend lines for each data set for sediments in lithologic Subunit 5C above the anomalous sediments.

**Figure F28.** (top) Time-migrated seismic SCREECH profile 2MCS with location of main seismic reflections and location of Site 1276; (bottom) Time-migrated IFP-CNEXO seismic profile GP-19 (Bouguigny and Wilm, 1979) with location of main seismic reflections and location of Site 398. CMP = common midpoint.

**Figure F29.** Correlation between seismic sequences and lithologic breaks and age at Site 1276 and that at Site 398 (Shipboard Scientific Party, 1979). CMP = common midpoint.

**Figure F30.** Isopach map of acoustic Unit 4 beneath the orange reflection on the Iberia margin. Sources are: (1) the isopach map of acoustic Unit 4 by Réhault and Mauffret (1979) from available seismic data in 1975; (2) MCS lines acquired in 1997 by the *Maurice Ewing* during the Iberian Seismic Experiment (ISE, Dale Sawyer, Principal Investigator), MCS line IAM 9 (Pickup et al., 1996), and MCS line *Lusigal* 12 (Beslier, 1996); (3) the Iberia Abyssal Plain basement map (Shipboard Scientific Party, 1998) compiled from all available seismic data in the IAP; and (4) a detailed bathymetric map of the northeast Atlantic Ocean (Loubrieu et al., 2002).

**Figure F31.** Sedimentation rates at Sites 398 (Shipboard Scientific Party, 1979) and 1276; timescale from Berggren et al. (1995) and Gradstein et al. (1995). Site 398 seismic sequence (numbers) (Shipboard Scientific Party, 1979) and Site 1276 seismic sequence (letters) are shown.

**Figure F32.** Schematic illustration of actual Site 1276 installation and cored intervals. The depth of the seafloor was determined by observing a reduction in drill string weight, so the seafloor depth of 4549.1 m below sea level is likely deeper than the true sediment/water interface. The exact sediment thickness over the reentry cone is unknown. ODL = Overseas Drilling, Ltd.

**Figure F33.** Breakdown of operational activities while on site.

Table T1. Predicted depths of major reflection boundaries at Site 1276 from MCS velocity data.

Reflection boundary	Predicted depth (mbsf)	Average interval velocity to overlying boundary (km/s)
Base of turbidites	50	~1.87
Base of fan	711	~1.87
Horizon A	966	2.22
Reflection U	1866	2.73
Basement	2080	3.50

Table T2. Leg 210 coring summary.

Hole	Latitude	Longitude	Seafloor depth (mbrf)	Number of cores	Interval cored (m)	Core recovered (m)	Recovery (%)	Interval drilled (m)	Total penetration (m)	Time on hole (days)
1276A	45° 24.3198' N	44° 47.1496' W	4560.0	103	936.9	796.72	85	800.0	1736.9	46.78
1277A	45° 11.8002' N	44° 25.5999' W	4639.4	8	76.4	29.24	38	7.0	83.4	2.22
<b>LEG 210 TOTALS:</b>				<b>111</b>	<b>1013.30</b>	<b>825.96</b>	<b>82%</b>	<b>807.0</b>	<b>1820.3</b>	<b>49.00</b>

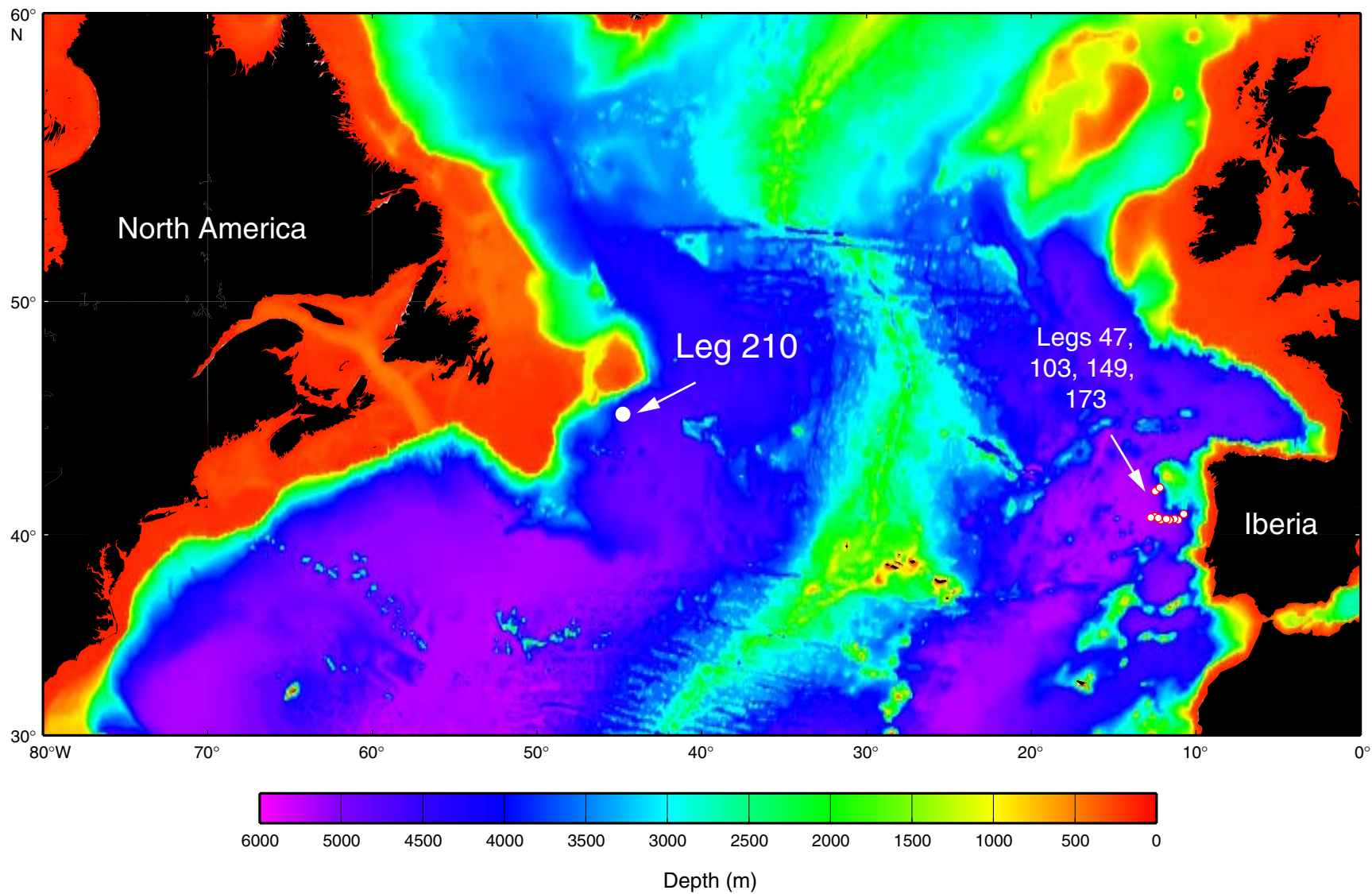


Figure F1

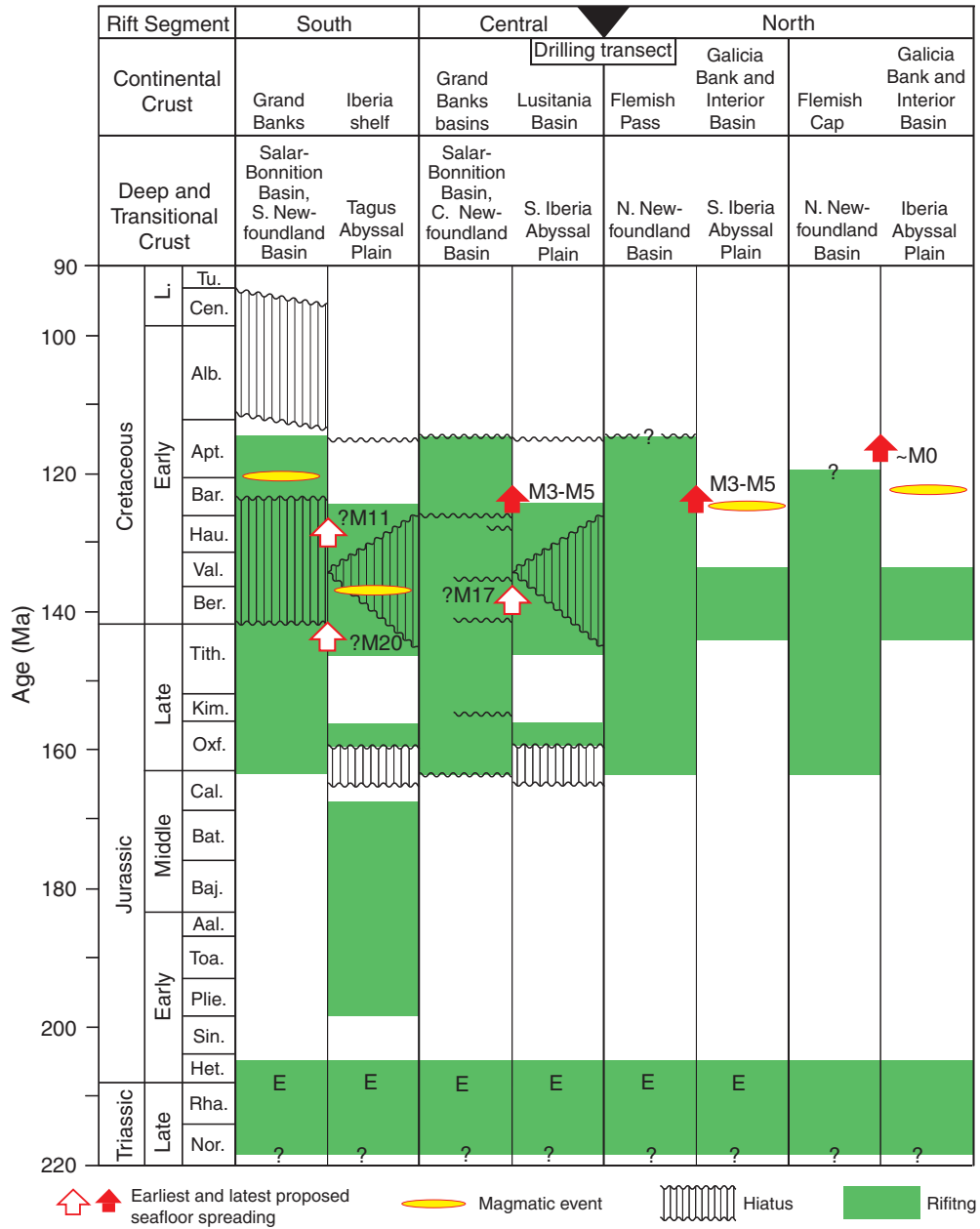


Figure F2

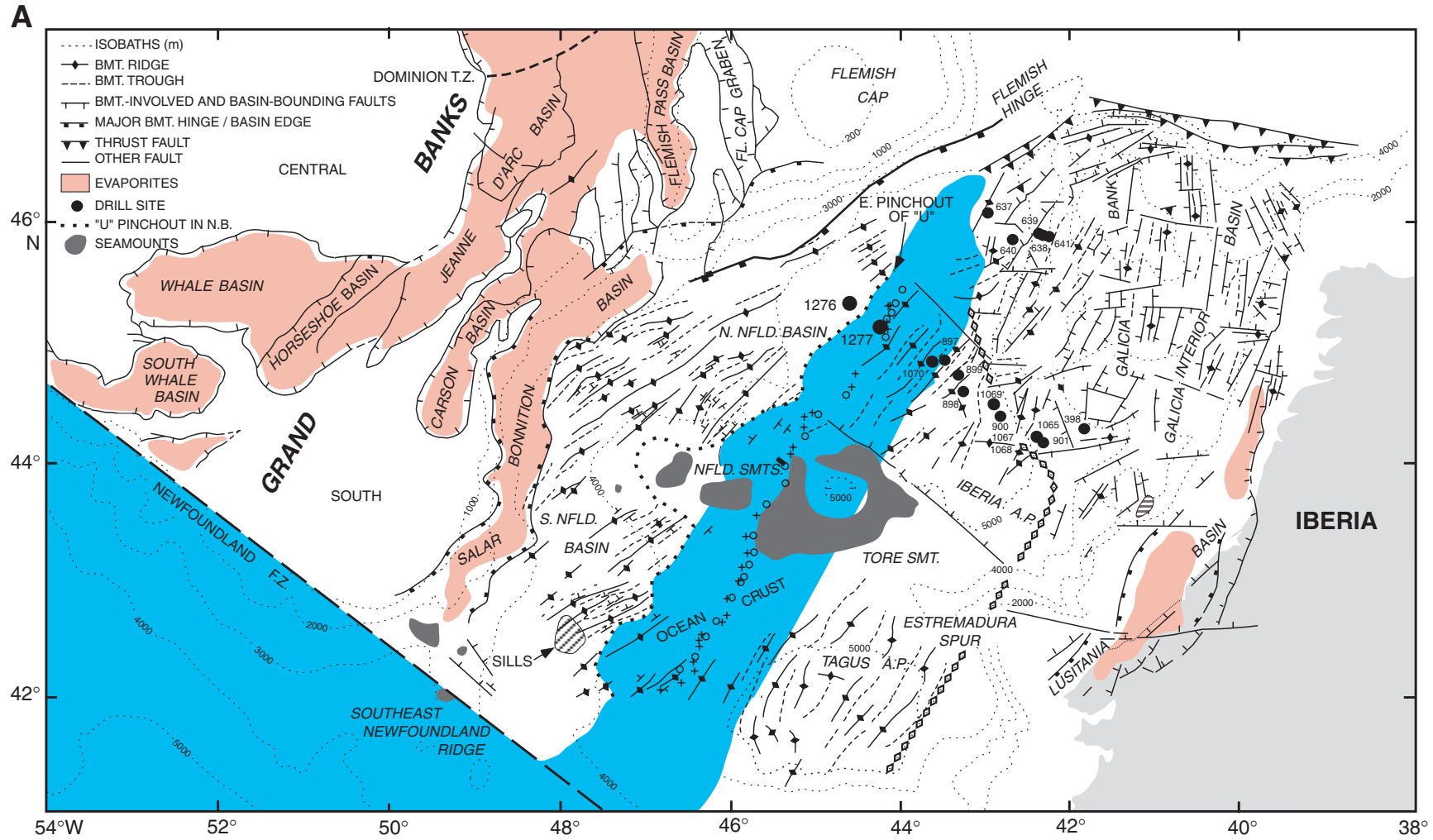


Figure F3

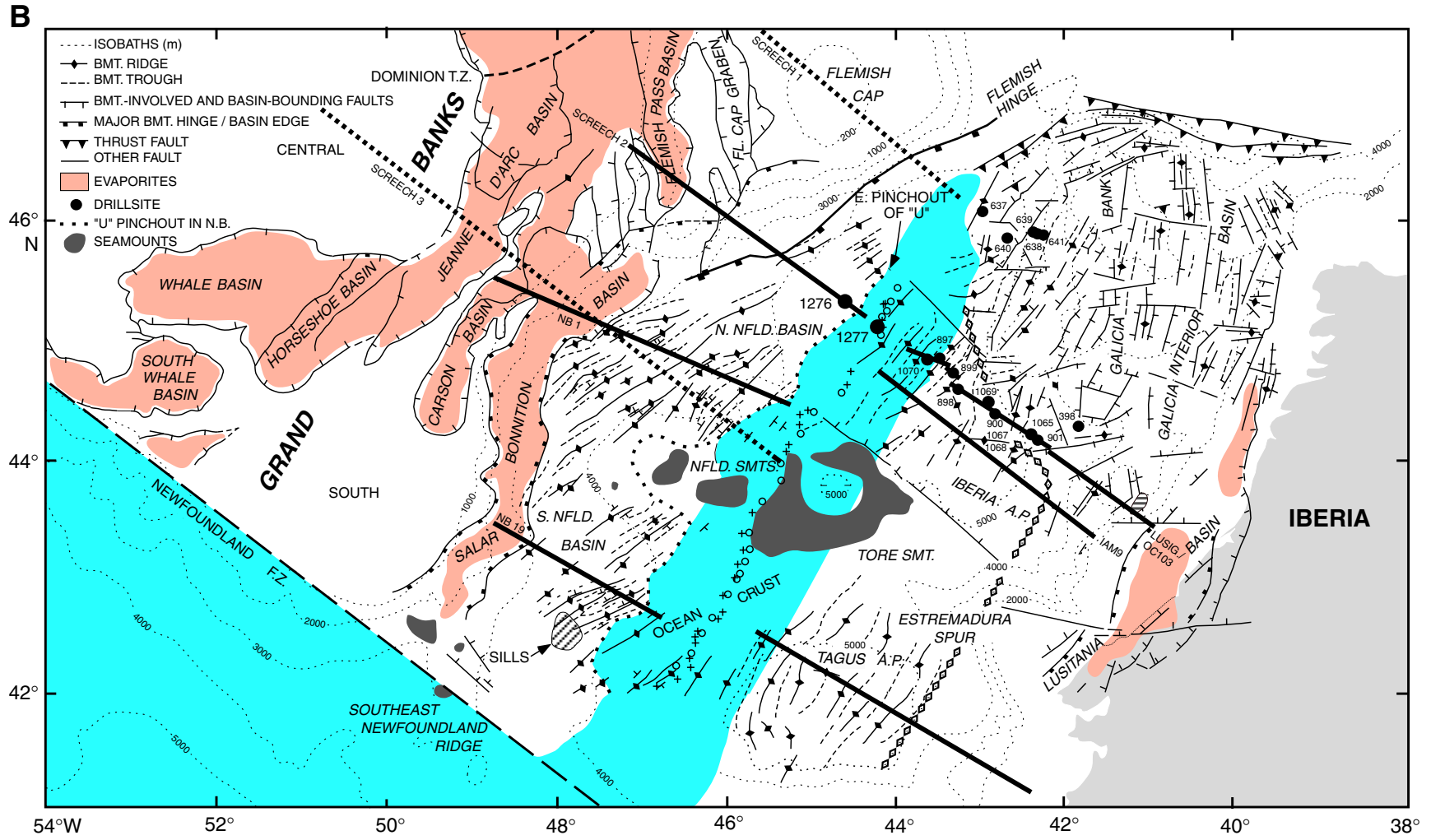
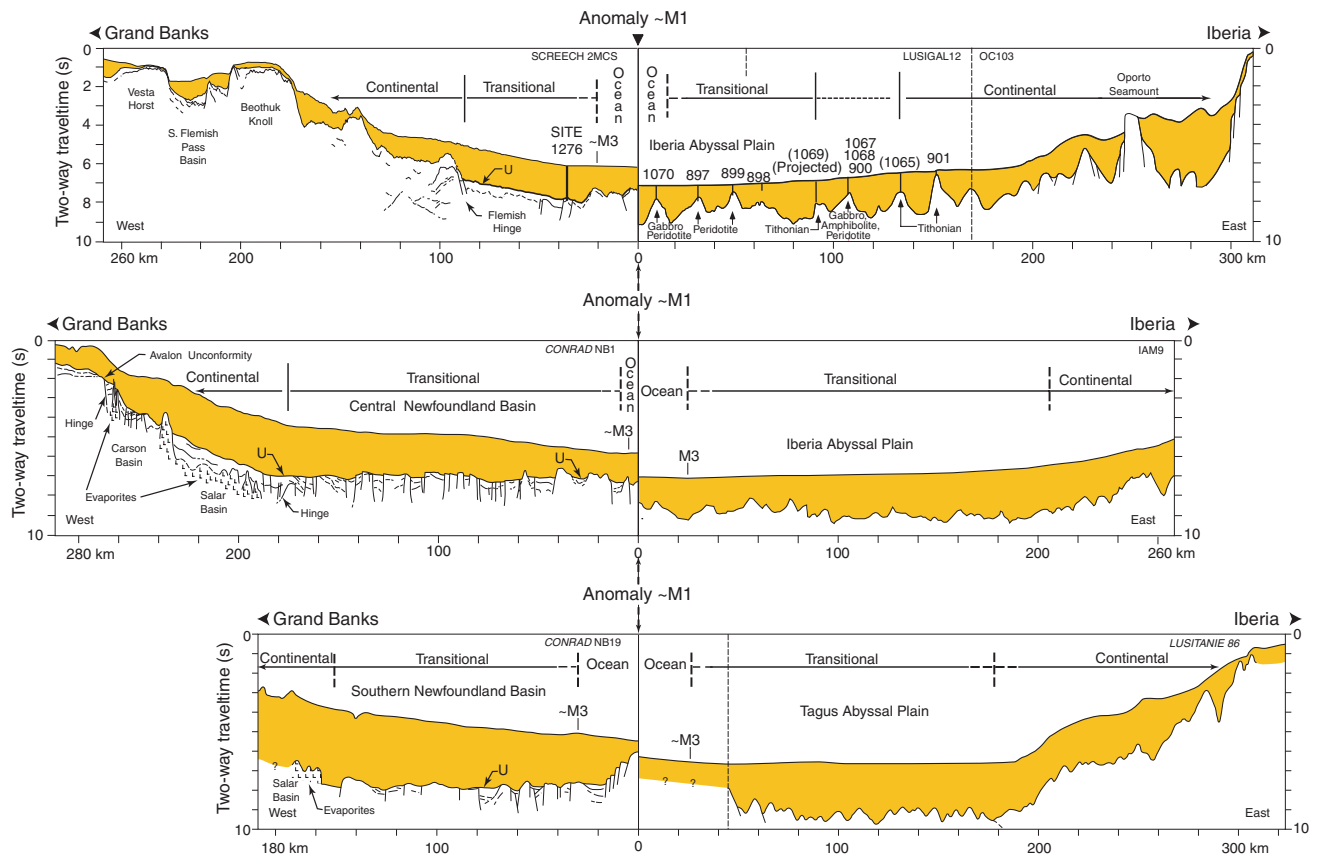


Figure F3 (continued)



**Figure F4**

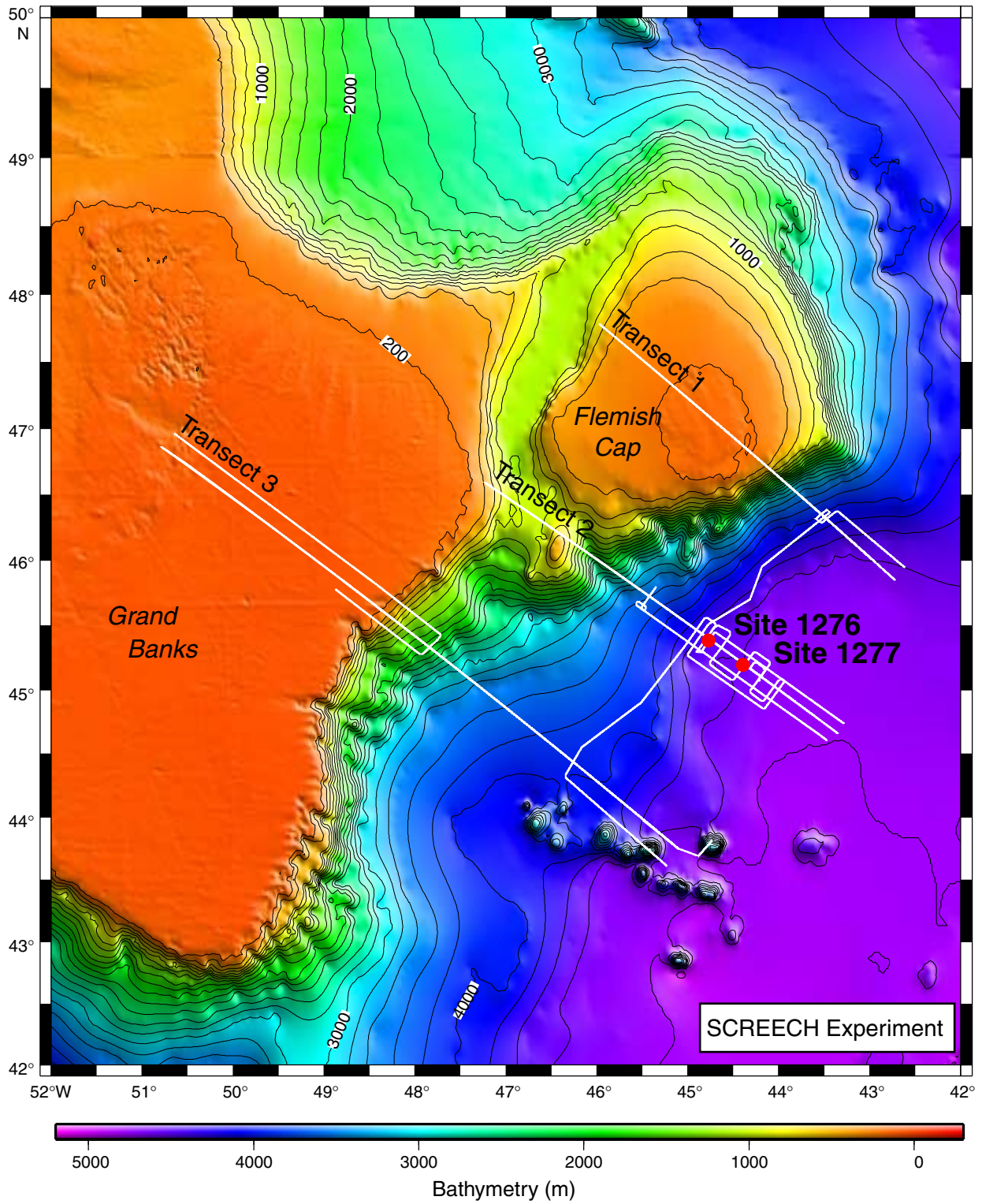


Figure F5

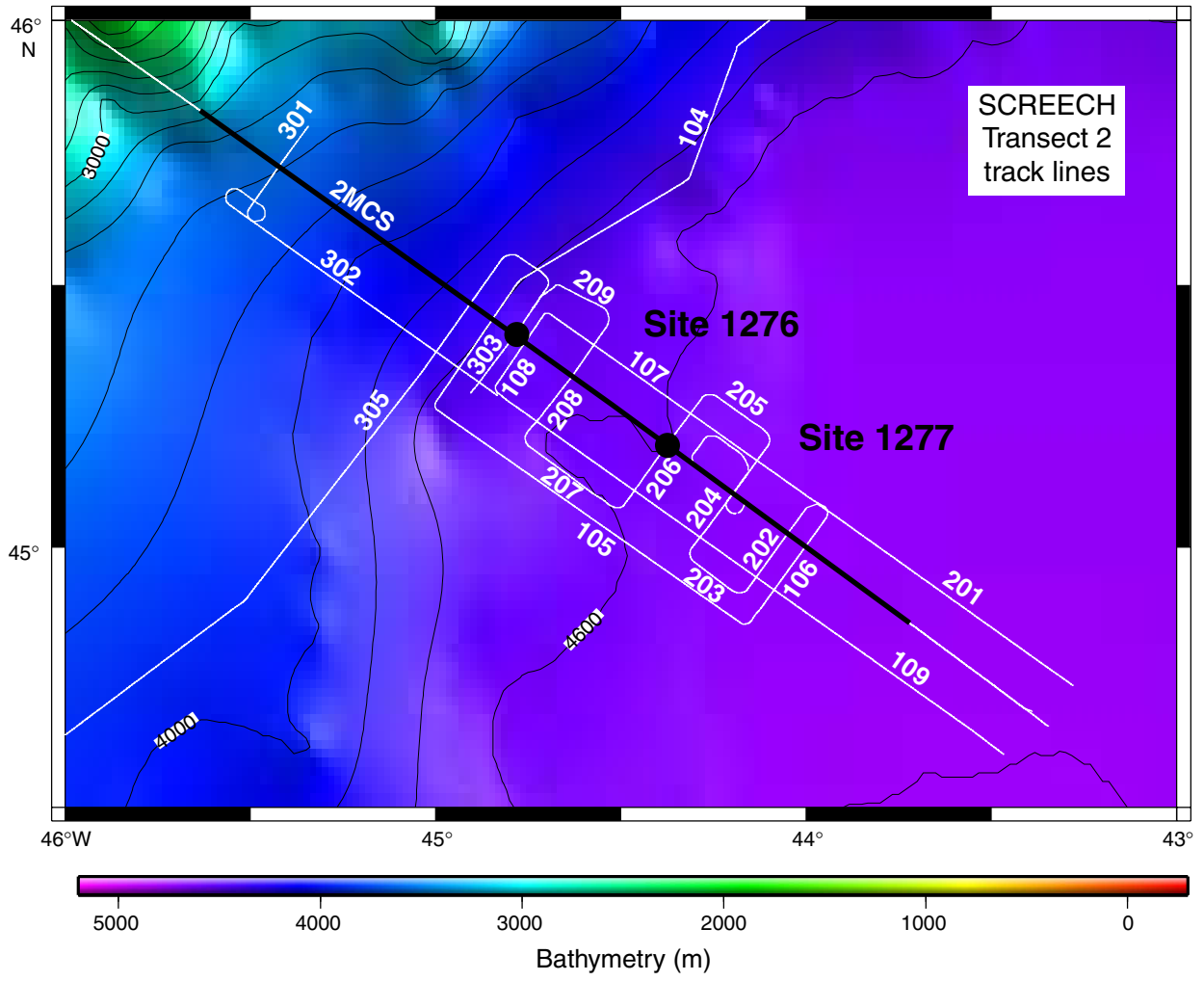


Figure F6

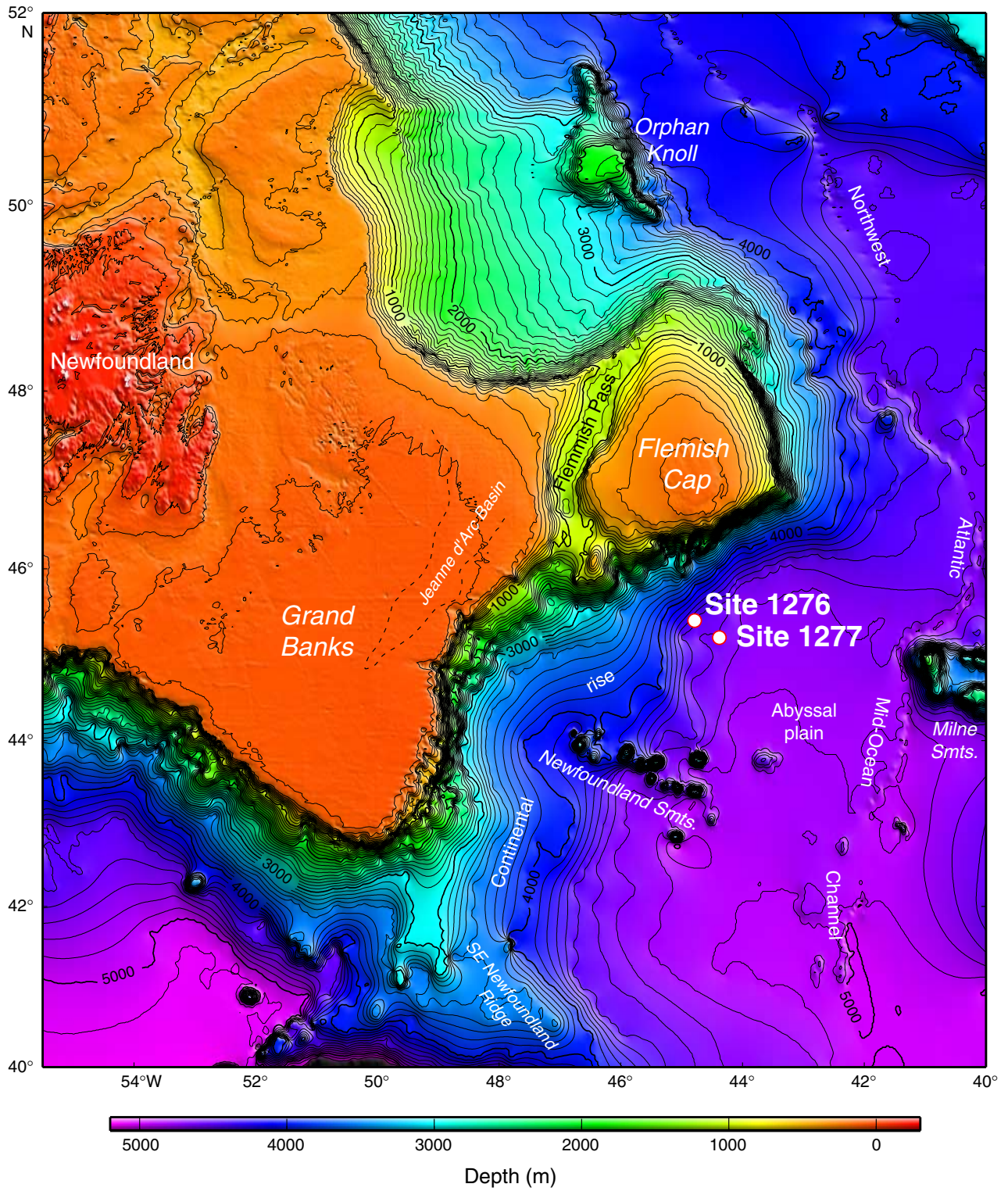


Figure F7

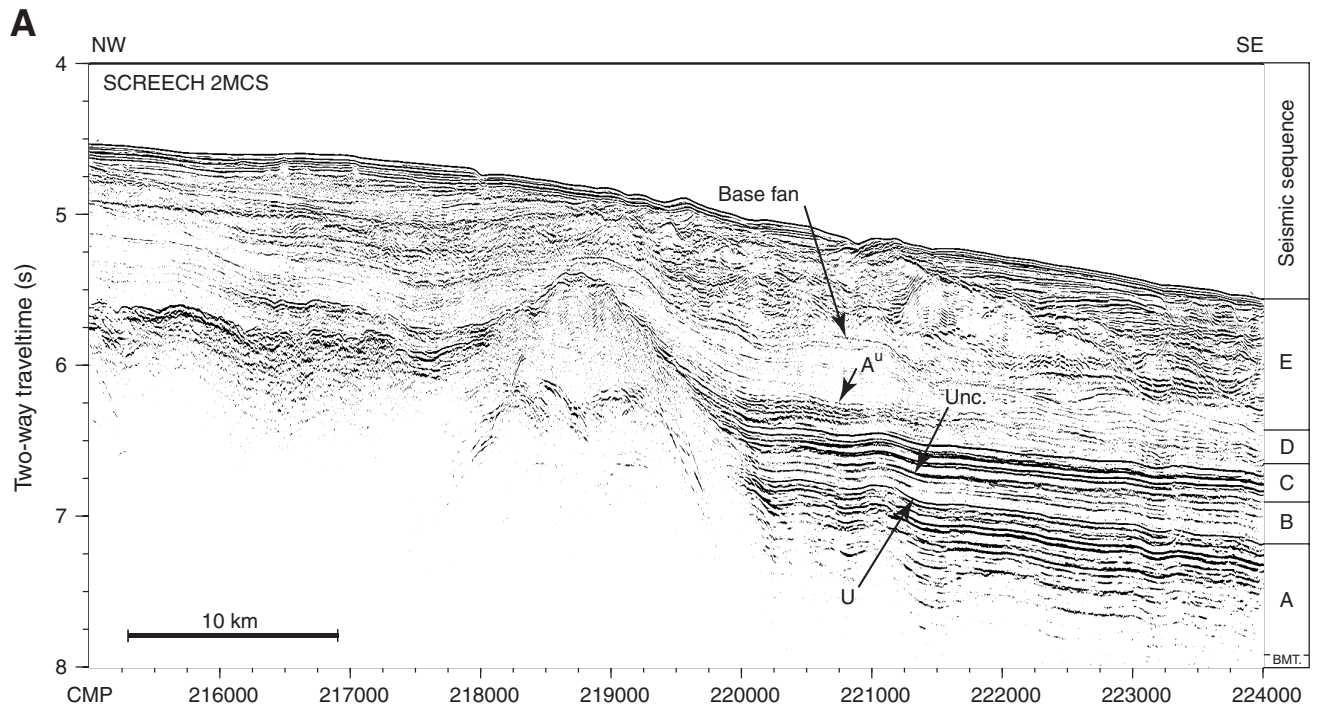


Figure F8

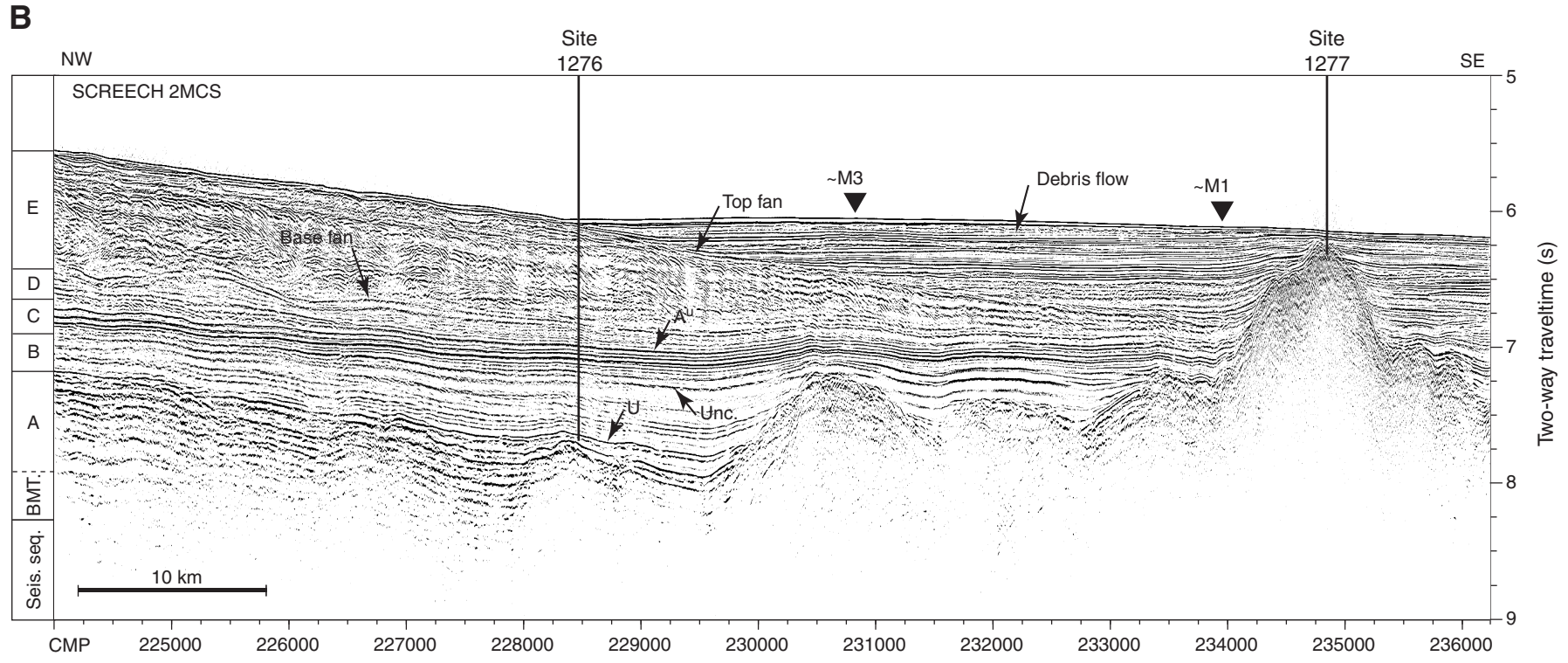


Figure F8 (continued)

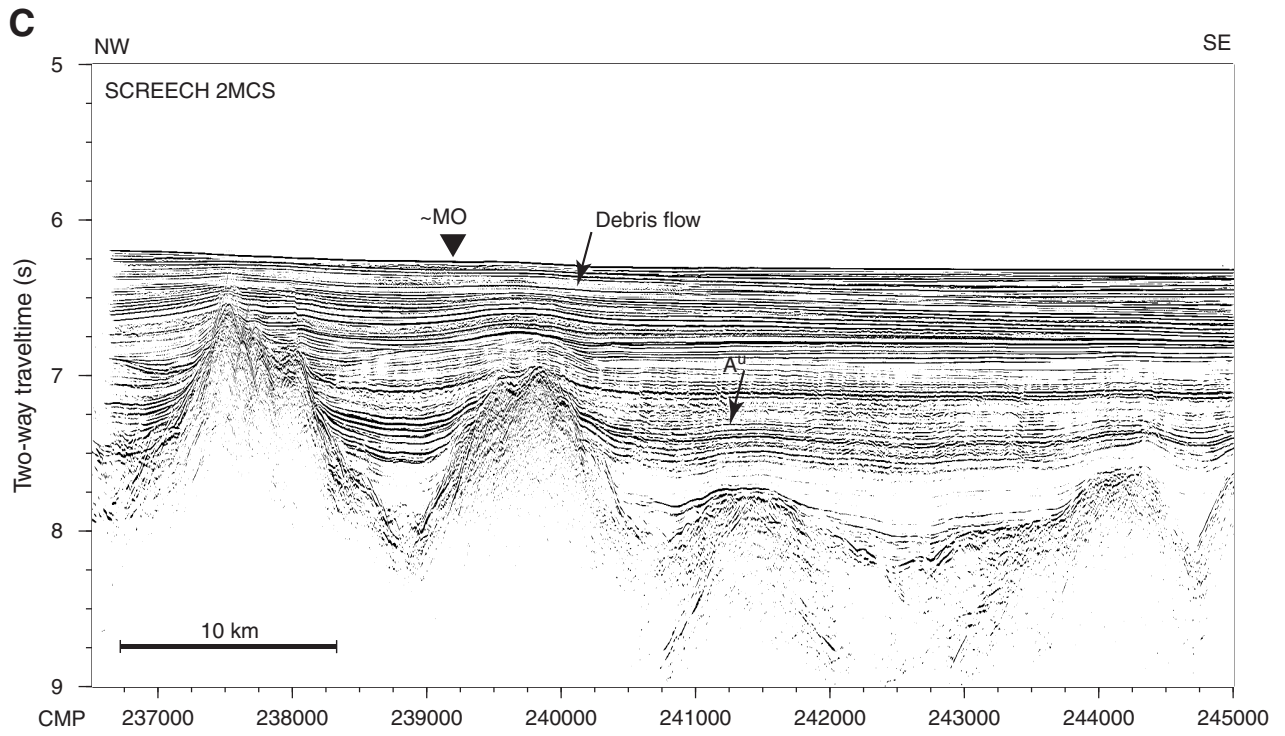


Figure F8 (continued)

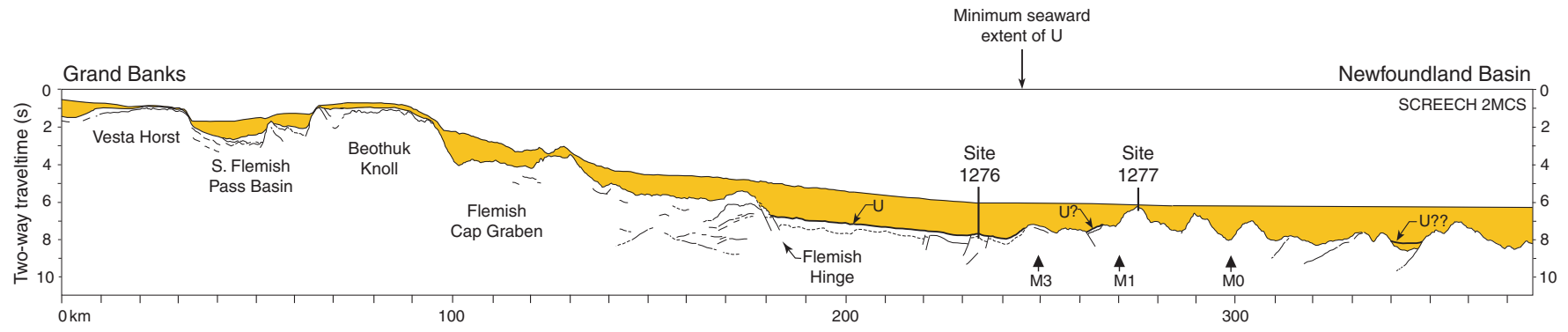


Figure F9

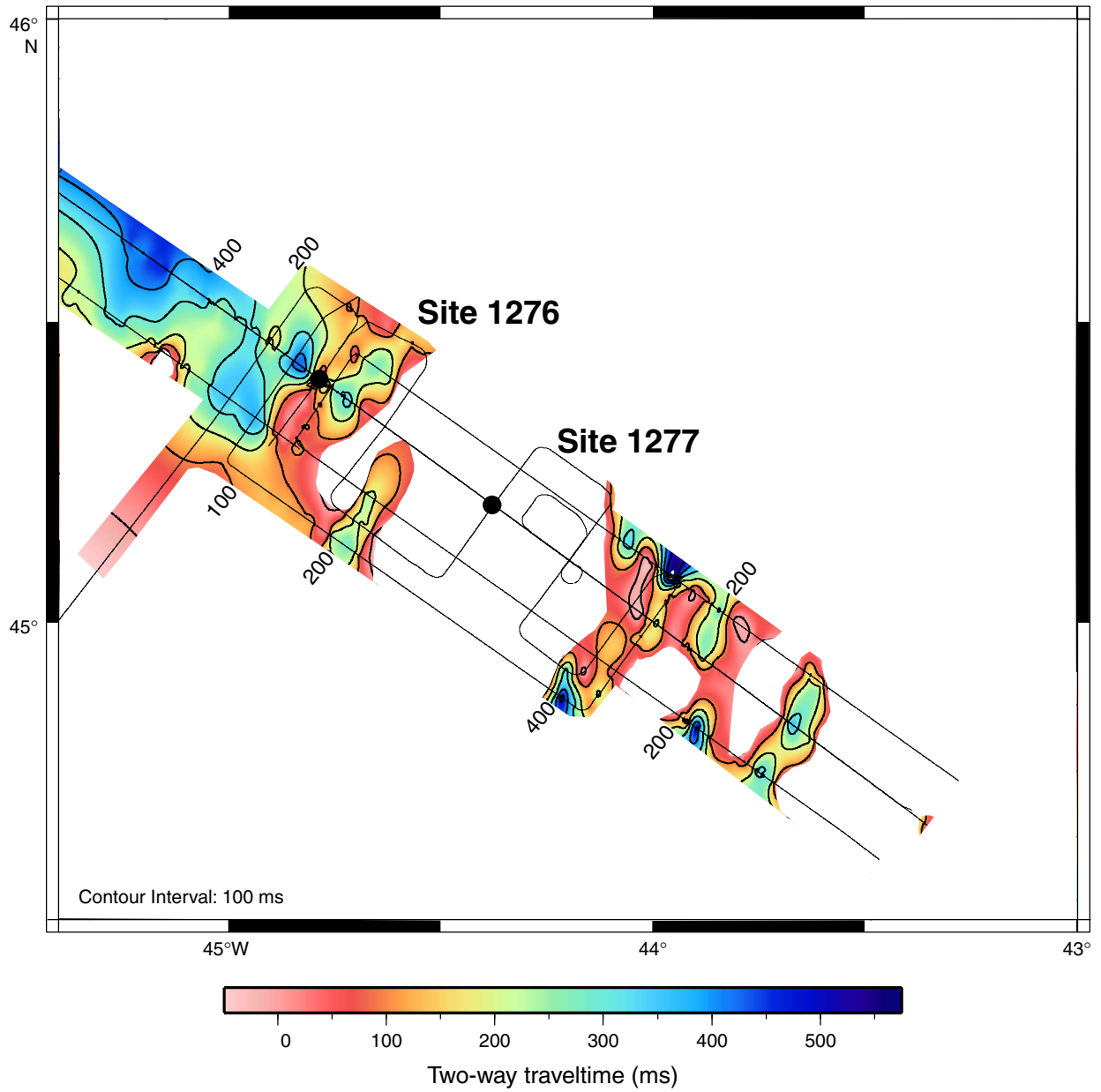


Figure F10

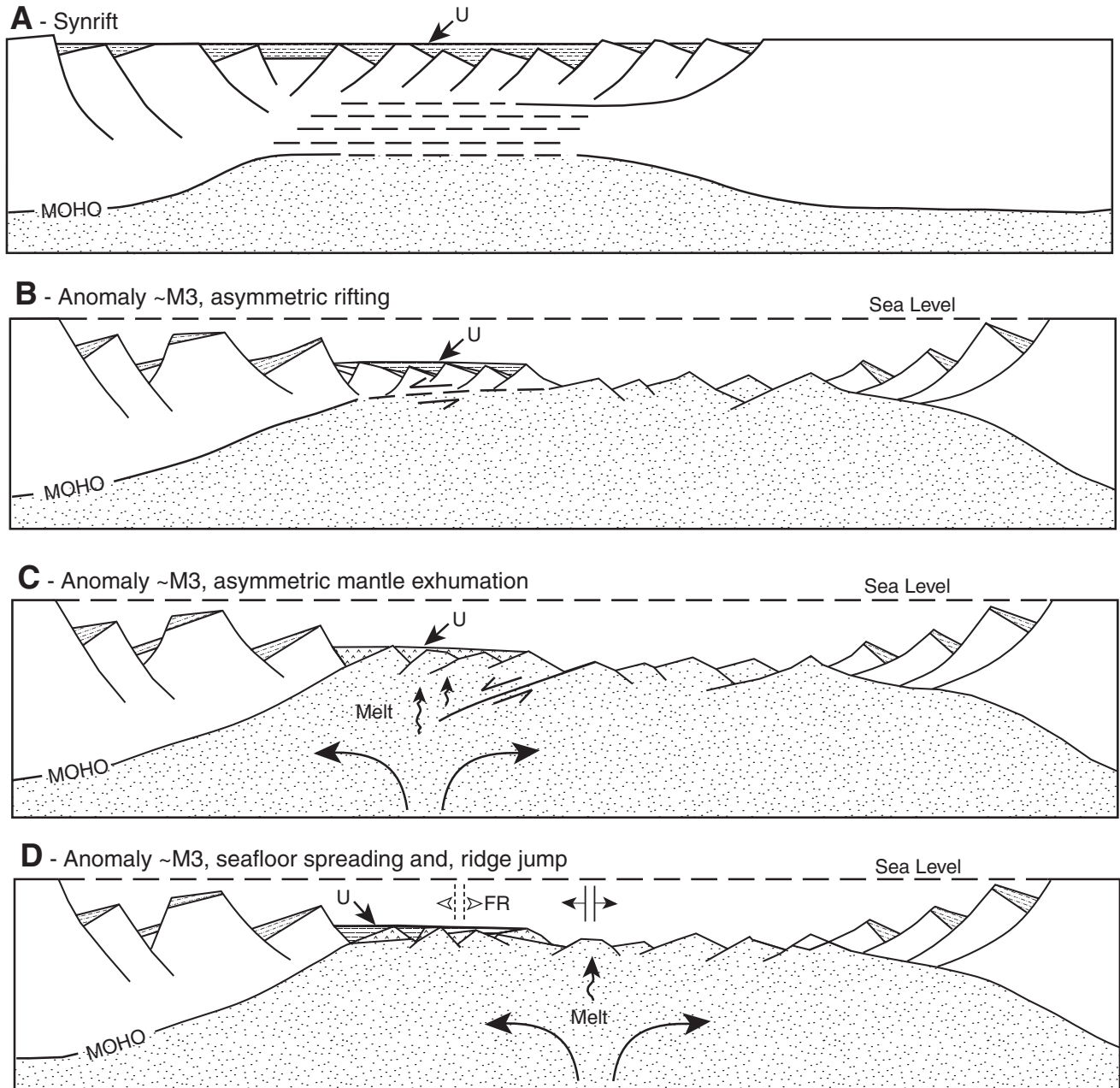


Figure F11

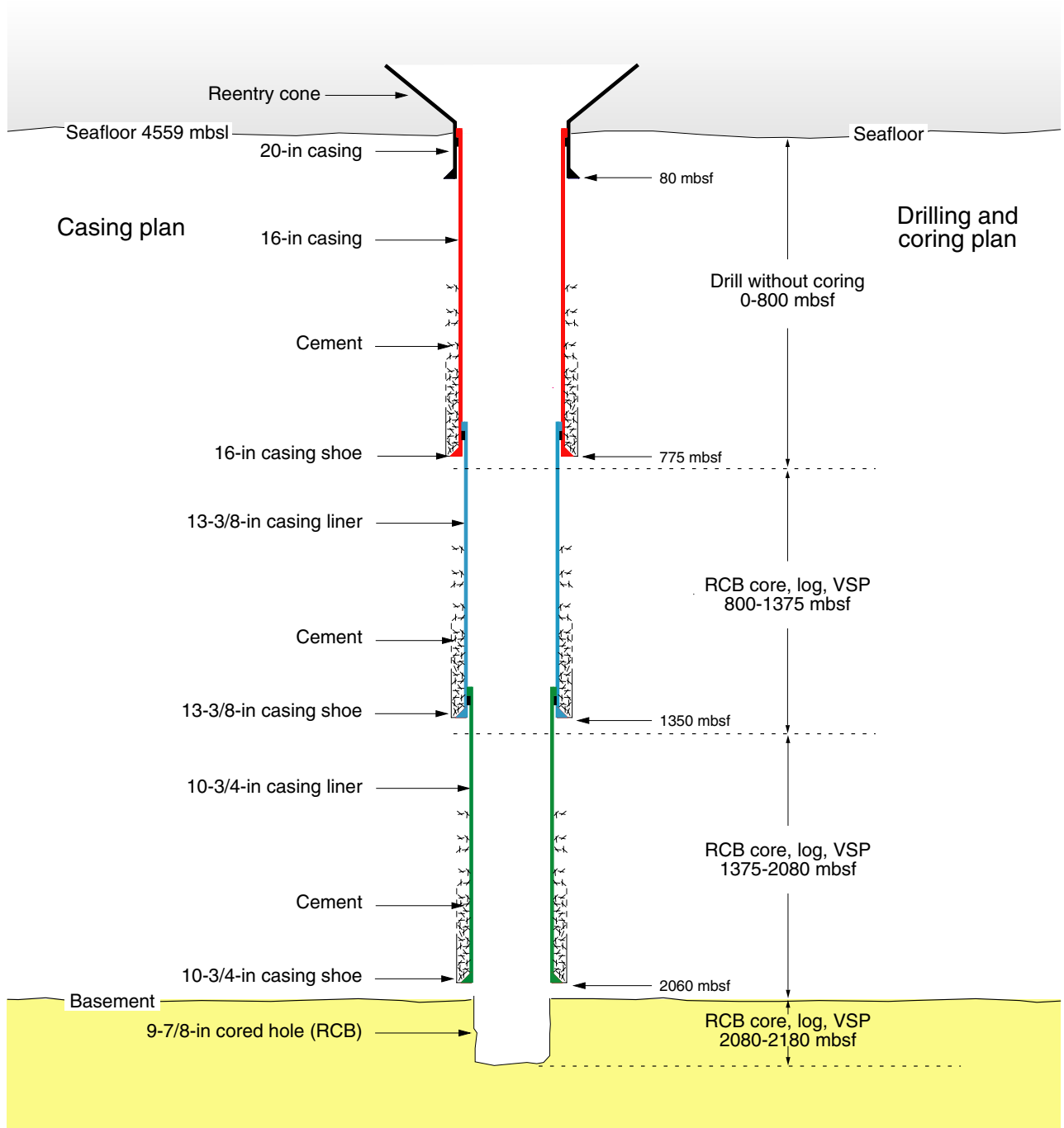


Figure F12

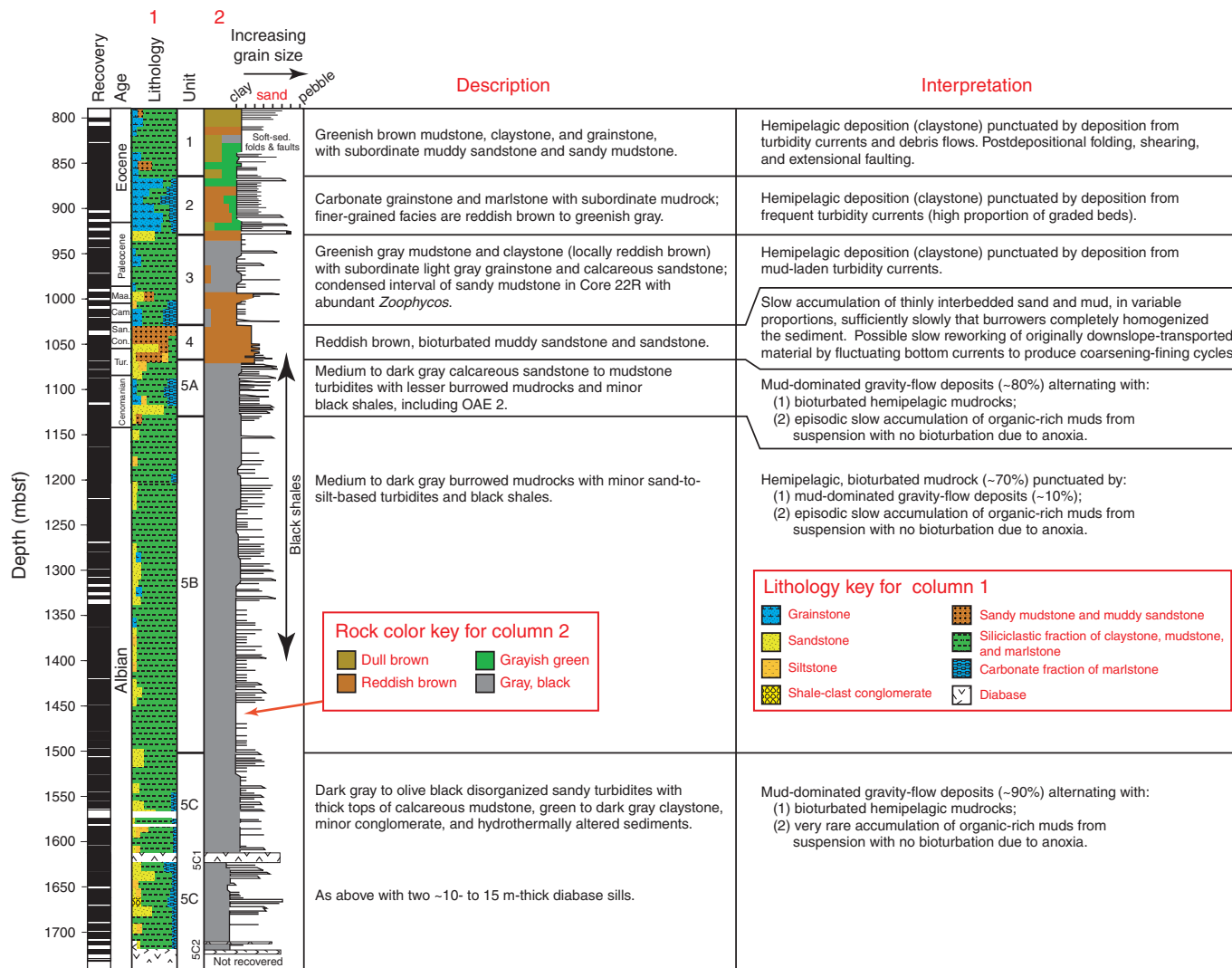


Figure F13

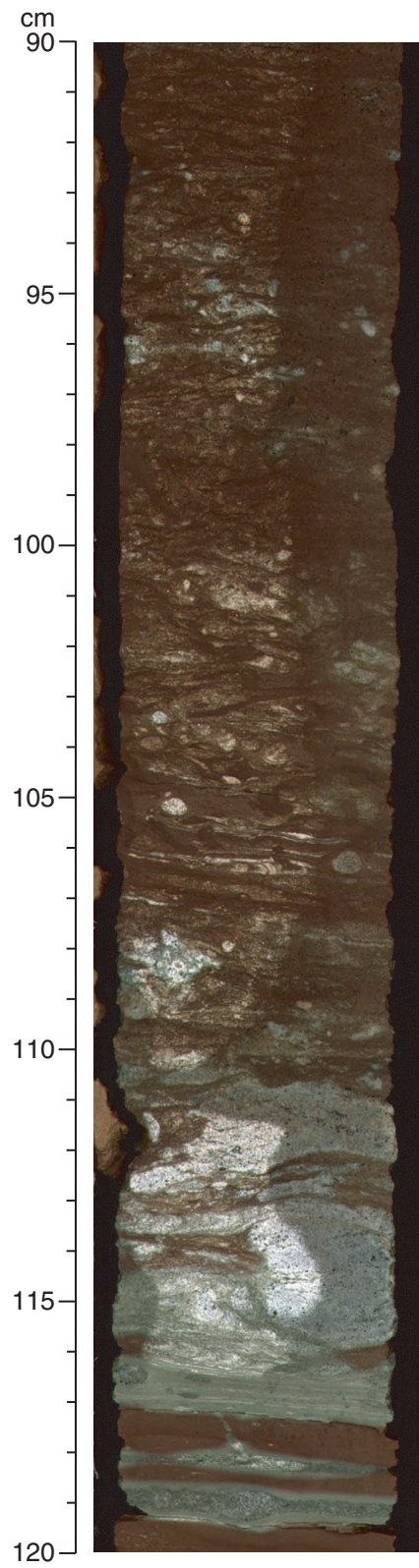


Figure F14

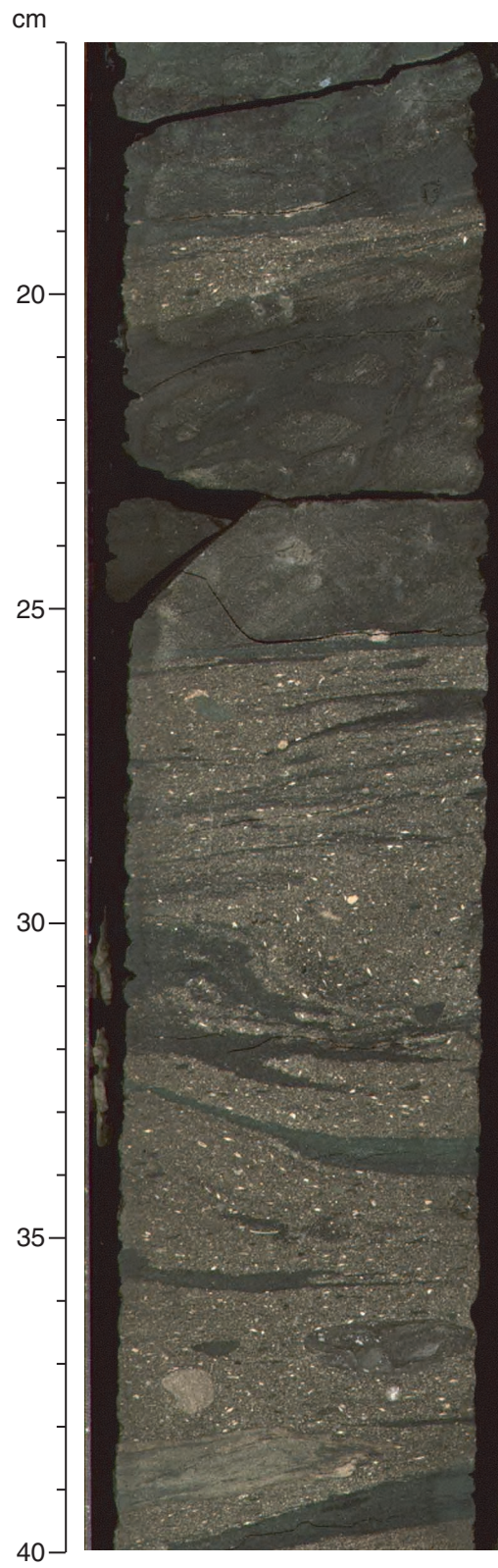


Figure F15

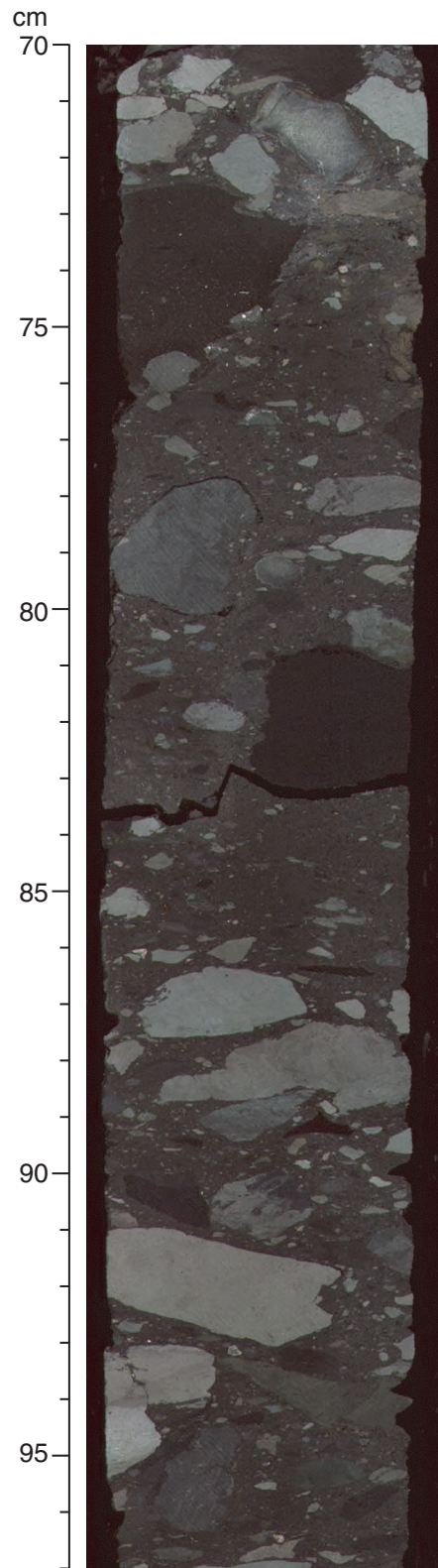


Figure F16

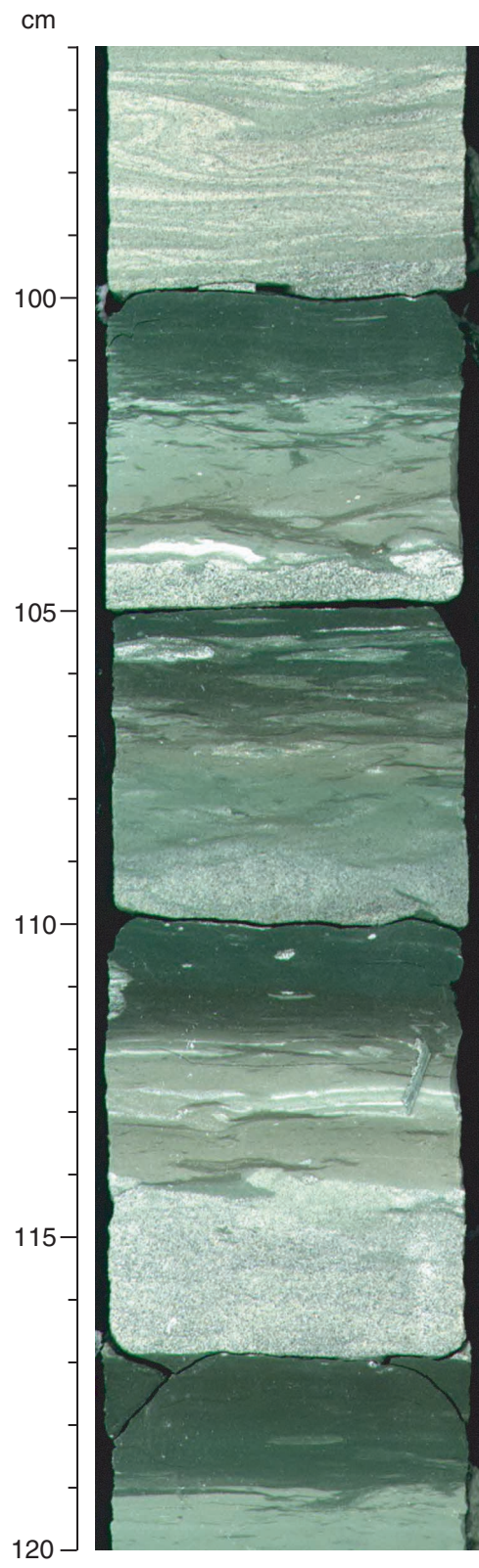


Figure F17

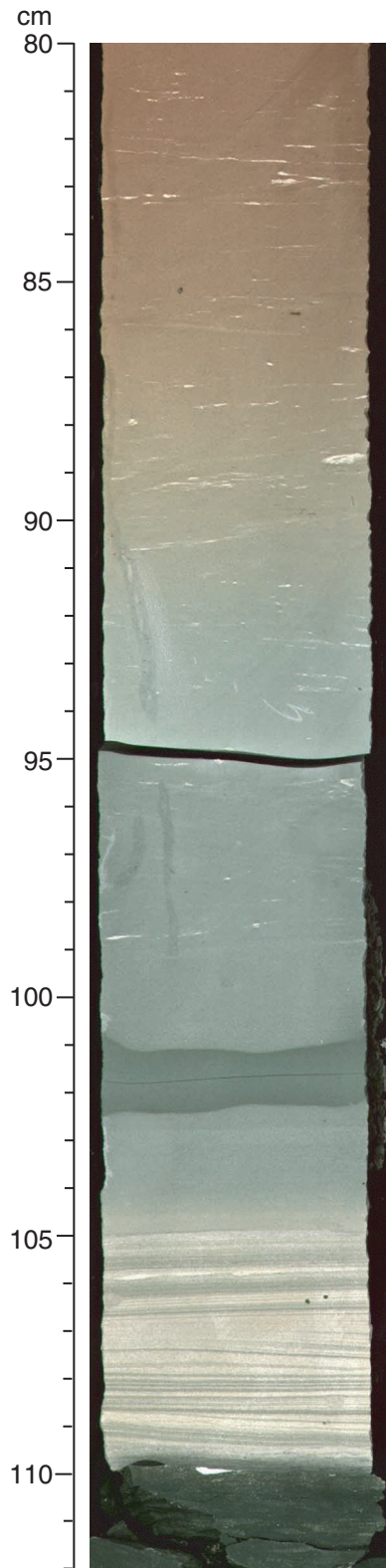


Figure F18

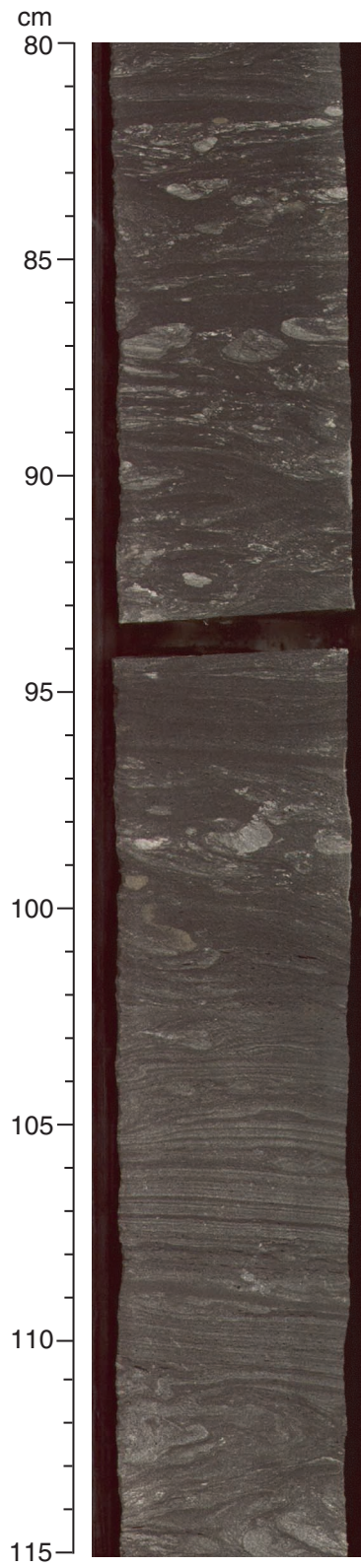


Figure F19

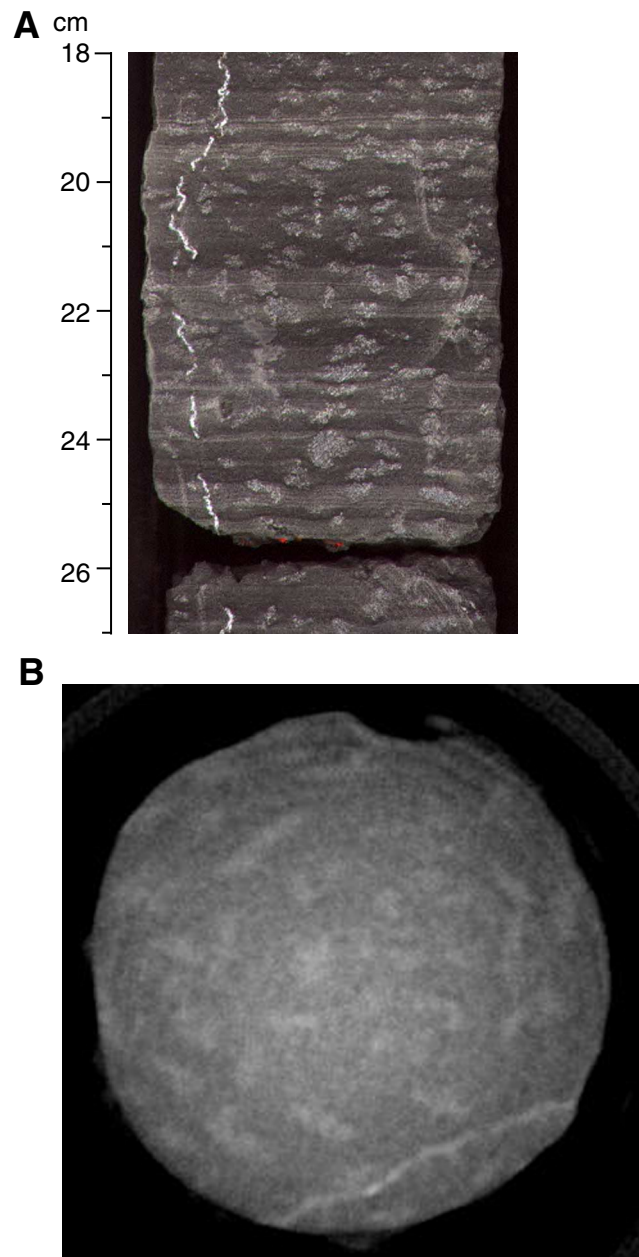


Figure F20

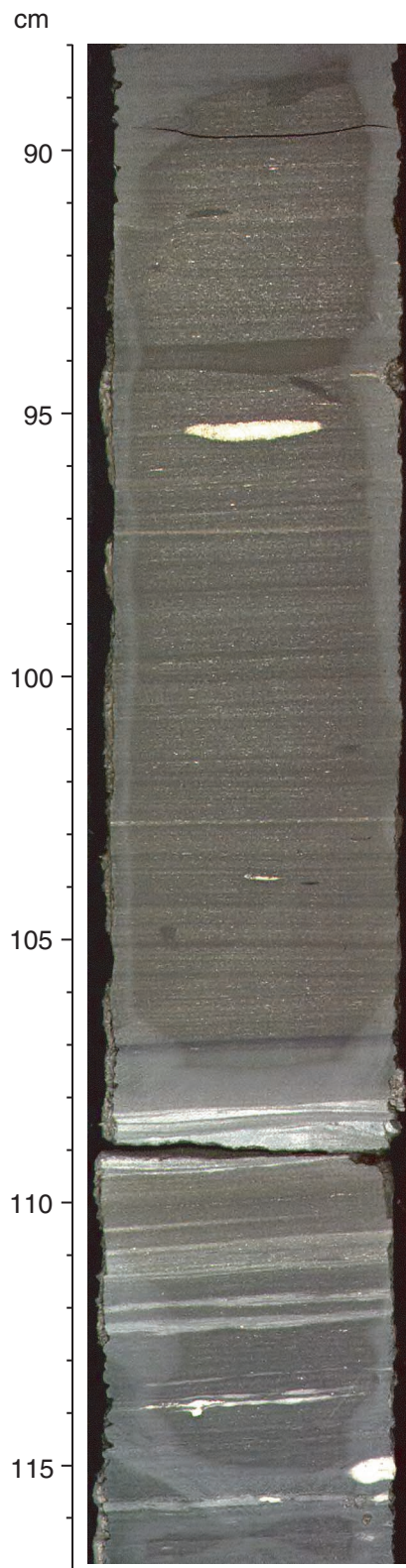


Figure F21

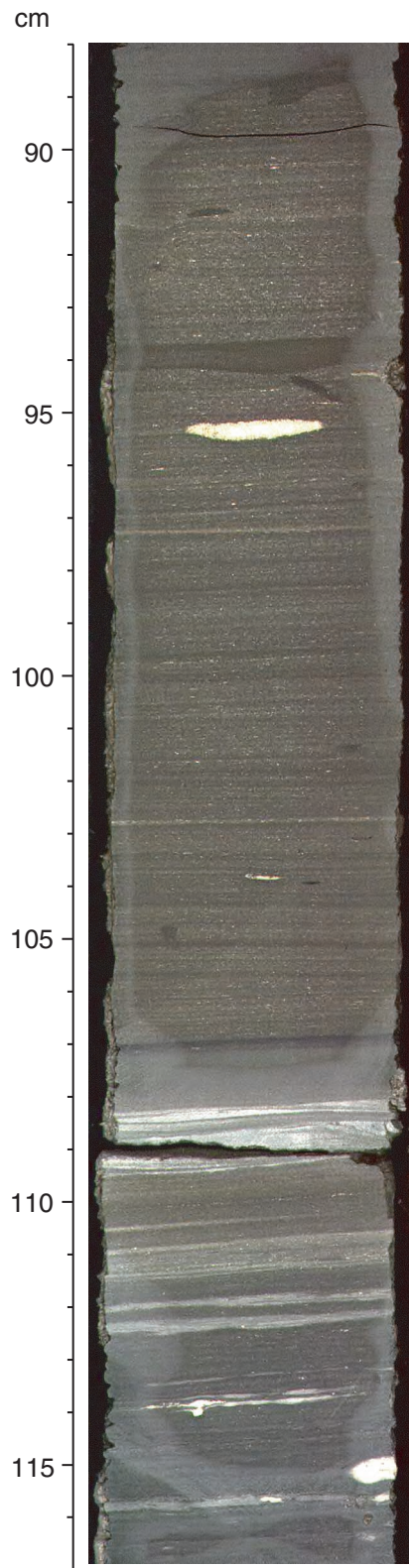


Figure F22

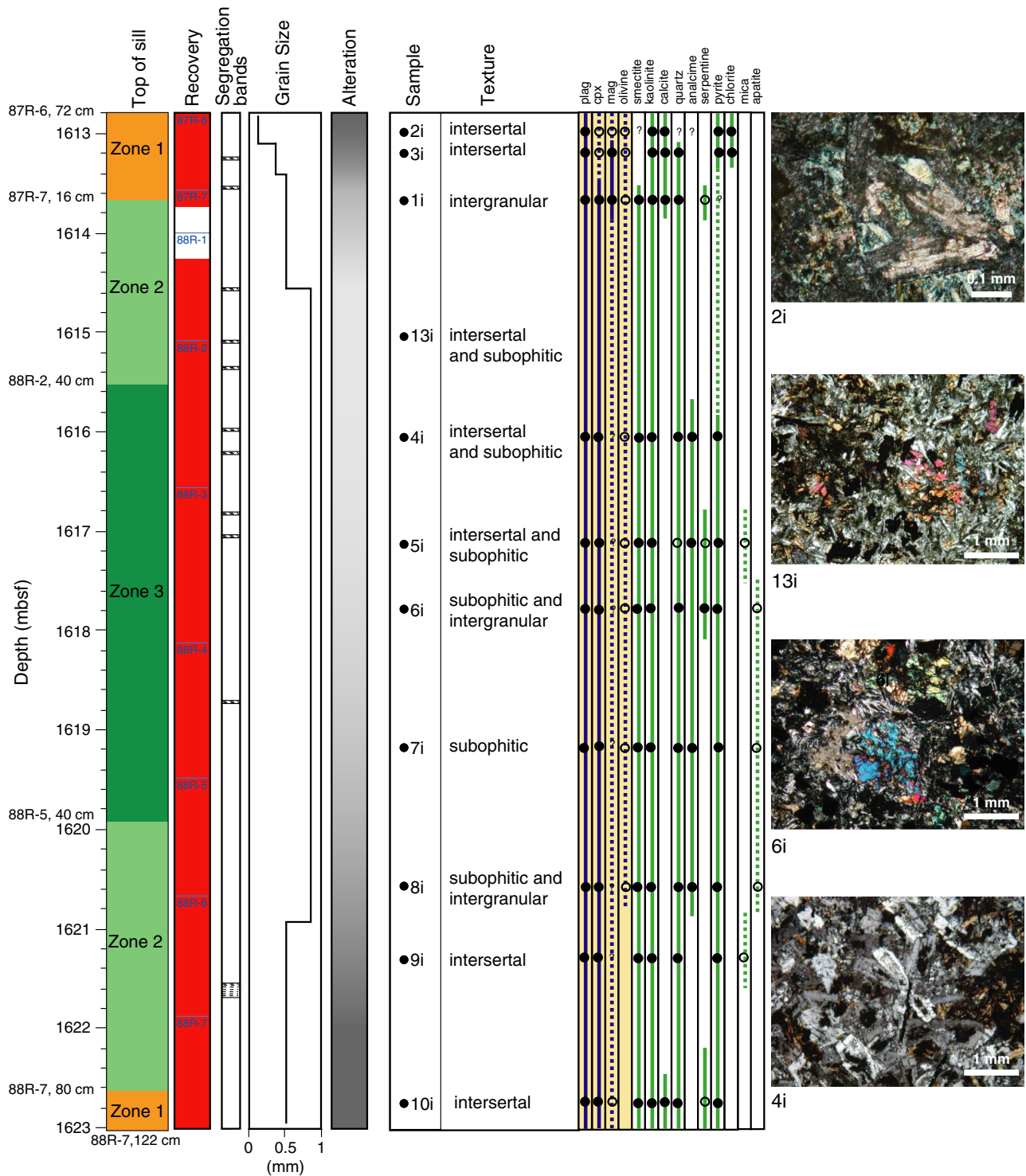


Figure F23

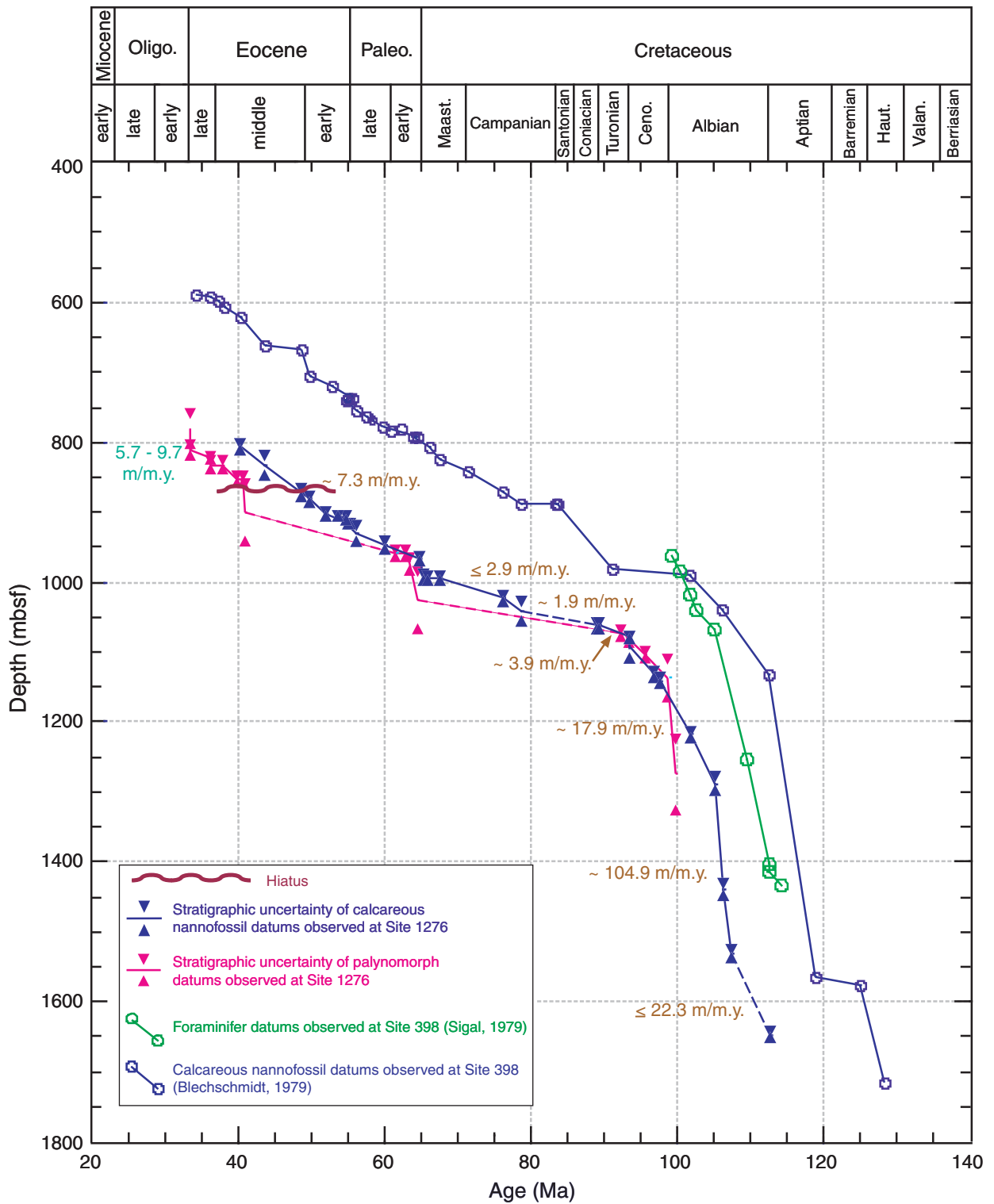


Figure F24

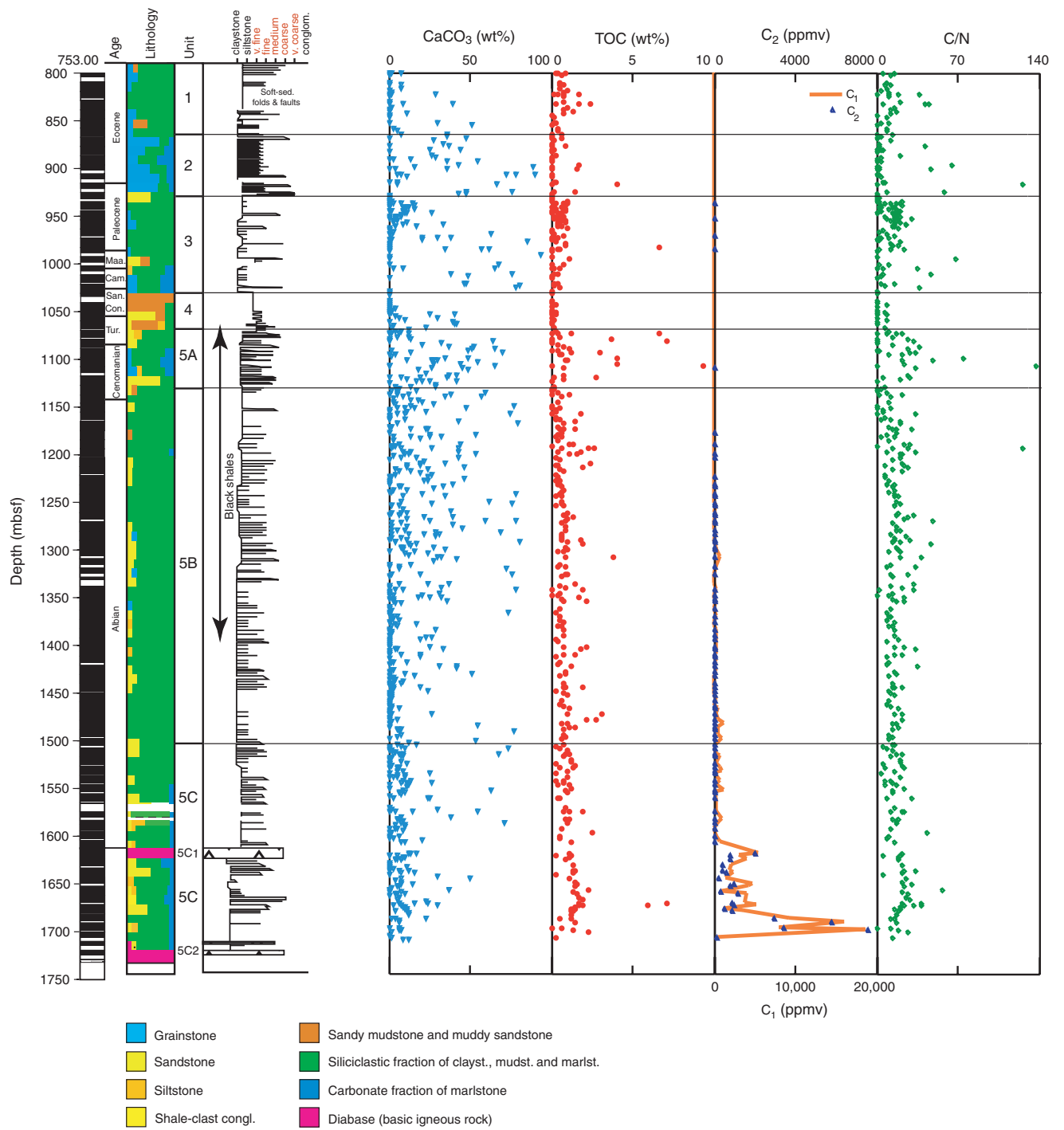


Figure F25

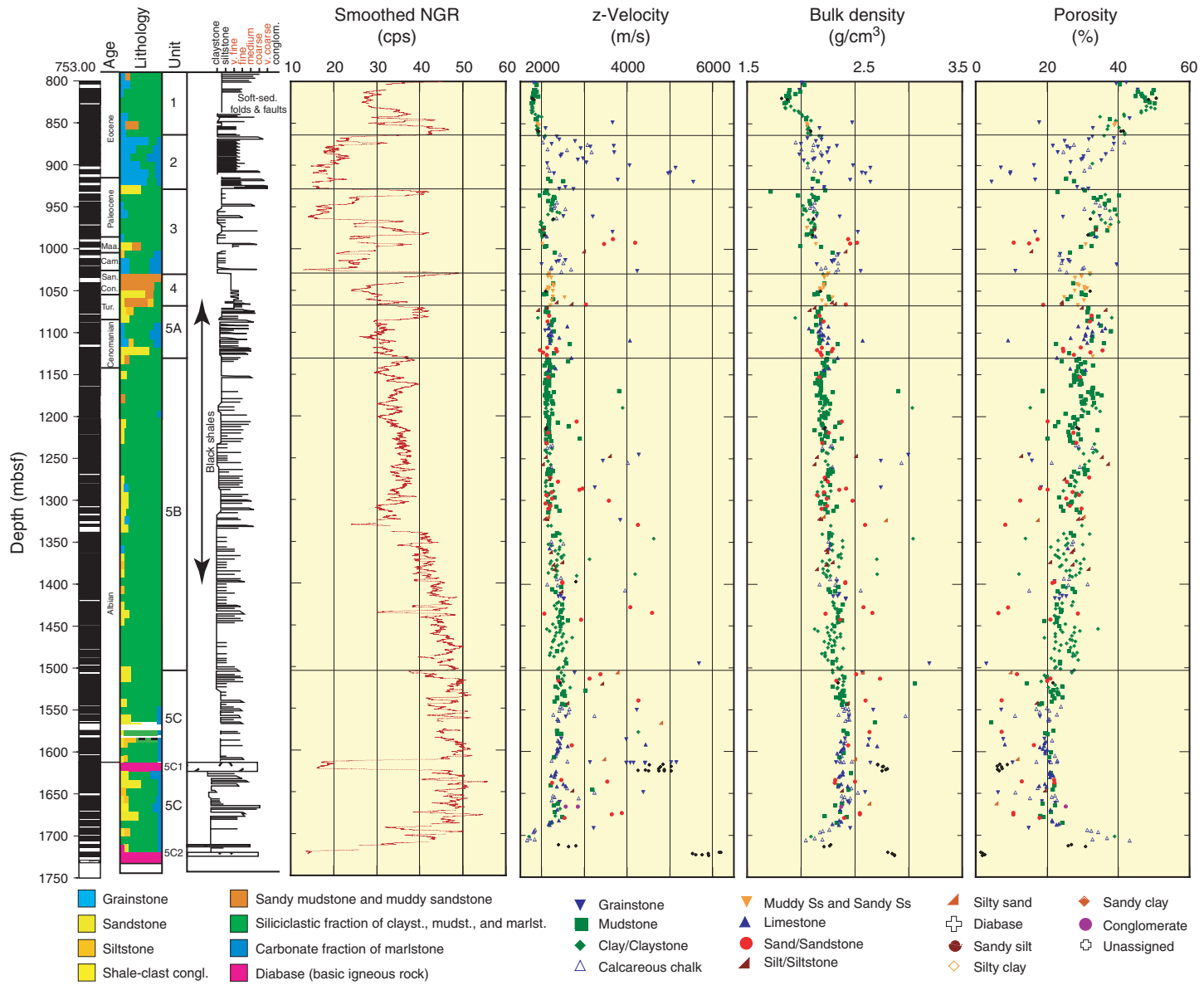


Figure F26

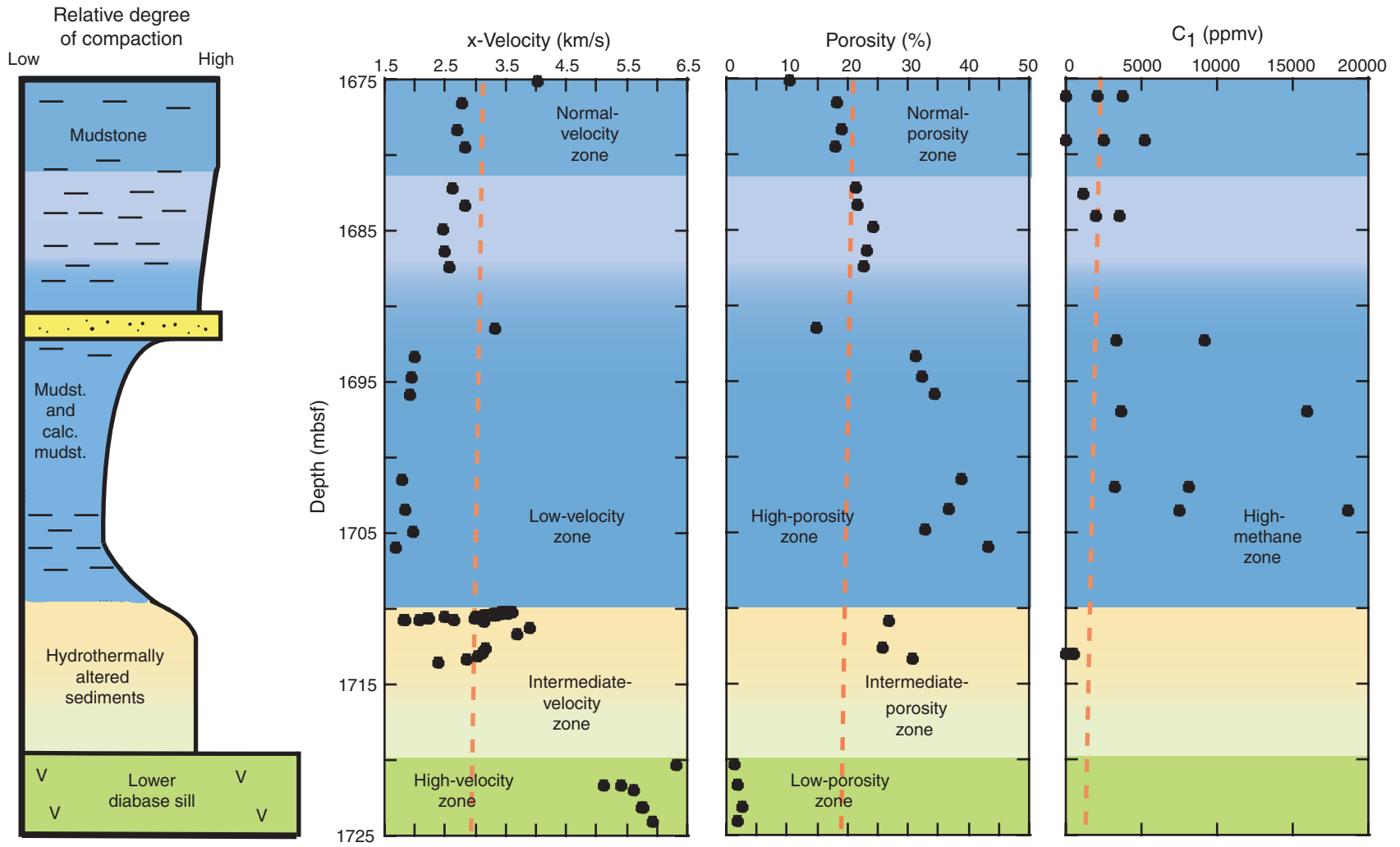


Figure F27

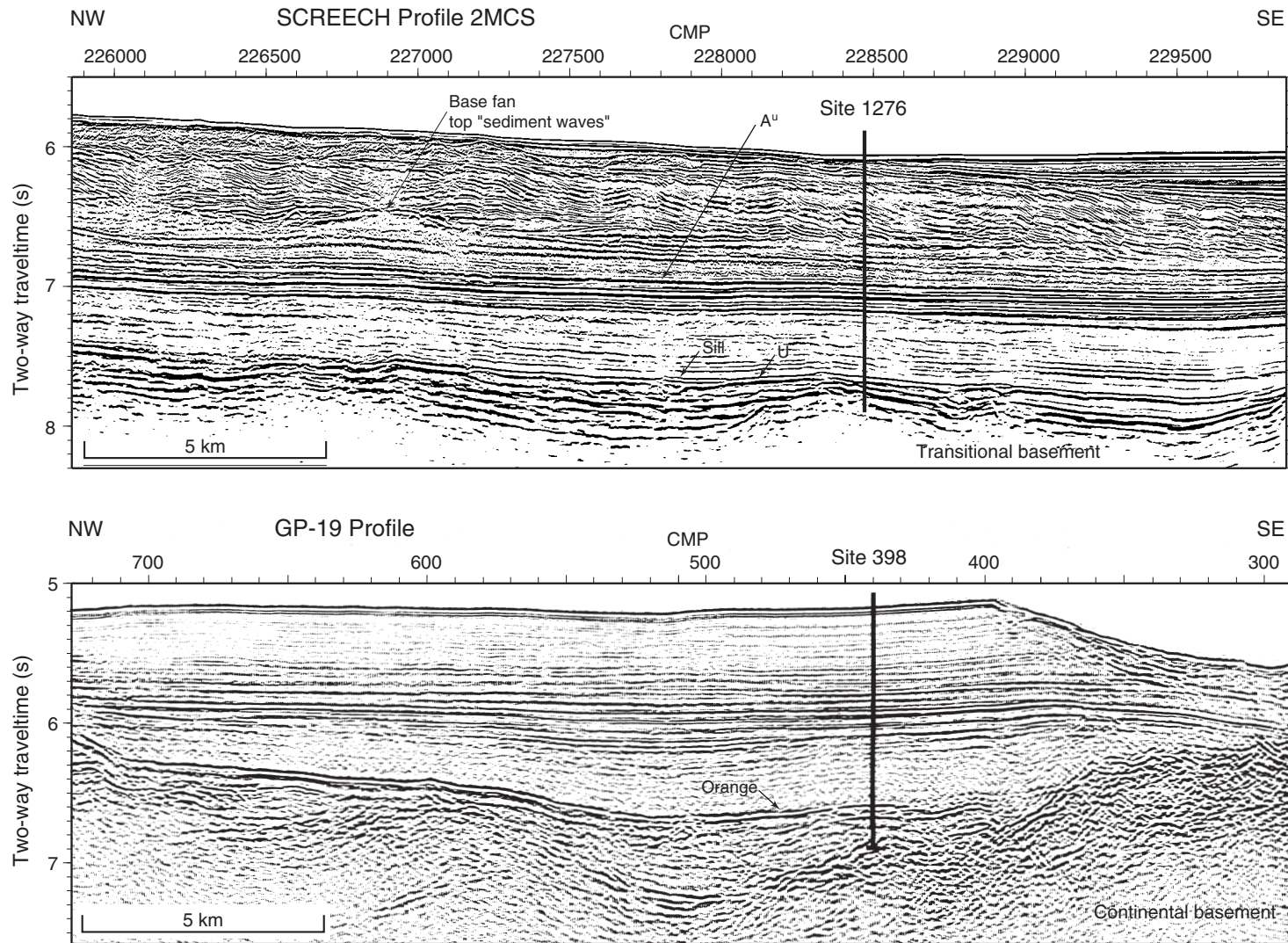


Figure F28

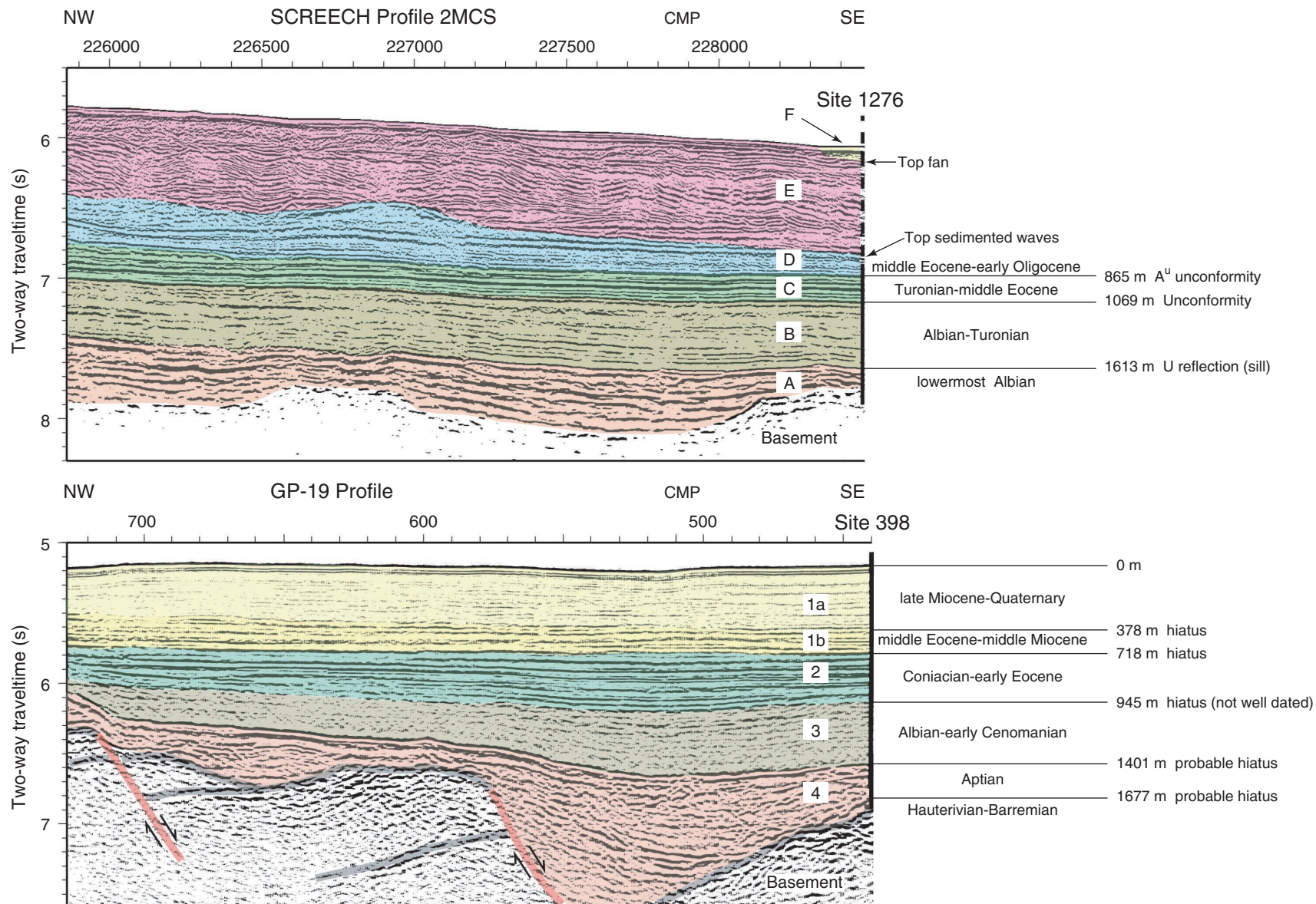


Figure F29

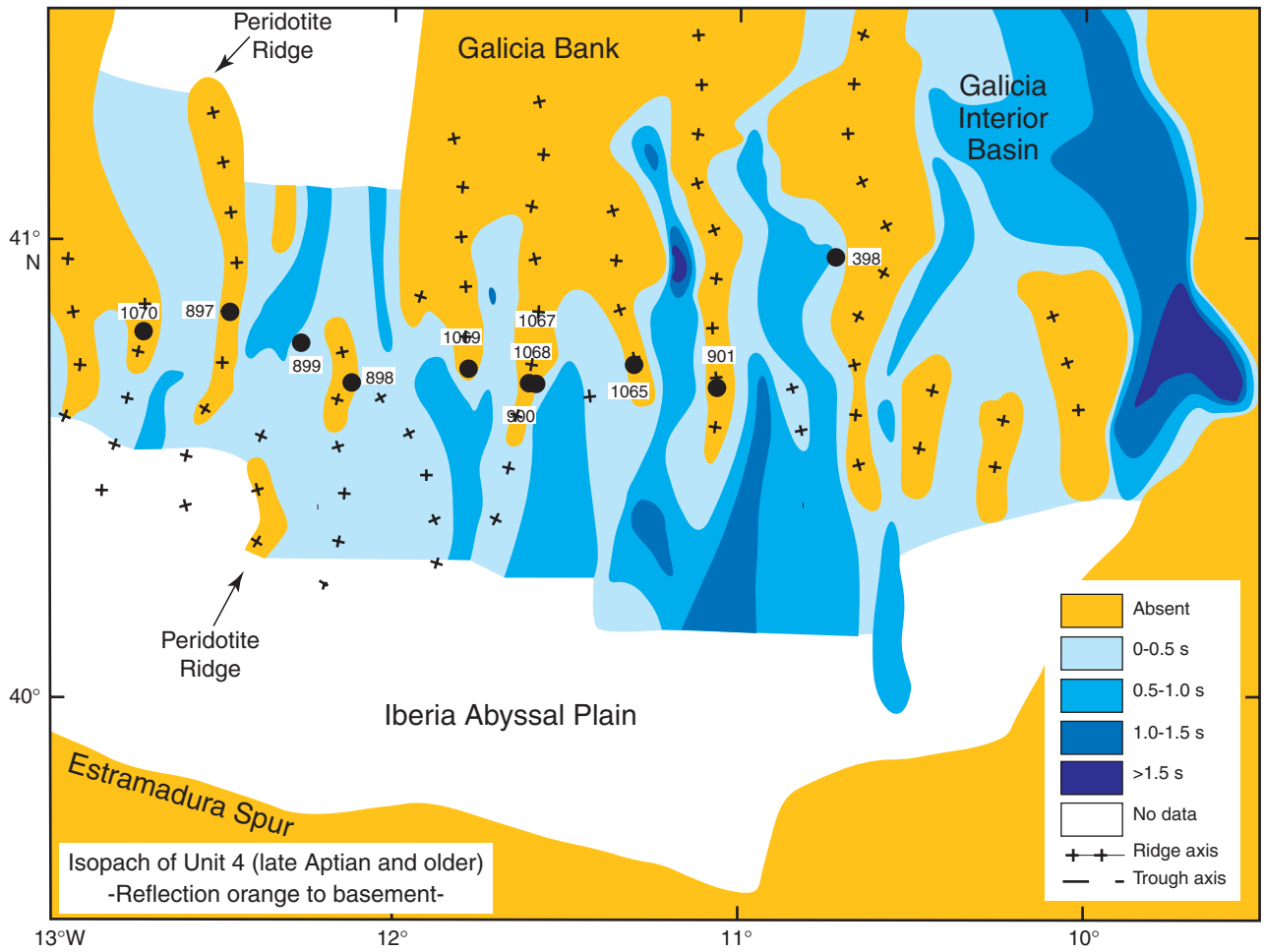


Figure F30

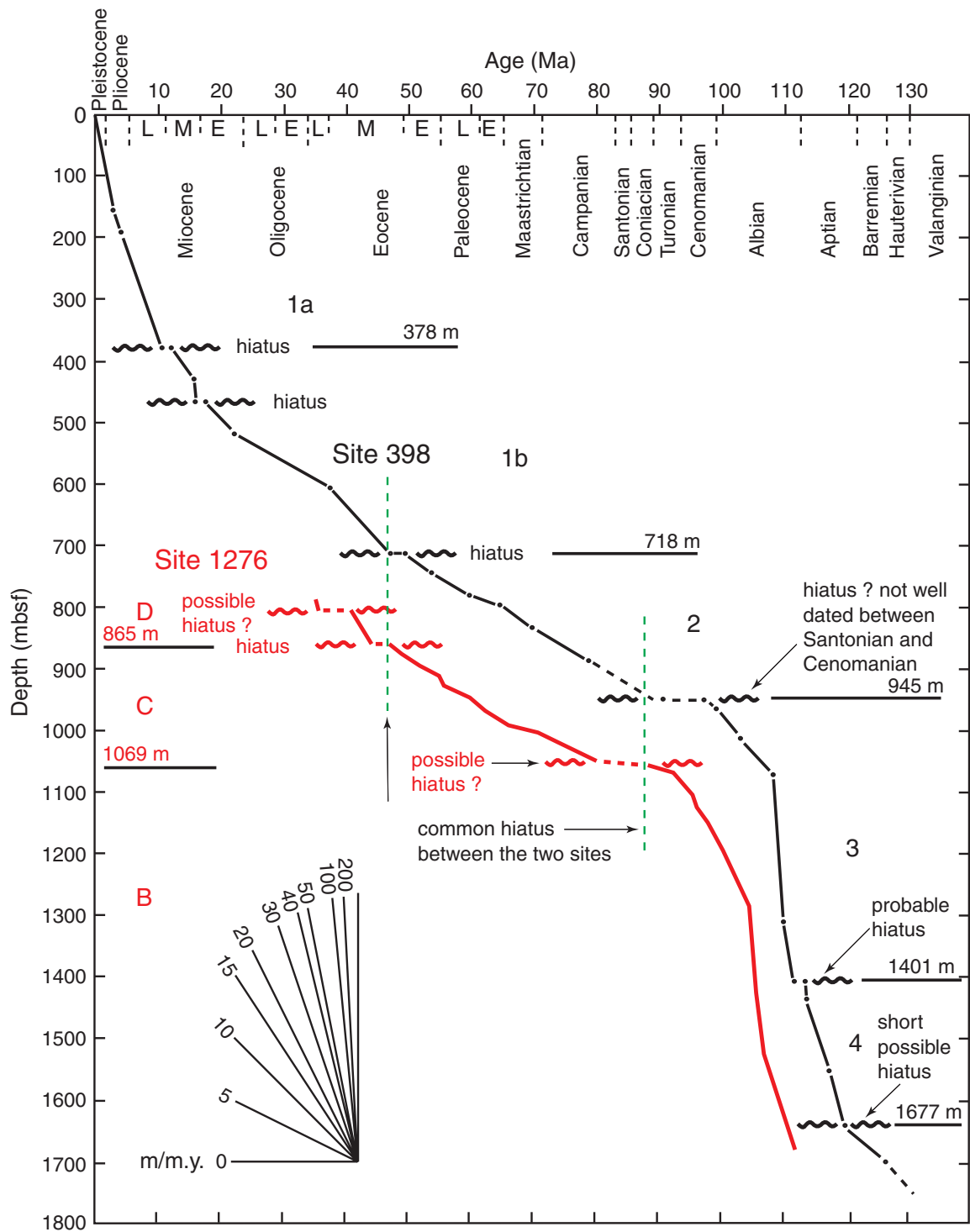


Figure F31

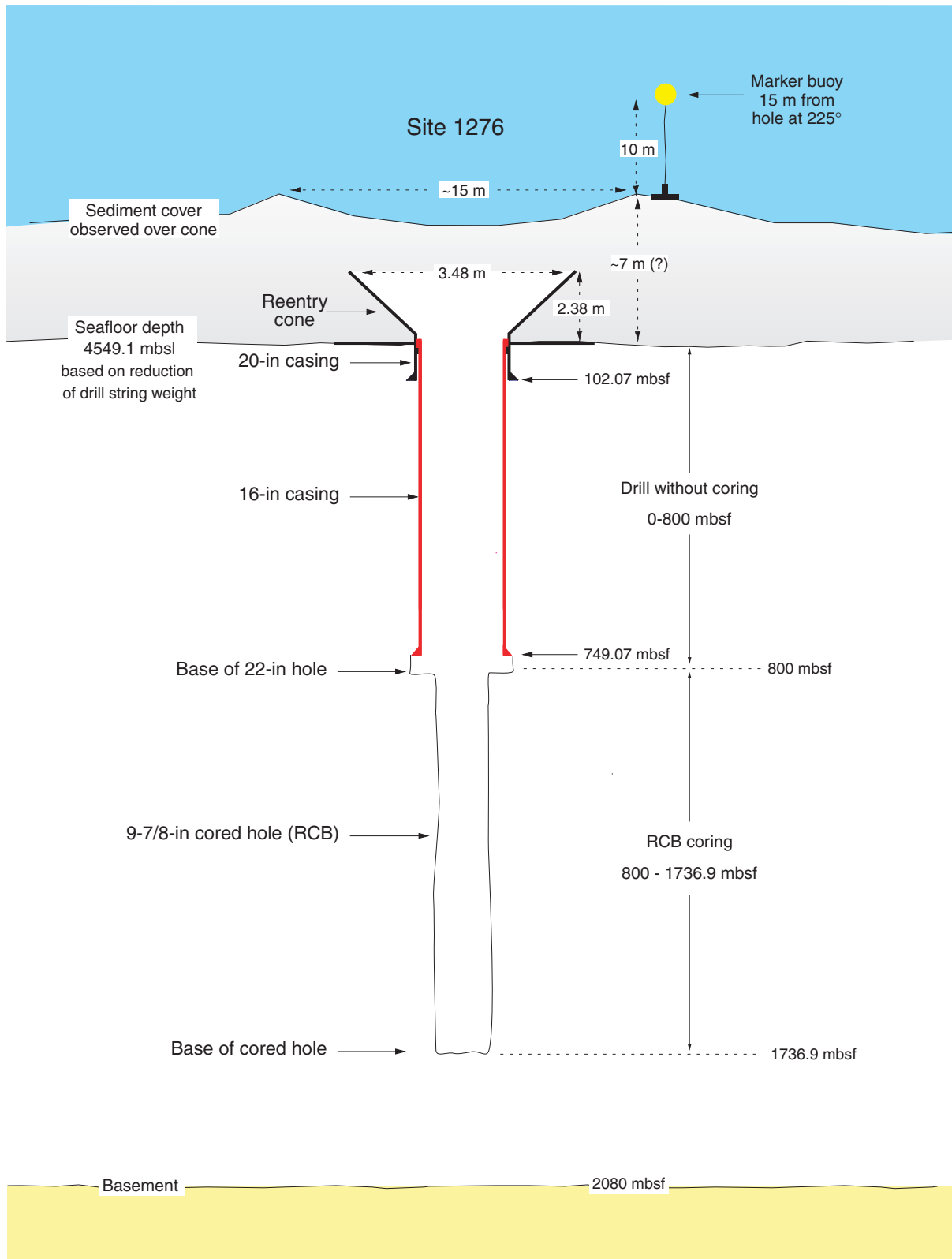


Figure F32

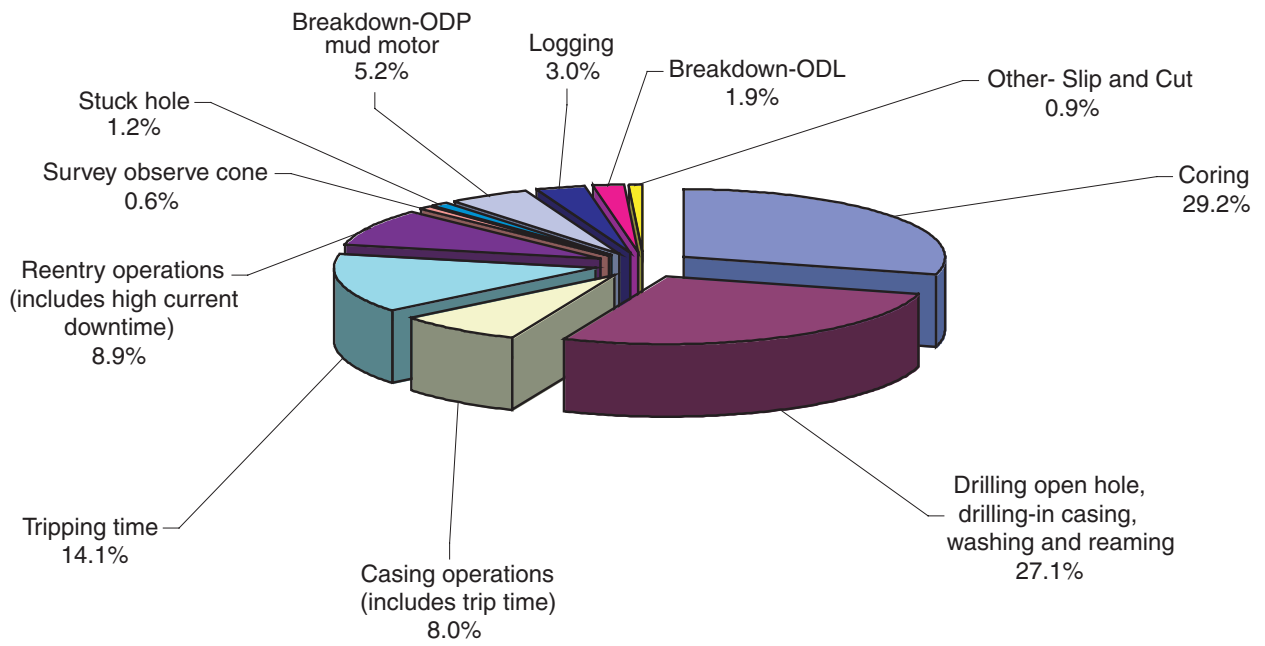


Figure F33